W-PM-A1 MEMBRANE POTENTIALS OF MITOCHONDRIA: DISTRIBUTION OF K^+ IN THE PRESENCE OF VALINOMYCIN. H. Tedeschi, Department of Biological Sciences, State University of New York at Albany, Albany, N.Y. 12222.

Mitchell and Moyle [Eur. J. Biochem. 7, 471 (1969)] have followed the distribution of K^+ in isolated mitochondria in the transition from anaerobic to aerobic conditions. The membrane potential generated by metabolism was calculated using the Nernst equation, $\Delta E = -59 \log[(K^+)_i/(K^+)_o]$. The assumptions of this procedure are not justified. The K^+ net influx approximately corresponds to the H^+ net efflux. The internal negative charge (X^-) neutralized by the K^+ corresponds quantitatively to the H^+ efflux. Under these conditions the Gibbs-Donnan ratios will be $r = (X^-)/(K^+)_o$. As shown in the Table, the Donnan ratios and not the membrane potentials are responsible for the observed distribution. Hence the evidence does not support the presence of a significant metabolically induced membrane potential in the mitochondria. Paradoxically, the increase in permeability induced by valinomycin might produce a diffusion potential approximated by the Nernst equation. However, this potential is not directly dependent on metabolism and is not the result of an electrogenic process.

Experiment #	-59 log r	Apparent membrane potential (Mitchell and Moyle, 1969)
I	-189	-199
II	-183	-171
III	-142	-139
IV	- 73	- 83

W-PM-A2 K^+ FLUXES AND THE MITOCHONDRIAL MEMBRANE POTENTIAL. Joyce Johnson Diwan and Henry Tedeschi, Biology Department, Rensselaer Polytechnic Institute, Troy, N. Y. 12181 and Department of Biological Sciences, State University of New York at Albany, Albany, N. Y. 12222

Rottenberg (J. Membr. Biol., 11: 117, 1973) has proposed that K^+ transport in isolated mitochondria is a passive process driven by an electrical potential across the mitochondrial membrane. This conclusion is based on questionable premises and we therefore decided to examine this problem more incisively. Unidirectional K^+ fluxes into isolated rat liver mitochondria were monitored by means of the radioisotope ^{42}K, the mitochondria being separated from incubation media by rapid centrifugation through silicone. Net K^+ fluxes were determined from atomic absorption measurements and unidirectional K^+ effluxes were calculated as the difference between influx and net flux. Effects on the unidirectional K^+ fluxes of the respiratory inhibitors NaCN and antimycin A and the uncoupler dinitrophenol were examined. Both the K^+ influx and K^+ efflux were found to be decreased when respiration was inhibited. These results are not consistent with the fluxes being passively driven by a metabolism-dependent membrane potential. These and other studies (Diwan & Lehrer, in preparation) support the conclusion that K^+ is transported across the mitochondrial membrane by an energy-linked, carrier mechanism. Other results (see Kinnally & Tedeschi, these abstracts) indicate the absence of a significant electrogenically generated membrane potential in mitochondria. Supported by USPHS Grant GM-20726 and American Cancer Society Grant BC-161.

W-PM-A3 PHOSPHORYLATION WITHOUT PROTONMOTIVE FORCE. Kathleen Walsh Kinnally and Henry Tedeschi, Department of Biological Sciences, State University of New York at Albany, Albany, N.Y. 12222.

The total protonmotive force [e.g. see Mitchell and Moyle, Eur. J. Biochem. 7, 471 (1969)] was estimated in metabolizing rat liver mitochondria. The ΔpH was estimated from the distribution of 5,5 dimethyl-oxazolidine 2,4 dione (DMO) by the method of Addanki et al. [J. Biol. Chem. 243, 2337 (1968)]. The membrane potential was estimated from the fluorescence changes observed upon energization in the presence of the cyanine dye, 3,3' dipropylthiocarbocyanine [diS-C_3(5)] by the method of Laris et al. [Biochim. Biophys. Acta 376, 415 (1975)]. The total protonmotive force estimated was not sufficient to support the observed phosphorylation of ADP. In some experiments it provided as little as 1/10 of the total required electrochemical gradient. Aided by grant B-161 of the American Cancer Society, Inc.

W-PM-A4 THE MEMBRANE POTENTIAL OF MITOCHONDRIA MEASURED WITH MICROELECTRODES. Bruce L. Maloff, Stylianos P. Scordilis and Henry Tedeschi, State University of New York at Albany, Albany, N.Y. 12222.

The electrical parameters of the mitochondrial membrane were studied with microelectrodes in liver mitochondria from cuprizone treated mice. The size of the mitochondria varied from about 5 to 10 μm. The measured potentials were not changed significantly with the initiation of metabolism. They ranged between 10 and 25 mv, positive inside. The resistances were 1-2 meg Ω. The data are essentially equivalent to those previously reported by Tedeschi and Tupper for isolated giant Drosophila mitochondria [Proc. Nat. Acad. Sci. 63, 370, 713 (1969), Science 166, 1539 (1969)]. The measured electric potentials probably correspond to potentials across the mitochondrial membrane since their magnitude changes predictably with the K^+ concentration of the medium in the presence of valinomycin. The results are not consistent with a role of the membrane potential in the coupling between oxidation and phosphorylation. Similar conclusions can be reached from experiments with rat liver mitochondria using a cyanine dye (Kinnally and Tedeschi, these abstracts) and studies of the unidirectional fluxes of K^+ (Diwan and Tedeschi, these abstracts). Aided by grants from the American Cancer Society Inc., BC-161 and USPHS NSO 7681. We thank J. Suchy and C. Cooper for making their studies of giant mice mitochondria available to us before publication [Exp. Cell Res. 88, 198 (1974)].

W-PM-A5 FURTHER STUDIES OF THE MITOCHONDRIAL MEMBRANE POTENTIAL UTILIZING GUANIDINE AS A PROBE ION. B.C. Pressman and J. Fields*, Department of Pharmacology, University of Miami, Miami, Florida 33152

Determination of the mitochondrial membrane potential from the equilibrium transmembrane guanidine gradients sets an upper limit of ca. -50 mV (internal) subject to correction to more positive values if part of the intramitochondrial guanidine lodges in the membrane rather than the matrix. Nigericin does not affect guanidine uptake indicating it does not accumulate via an H^+-for-guanidine exchange; DNP induces efflux of 80% of the guanidine confirming that the guanidine gradient is energy controlled. 150 mM guanidine salts of SCN^-, NO_3^- and Ac^- are as effective as NH_4Ac in inducing passive swelling of mitochondria indicating mitochondria are intrinsically permeable to the guanidinium ion and that its salts do enter the matrix. Swelling was confirmed both by light scattering decrease and a micromitocrit procedure for glutaraldehyde-fixed mitochondria which will be described. Since the diffusion potentials of the equilibrium transmembrane gradients of several cations (K^+, Mn^{++}, Ca^{++}, etc.) differ significantly from each other and exceed the upper limit established by the observed guanidine gradient, it follows that the mitochondrial membrane must contain one or more energy-linked cation pumps. These results are incompatible with the chemoiosmotic hypothesis which: (1) predicts permeant cations are accumulated passively by attaining equilibrium with the membrane potential produced by an electrogenic proton pump; (2) requires much greater proton pump-induced membrane potentials to drive the synthesis of ATP than the limits set by the guanidine gradients.

W-PM-A6 TRANSPORT OF DIVALENT CATIONS AGAINST AN ELECTROCHEMICAL GRADIENT IN MITOCHONDRIA. J.S. Puskin, T.E. Gunter, K.K. Gunter, and P.R. Russell*, Department of Radiation Biology and Biophysics, University of Rochester Medical Center, Rochester, N.Y. 14642.

Steady state concentration gradients of free Mn^{2+} were measured in energized valinomycin -treated rat liver mitochondria with EPR spectroscopy. Using values of membrane potential derived from steady state K^+ gradients measured on the same mitochondria, the electrochemical activity of Mn^{2+} was generally found to be higher in the external solution than in the matrix space. This is inconsistent with only a passive electrogenic uniport model of divalent cation transport.

The inadequacy of the uniport model is corroborated by the demonstration that Ruthenium Red or La^{3+} disturb steady state distributions of Ca^{2+} or Mn^{2+} ions without appreciably altering membrane potential. The data suggest two separate mechanisms for Ca^{2+} movements under energized conditions: (a) a passive "leak" inwards down an electrochemical gradient and (b) an outwardly-directed pump (or electrogenic antiport).

This work was supported by ERDA and has been assigned Report No. UR-3490-856.

W-PM-A7 FACTORS INFLUENCING THE TOTAL PROTON MOTIVE FORCE IN PLANT MITOCHONDRIA. A.L. Moore* and W.D. Bonner, Jr. Department of Biochemistry and Biophysics, University of Pennsylvania, Philadelphia, Pa. 19174.

The proton motive force (Δp) across the inner membrane of purified mung bean and potato mitochondria was estimated from the ΔpH as measured by ^{14}C-dimethyloxazolidine-dione distribution and from $\Delta\psi$ (the membrane potential) as measured by ^{86}Rb distribution (in the presence of valinomycin). Changes in the components of Δp were monitored continuously during coupled oxidative phosphorylation. The addition of ADP resulted in a fall of $\Delta\psi$ and ΔpH (ie.State 3) which increased steadily returning to their initial values as respiration returns to the State 4 rate. The value of Δp under these conditions was consistently lower than that obtained with rat-liver mitochondria under comparable conditions. The components of Δp during State 4 succinate supported respiration were unaffected by 0.5 - 1.0mM $CaCl_2$, confirming earlier reports from this laboratory on the lack of an active Ca^{2+} transport system in some plant mitochondria. The hydolysis of exogenous ATP failed to generate an optimal Δp in mung bean mitochondria consistent with their relative insensitivity to atractyloside. Data will also be presented on the relative contributions of the membrane potential and ΔpH in purified plant mitochondria in the presence of various electrophoretic and electroneutral translocatable species. Reference will be made as to the effect of the cyanide-resistant pathway on the components of Δp during coupled respiration.

This work was supported by grants from the National Science Foundation and the Herman Frasch Foundation.

W-PM-A8 ENERGY-LINKED SPECTRAL RESPONSES OF THE PROBE MC-V IN MEMBRANES. J. C. Smith* and B. Chance, Johnson Research Foundation, University of Pennsylvania Medical School, Philadelphia, 19104

The probe MC-V has recently been identified as bis-[3-phenyl-5-isoxazolone-(4)]-pentamethine oxonol. The anionic form of the probe appears to be the fluorescent species, the neutral form being insoluble in aqueous media (1). MC-V has been studied in ATPase vesicles, $ATP\text{-}Mg^{++}$ and EDTA submitochondrial particles (SMP) and in pigeon heart, beef heart, and rat liver mitochondria. In these preparations, and in R. rubrum chromatophores energized with light (2), a fluorescence decrease and a red shift of the 620-650 nm absorption spectrum is associated with membrane energization by succinate, ATP, or NADH. The uncoupler-sensitive, energy-linked fluorescence decrease and absorption red shift are reversed by reagents known to affect the $\Delta\Psi$ and ΔpH components of the protonmotive force. With the exception of ATPase vesicles, valinomycin alone will not reverse the energy-linked spectral changes. Nigericin or nigericin + K^+, however, appears to reverse the spectral changes caused by membrane energization in ATPase vesicles, EDTA SMP, and mitochondria. In reconstituted ATPase vesicles, EDTA or $ATP\text{-}Mg^{++}$ SMP, the addition of NH_4Cl causes an enhancement of the energy-linked MC-V spectral changes. The NH_4Cl behavior seems to be anomalous in relation to that of nigericin which collapses ΔpH. After NH_4Cl addition, valinomycin reverses the MC-V spectral responses, a change in $\Delta\Psi$. In mitochondria, NH_4Cl appears to act as a weak uncoupler. The ATP-induced fluorescence decrease in mitochondria is reversed by atractolyside and the succinate-induced decrease by nigericin. MC-V thus may be capable of measuring both $\Delta\Psi$ and ΔpH at least in the ATPase vesicle and SMP preparations. Supported by NIH GM05226, GM12202, and PMI. (1) with P. Russ and B. S. Cooperman, submitted to Biochemistry, (2) B. Chance and M. Baltscheffsky, Biomembranes, Vol. 7, p. 33.

W-PM-A9 MEMBRANE POTENTIAL OF *THERMOPLASMA ACIDOPHILA*. Jean-Cheui Hsung and A.Haug*, Department of Biophysics and ERDA Plant Research Laboratory, Michigan State University, East Lansing,Michigan 48 824.

Thermoplasma acidophila is a mycoplasma-like organism which grows optimally at 59°C and pH 2. The intracellular pH, lying between 6.4 and 6.9, independent of external pH changes, has been measured by the distribution of a radioactive weak organic acid (J.C.Hsung and A.Haug, Biochim.Biophys.Acta 389,477, 1975). The membrane potential Ψ is measured by the distribution of radioactive $KS^{14}CN$, which almost completely dissociates at pH≥2. The membrane potential is calculated from $\Psi=(RT/nF)\lg\{[SCN^-]_{in}/[SCN^-]_{out}\}$. The cells are harvested at late log phase after 26 hours of growth, washed and resuspended in 1.5 mM $(NH_4)_2SO_4$, 4.2 mM $MgSO_4$, 1.7 mM $CaCl_2$, 0.022 N KCl, 0.04 M sucrose, and 0.01 M glycine buffer, pH 2, and incubated with 0.1 μC KSCN, 60 mC specific activity, per 2 ml of cells with 20-30 mg protein/2 ml. The measured membrane potential lies between 105 and 118 mV, positive inside the cell. Increasing the external KSCN concentration to 0.01 N with cold KSCN, the membrane potential is reduced to 90 mV, and upon further increase to 0.1 N, the potential is lowered to 55 mV. The membrane potential does not change when the cells are preincubated with 10 mM NaN_3, a respiratory inhibitor. Enhancing the external pH to 3.85, the membrane potential is reduced to 80 mV, and when the external pH is changed to 6, the potential is practically diminished to values smaller than 15 mV. These results suggest that at least part of the pH gradient across the cell membrane is maintained by a passive Donnan equilibrium across the plasma membrane.

This work was supported by U.S.-ERDA Contract No. E-(11-1)-1338.

W-PM-A10 METABOLISM-DEPENDENT CHANGES OF MEMBRANE POTENTIAL IN NEUROSPORA, TRACKED WITH AN OPTICAL PROBE. Avraham Naparstek* and Clifford Slayman, Yale School of Medicine, New Haven, Conn. 06510.

Recent evidence linking biological membrane potentials to the transport of non-ionic substrates and to transfer of energy from redox processes to phosphate anhydride bonds has produced a need to determine membrane potentials in cells or organelles that are too small to be punctured with microelectrodes. Fluorescent dyes of the cyanine class have been used on cell and mitochondrial suspensions, but have the disadvantage--in work with microorganisms--of severe non-linearity at high membrane potentials (i.e., beyond -150 mV). We have therefore carried out experiments with a structurally different dye, merocyanine-I, known to give linear responses over a 200-mV range with squid nerve (J. Membr. Biol. 19:1).

Absorption measurements were made on cells harvested from 9-hour shaking cultures and resuspended in a standard buffer plus 5μM dye. Differential absorption was determined (at 570 nm, minus 525nm) with a double-beam spectrophotometer, and was calibrated with microelectrode measurements of membrane potential, made in separate experiments. The cells were depolarized in steps from the resting potential (ca. -200 mV, cytoplasm negative), by successive addition of glucose (to carbon-starved cells; PNAS 71:1935), cyanide, and azide. The maximal absorption change observed for a 200-mV depolarization was 5×10^{-4} O.D., absorption increasing at 570nm, relative to 525nm; and the response was linear over the whole range of membrane potentials. The results confirm both the feasibility of using merocyanine dyes on cell populations, and the metabolic dependence of membrane potential, which had been deduced from microelectrode measurements on single hyphae of Neurospora. Supported by Program Project Grant AM17433 from the National Institutes of Health.

W-PM-A11 COUPLING OF LIGHT-INDUCED CHEMICAL AND ELECTRICAL GRADIENTS TO GLUTAMATE TRANSPORT IN HALOBACTERIUM HALOBIUM ENVELOPE VESICLES. J. K. Lanyi and R. E. MacDonald*, NASA-Ames Research Center, Moffett Field, CA 94035 and Section of Biochemistry, Molecular and Cell Biology, Cornell University, Ithaca, NY 14850.

Illumination of H. halobium cell envelope vesicles causes the electrogenic extrusion of H^+, owing to the action of light on bacteriorhodopsin. In the presence of Na^+ (on the exterior of the vesicles), and K^+ (on the interior) light-induced transport of glutamate against large concentration gradients is observed. When high Na^+ gradients (exterior/interior $\gg$ 1) are provided transport takes place also in the dark. The light-induced uptake is inhibited by the uncoupler FCCP and by the membrane-permeant cation $TPMP^+$, while the Na^+-gradient dependent dark uptake is insensitive. Previous illumination energizes the vesicles, which then are able to take up glutamate in the dark. The time-course for the production of the energized state for transport and for its decay after illumination is inconsistent with the idea that glutamate accumulation is driven directly by the proton motive force. Rather, observed similarities between the light-induced transport and the Na^+-gradient induced transport of glutamate in these vesicles suggest that the energized state consists in both cases of a transmembrane Na^+gradient. Rapid efflux of (^{22}Na) from the envelope vesicles does indeed take place during illumination. The effects of FCCP and $TPMP^+$ on the development and decay of such Na^+ gradients suggest that under these conditions Na^+ is translocated by electrogenic antiport with another cation. The light-induced proton motive force in the H. halobium cell envelope vesicles is thus coupled to Na^+ efflux and thereby indirectly to glutamate uptake as well.

W-PM-A12 LIGHT ENERGY TRANSDUCTION IN HALOBACTERIUM HALOBIUM. R. A. Bogomolni, R. H. Lozier and W. Stoeckenius, Department of Biochemistry and Biophysics, University of California, San Francisco, CA 94143 and NASA-Ames Research Center, Moffett Field, CA 94035.

The purple membrane of H. halobium functions as a light driven proton pump, conserving light energy as electrochemical potential. The quantum efficiency of the pump in the intact bacterium is 0.7±0.2 protons per photon absorbed by bacteriorhodopsin. Action Spectra for the proton translocations are similar to the bacteriorhodopsin absorption spectrum implying lack of energy transfer from the carotenoids in distinction with the chlorophyll containing photosynthetic organisms. The light-induced changes in pH of bacterial suspensions are complex and appear to be contributed by a light driven proton efflux and influxes coupled to ATP synthesis, a passive leak and possibly transmembrane ion exchange processes. Simultaneous measurements of light-induced ATP concentration changes and pH changes of the suspensions indicate that the proton inflow as well as the ATP synthesis are triggered when a threshold value of the proton motive force and possibly a critical internal pH is attained. Preliminary measurements of the time course of the light-induced transmembrane potential changes with a lipophillic permeant cation selective electrode or by the fluorescence change of a cyanine dye show the electrogenic nature of the light driven proton pump in vivo. The potential changes closely follow the kinetics of the pH changes. Under some assumptions an estimation of the steady-state light-induced potential change is possible, and yields values around 20 to 50 mV negative inside at intermediate light levels. This small value suggests that considerable flow of other ionic species must occur and that the primary energy storage is in the form of ionic gradients. Control of respiration by light is released by uncouplers but not by permeant cations suggesting regulation of electron transport by the protonmotive force ,and possibly by the internal pH.

W-PM-A13 KINETICS AND STOICHIOMETRY OF LIGHT-INDUCED PROTON RELEASE AND UPTAKE FROM PURPLE MEMBRANE FRAGMENTS, HALOBACTERIUM HALOBIUM CELL ENVELOPE VESICLES, AND PHOSPHOLIPID VESICLES CONTAINING ORIENTED PURPLE MEMBRANE. R. H. Lozier, R. A. Bogomolni, and W. Stoeckenius, University of California, San Francisco, CA 94143 and NASA Ames Research Center, Moffett Field, CA 94035

The kinetics and stoichiometry of light-induced proton release and uptake by purple membrane fragments in aqueous suspensions has been measured spectroscopically using pH indicating dyes. Approximately one proton per bacteriorhodopsin molecule undergoing its photochemical reaction cycle appears transiently in the aqueous phase with a half-rise time of 0.4 msec and a half-decay time of ~10 msec at 21°C. A cell envelope vesicle preparation containing purple membrane preferentially oriented so as to pump protons out (same orientation as whole cells) shows a net acidification with a half-time less than 1 msec, a partial relaxation in the 10 msec time range, and a complete relaxation of the pH signal with a half-time of several seconds. Phospholipid vesicles containing purple membrane oriented preferentially so as to pump protons in show a small fast transient acidification followed by a net alkalinization in the 10 msec time range and a slow relaxation to the baseline in the several second time range. These experimnts show that purple membrane undergoes a stoichiometric light-induced proton release from the outer surface followed by a proton uptake by the cytoplasmic surface on the same time scale as the photochemical reaction cycle of bacteriorhodopsin. The partial relaxation in the 10 msec time range in the cell envelope vesicles as well as the fast transient acidification in the phospholipid vesicles is accounted for by the misoriented fraction of the purple membrane and the leakage of the indicator dye into the vesicles. The relaxation in the range of seconds is due to the passive leak of protons through the membrane.

W-PM-A14 PHOTO-INDUCED ELECTRICAL GRADIENTS WITH A PURPLE MEMBRANE PREPARATION FROM HALO BACTERIUM HALOBIUM. P.K. Shieh and L. Packer. Membrane Bioenergetics Group, Energy and Environment Division, Lawrence Berkeley Laboratory, University of California, Berkeley, Calif. 94720

Light-induced pH gradients and electrical potentials of purple membrane vesicles from H. Halobium has been reported (Renthal and Lanyi, Biochemistry, in press). Quantitative studies of this system suffer from the instability of lipid-containing vesicles and random orientation of bacterial rhodopsin. Therefore, we have sought for an in vitro system capable of providing a stable support for a purple membrane preparation (J. Lanyi, collaboration). A membrane was constructed from polyacrylamide plastic (PM) into which part of 2 μM solution of bacterial rhodopsin was incorporated. Physical-chemical characteristics of this membrane system investigated were: resistance ($10^5 \Omega \cdot cm^2$); capacitance (1.8 μF); thickness (88~190Å), and ion-selectivity (H^+). Redox electrode characteristics of this plastic membrane in an open circuit manifests a photo-emf of about 100 mv in a Fe^{3+}/PM/Eosin, NaI system where the oxidation and reduction take place on each side of the purple membrane under illumination. Photo-induced voltage generation coincides with the absorption spectrum of PMs (λ_{max}=563 nm).

The magnitude and polarity of the photo response in this system is affected by an electric field across the membrane. Maximum photo response of ~ 500 mv is observed under an applied field. This was explained in terms of a separation of charge carriers generated by light. The enhanced photo response observed under applied field conditions appeared due to the higher efficiency of charge carrier separation. These results suggest that artificial membranes impregnated with bacterial rhodopsin may be considered for the development of a fuel cell powered by solar energy. (Supported by ERDA)

W-PM-B1 EXTERIOR DETECTION OF THE RESTING POTENTIAL OF A FREE-FLOATING CELL. R.J. King*†, C.P. Bean and E. E. Uzgiris. General Electric Research and Development Center, Schenectady, N.Y. 12301.

Owing to the high impedance of the cellular plasma membrane, almost all of the drop of the resting potential appears across that membrane. A small fraction, however, does extend into the bathing solution. Using conventional continuum electrostatic theory this fraction (f) is closely given by $f = \varepsilon_{mem}\lambda_D/\varepsilon_{sol}\Delta$ where ε_{sol} and ε_{mem} are dielectric constants of the bathing solution and membrane respectively while Δ is the membrane thickness and λ_D is the Debye screening distance appropriate to the ionic concentration of the bathing solution. For normal physiological conditions of 0.15N NaCl concentration and resting potentials of say, - 80 mV, the potential at the exterior surface of the cell membrane is negative by only 0.4 mV. For dilute salt conditions, e.g., 0.005N, where the Debye distance is approximately 45 Å the corresponding potential at the outside surface is - 2.6 mV. This latter value is 10% or so of cellular zeta potentials as determined by electrophoresis in such dilute solutions made isoosmotic with sucrose.[1] The precision of laser Doppler spectroscopy[2] allows such a difference to be detected reliably when cells are exposed to chemical agents or physical treatments that destroy the transmembrane potential. We report such measurements.

†Presently at Stanford University Medical School, Palo Alto, CA. 94305.

1. E. E. Uzgiris and J. H. Kaplan, Anal. Biochem. 60, 455 (1974).
2. E. E. Uzgiris, Rev. Sc. Instrum. 45, 74 (1974).

W-PM-B2 NEW AND MORE SENSITIVE MOLECULAR PROBES OF MEMBRANE POTENTIAL: SIMULTANEOUS OPTICAL RECORDINGS FROM SEVERAL CELLS IN THE CENTRAL NERVOUS SYSTEM OF THE LEECH. B.M. Salzberg, L.B. Cohen, W.N. Ross, A.S. Waggoner and C.H. Wang.* Dept. of Physiology, Yale University, New Haven, Ct. 06510 and Dept. of Chemistry, Amherst College, Amherst, Mass.

We have continued our search for sensitive probes of membrane potential and have found four molecules which provide fluorescence or absorption changes in giant axons from Loligo pealii that are larger than those obtained (∿5:1) with Merocyanine 540. The new dyes are (with signal-to-noise ratio and the mode in which it was obtained in parentheses) a cyanine, 1,1'-di-δ-sodium-sulfobutyl-3,3,3',3'-tetramethyl-4,5,4',5'-dibenzo-indotricarbocyanine iodide (12:1 abs.); two dyes of the oxonol class, Bis-[1,3-dibutyl-barbituric acid-(5)]-pentamethinoxonol (17: 1, fluor.) and Bis-[3-carbopropoxy-1-phenyl-5-pyrazolone(4)]-pentamethinoxonol (10: 1,abs.), and, a merocyanine-rhodanine dye, 5-[(1-γ-sodium sulfopropyl-4(1H)-quinolylidene)-2-butenylidene]-3-ethylrhodanine (40: 1, abs.). All four inflict much less photodynamic damage on nerve membrane than does Merocyanine 540.

The merocyanine-rhodanine dye has been used to record simultaneously from three sensory neurons in the central nervous system of the medicinal leech, Hirudo medicinalis. One of the cells was impaled with a microelectrode, and stimulated past threshold. Absorption at 750±50 nm was monitored in all three cells at once and only from the stimulated neuron was an optical spike recorded. We expect that this technique can be employed in an expanded version of this same apparatus, where 20-30 neurons are monitored simultaneously.

We are grateful to the Polaroid Corp. and to Eastman Kodak Co., for their very generous gifts of the pyrazolone oxonol and cyanine dyes, respectively. Supported in part by USPHS grants NS-08437 and NS-10489 and NIH Fellowship 1 F22-NS-00927.

W-PM-B3 INTRACELLULAR Ca^{2+} DEPRESSES NET LATE OUTWARD CURRENT IN SNAIL NEURONS. H.D. Lux*, R. Eckert, G. Hofmeier*, and C. Heyer*, Max Planck Institute for Psychiatry, Munich 40, Germany.

Voltage clamp experiments were performed on soma membranes of bursting pacemaker neurons of H. pomatia with holding potentials (V_h) of about -50mV. In one series intracellular Ca^{2+} was increased by 10^{-6} to 10^{-3}M by injection of known quantities of $CaCl_2$ (or $CaCl_2$ + EGTA). As a result of injection the slope of the late I-V plot was depressed significantly, the slope conductance between -10 and +30 mV (absolute) dropping by as much as 50%. With injections of pure $CaCl_2$ the effect was fully reversible within minutes. In another series a 300msec test pulse (V_2) fixed at +10 mV (absolute) was applied 1 sec after a conditioning depolarization (V_1). V_1 was applied to allow Ca^{2+} to enter the cell through the slow Ca system (Eckert and Lux, 1975, Brain Research 83, 486). As V_1 was increased from V_h to about zero mV the net outward current (I_2) during V_2 exhibited a graded decline to a minimum of 60% to 80% of the control intensity of I_2 seen without the V_1 conditioning pulse. The depressing action of V_1 on I_2 decayed with a time course of many seconds. With further rise in V_1, I_2 gradually increased, and with V_1 approaching +150 mV, I_2 returned to 95% of the intensity seen in the absence of V_1. Failure of V_1 to suppress I_2 coincided with potentials in the region of the "N"-shaped drop in I_1 described by Meech and Standen (1975, J. Physiol. 249, 211). These findings suggest that a rise in $[Ca]_{in}$ either facilitates a late inward current (Lux and Eckert, 1974, Nature 250, 574) or depresses a component of the late K conductance.

W-PM-B4 VOLTAGE DEPENDENCE OF BOTH CONDUCTANCE AND ABSOLUTE PERMEABILITY IN THE ABSENCE OF CONSTANT FIELD IN A CHOLINERGIC K^+ CHANNEL. T.L. Schwartz and R.T. Kado, Biological Sciences Group, University of Connecticut, Storrs, Ct. 06268, and Laboratoire de Neurobiologie Cellulaire, C.N.R.S., 91190 Gif-sur-Yvette, France.

Medial cells in the isolated pleural ganglia of Aplysia californica were voltage-clamped in both the absence and presence of carbachol. Drug was applied iontophoretically in a manner that excited only a K^+ selective, somatic, channel. Channel conductance was dependent on both potential and external potassium concentration. A constant-field permeability coefficient could not account quantitatively for this voltage dependence. Absolute permeability, defined with no assumptions regarding the electrical field in the membrane and corrected for phase-boundary potentials, was determined. It was both voltage and concentration dependent, and accounted well for the conductance-voltage relationships. The voltage dependence of the permeability was more severe in low than in high K^+. In 5mM K^+ it increased by a factor of 2.6 when the membrane was hyperpolarized from -30 to -120mV, while in 20mM K^+ it increased by only a factor of 1.7. Permeability became concentration independent at approximately -65mV. Assuming, for purposes of comparison, that one third of the available sites were activated, a permeability of $2(10)^{-6}$cm/sec existed at this voltage. Permeability voltage dependence seemed consistent with concentration profile shifts due to simple electrodiffusion. (Supported in part by grants to T.L. Schwartz from NIH(NS08444), EMBO, and the University of Connecticut Research Foundation, and grants to both authors from the DGRST, France.)

W-PM-B5 INWARD RECTIFICATION IN APLYSIA GIANT NEURONS. D.C. Eaton and M.S. Brodwick*, Department of Physiology and Biophysics, University of Texas Medical Branch, Galveston, Texas 77550.

The inward or "anomalously" rectifying conductance mechanism of Aplysia giant neurons was examined. In these neurons, at temperatures above 15°C, there is a marked non-linearity of the I-V relationship obtained from hyperpolarizing potential steps. The increased inward current can be almost totally blocked by the reduction of the bath temperature to less than 5°C. At these temperatures the I-V relationship is relatively linear. The inward rectification can also be significantly reduced by application of Rb^+ and Cs. Application of a solution containing Cs^+ may reduce conductance at large negative potentials (~ 100) to 10% of its value in a similar solution containing K^+. The conductance sequence is K>Rb>Cs. High concentrations of procaine (30 mM) and TEA^+ (200 mM) applied externally have little or no effect on the inward rectifier although they effectively block the outward rectifier associated with depolarizing potentials. In addition to the inward rectifying conductance, an additional conductance pathway has been observed at large negative potentials (> -140 mV). The conductance is very large and is not affected by application of Cs^+, Rb^+, TEA^+ or procaine. However, it may be partially reduced by application of solutions containing 20 mM Co^{++}. This conductance increase did not appear immediately after the test potential step, but gradually developed until it reached a steady state value approximately 100 msec after the onset of the command step.

W-PM-B6 SODIUM CURRENT INACTIVATION IN CRUSTACEAN AXONS. J.A. Connor, Department of Physiology & Biophysics, University of Illinois, Urbana, Ill. 61801 and University of Washington Friday Harbor Laboratory, Friday Harbor, Washington 98250

Inactivation characteristics of the sodium conductance system were investigated by means of voltage clamp in walking leg axons of the crab, Cancer magister. These axons are of small diameter, ca. 70 to 100 u, but display a range of physiological response among different identifiable fibers which makes analysis of the various conductance systems potentially very useful. A particular difference exploited has been between those fibers which fire repetitively in response to a maintained current stimulus and those which fire only once or twice. In repetitive axons the steady-state inactivation parameter, h_∞, (Hodgkin & Huxley, J. Physiol., 116, 497, 1952) does not depend on test voltage to a significant extent whereas in non-repetitive axons it does, shifting to the right as test voltage is made more positive (Goldman & Scheuf, J. Gen. Physiol., 59, 1972). Inactivation time course is different depending upon which of 3 measurement techniques is used: direct measure of Na current decay, τ_h; peak current amplitude as a function of conditioning pulse duration, τ_C; and reactivation following complete inactivation, τ_R. The decay time course of Na current is not well fit by a simple exponential at small depolarizations but for least squares fit of data, $\tau_R > \tau_C \geq \tau_h$. The τ_C and τ_h curves converge for large depolarizations. Quantification of the time constant differences is hindered by series resistance effects even though feedback compensation was used in these experiments. The findings suggest that a more general description of Na conductance kinetics than the Hodgkin-Huxley formulation may be in order.

Supported by NSF grant GB39946

W-PM-B7 OBSERVATIONS ON SODIUM CHANNEL INACTIVATION IN FROG NERVE. S.Y. Chiu* (Intr. by B. Hille), Dept. Physiol. & Biophys., Univ. Wash. Sch. Med., Seattle, Washington 98195

Kinetics of inactivation of Na channels in myelinated nerve were studied at 4° C under voltage clamp in the presence of TEA. In one type of experiment Na channels were first inactivated by a large maintained depolarization of 50 msec duration. The membrane was then allowed to recover for various times at different voltages; the extent of recovery was assayed by a test pulse. The time course of recovery is not exponential and shows an initial delay (Schauf, Biophys. J. 14:151, 1974) which depends on recovery voltages. In a second series of experiments, development of inactivation was measured from I_{Na} decaying under a maintained depolarization, and it exhibited two time constants. Their ratio for a given depolarization remains virtually unchanged when 75% of the external Na is replaced by the impermeant TMA-Cl, demonstrating that the two time constants do not result from 'series resistance' errors. Over a voltage range from (rest) -80 to -20 mV, the time constants of the development of inactivation determined by multiple pulse methods agreed with those determined from I_{Na} decays. The steady-state $h_\infty(V)$ curves are asymmetrical. These observations are quantitatively consistent with a three-state inactivation system: $0 \underset{\alpha_{10}}{\overset{\alpha_{01}}{\rightleftharpoons}} 1 \underset{\alpha_{21}}{\overset{\alpha_{12}}{\rightleftharpoons}} 2$ (open, closed, closed) with associated rate constants of the forms: $\alpha_{ij} = e^{A_{ij}V+B_{ij}}$ (A and B are constants, V voltage). Kinetics of the type $(1 - e^{-t/\tau_h})^n$ are inadequate in describing the observed delays in development of inactivation. This research is supported by the USPHS National Institutes of Health grant no. NS08174.

W-PM-B8 SODIUM INACTIVATION AND REACTIVATION DO NOT OCCUR BY IDENTICAL MECHANISMS IN THE MYXICOLA GIANT AXON. C. L. Schauf and T. L. Pencek. Departments of Neurological Sciences and Physiology, Rush Medical College, Chicago, Illinois, 60612.

In both Myxicola and lobster axons inactivation time constants determined from the decay in sodium current during a maintained depolarization (τ_h^s) are substantially smaller than the inactivation time constants determined at the same membrane potential using conditioning prepulses of variable duration (τ_h^p). This comparison, limited to depolarized potentials, suggests that the processes being examined when open channels inactivate are not identical to those occuring during depolarizing prepulses. In the present study we have determined values for the time constant of reactivation of the G_{Na} following depolarizations sufficient for complete inactivation (τ_h^{re}), and have compared them with the values of τ_h^p obtained using depolarizing prepulses. Over the 20mv range of data overlap, τ_h^{re} values were uniformly 30-50% larger than the values of τ_h^p determined simultaneously at the same potential in the same axon. The data suggest that inactivation and reactivation also do not occur by identical mechanisms, and further imply that, at least in Myxicola, there are three distinct experimental procedures necessary to fully characterize the sodium inactivation process. Since these results might be accounted for by the presence of a second inactivated state, studies were begun along these lines. Unlike squid, a second (slow) inactivation process cannot be resolved in Myxicola except with $[K^+]_o \geq$ 20mM, and even here there are only small reductions in the maximum I_{Na} following large 100ms hyperpolarizations. The major effect of high $[K^+]_o$ is a significant reduction in the slope of the $h_\infty(V)$ relation, which can be shown to be due largely to changes in holding potential alone, and thus only indirectly to high $[K^+]_o$. Rate constants for this process are approximately an order of magnitude slower than for fast Na^+ inactivation.(Supported by NIH RCDA 1-K04-NS-00004-01 and NMSS Grant 921-A-1)

W-PM-B9 CURRENT FLUCTUATIONS IN STROPHANTHIDIN-TREATED CARDIAC PURKINJE FIBERS. R.S. KASS*, W.J. LEDERER and R.W. TSIEN, Department of Physiology, Yale School of Medicine, New Haven, Connecticut 06510.

In voltage-clamped cardiac Purkinje fibers, strophanthidin produces a novel transient inward current (TI) which underlies increased diastolic depolarization. Membrane current fluctuations accompany the TI, and generate voltage "noise" in unclamped preparations. Intracellular potential remains synchronous over many cell lengths, indicating that the drug-induced noise is not due to intercellular uncoupling. The current fluctuations were studied with a simple shot noise approach which yielded a lower limit of 0.1 nA for the elementary event. This value is several orders of magnitude too large to be accounted for by a transient drug blockade of single pump sites turning over at 100 sec^{-1}. The autocovariance function of the current fluctuations showed a marked periodicity of 1-2 sec near -70 mV and 36°C. Spectral analysis confirmed the dominant low frequency character of the fluctuations and showed a shift toward higher frequencies with depolarization (left) and a shift toward lower frequencies with cooling. The spectral results suggested that the fluctuations and TI may share a common basis.

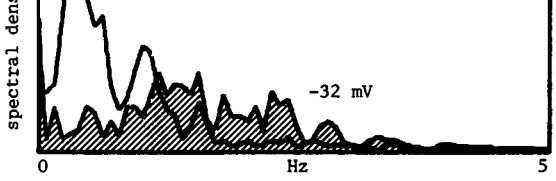

W-PM-B10 NON FIRST-ORDER K^+ CONDUCTION IMPEDANCE AND NOISE FEATURE IN SQUID AXON MEMBRANE. H.M. Fishman, L.E. Moore, D.J.M. Poussart* and E. Siebenga*. University of Texas, Galveston, Texas; Case Western Reserve University, Cleveland, Ohio; Laval University, Quebec.

The observation of sharp corners in power spectra of K^+ current noise, in small patches of squid axon membrane, suggests that the small-signal impedance $Z(j\omega)$ of the K^+ conduction process contains an additional RLC branch in parallel with the usual RL component (Fishman, Moore and Poussart, 1975, J. Mem. Biol., 23). The complex impedance was measured on axons with and without internal perfusion (.5M KF) using an axial-wire technique. The figure shows a low-frequency (1-30 Hz) impedance feature in both magnitude $|Z|$ and phase ϕ which differs significantly in form from that predicted by the HH formalism. The negative ϕ and "dip" in $|Z|$ at low frequencies are consistent with an additional RLC branch and are dependent on membrane potential, temperature, and $[K^+_i]$. This feature is most pronounced at hyperpolarized potentials of 5 to 10 mV but disappears for depolarizations of > 5 mV and hyperpolarizations of > 20 mV and after internal perfusion with 50mM KF + 50mM CsF. This impedance property cannot be attributed either to active transport, since it is observed during internal perfusion with 0.5M KF, or to K^+ accumulation in the Schwann cell space because 1) the potential dependence is contrary to K^+ accumulation outside and 2) the impedance function for K^+ accumulation does not produce low-frequency negative ϕ. These results are compatible with sharp corners observed in K^+ conduction noise spectra and together they suggest that K^+ conduction kinetics are not first order.

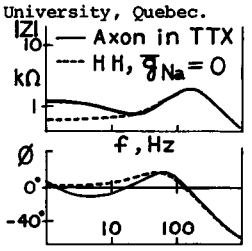

Aided by NS-11764 (HMF), NS-08409 (LEM) and A5274 (DJMP).

W-PM-B11 A NEW ANALYSIS FOR MEMBRANE NOISE: THE INTEGRAL SPECTRUM. Louis J. DeFelice and Barry A. Sokol*, Department of Anatomy, Emory University, Atlanta, GA. 30322

A new method of random data analysis has been developed as an alternative to conventional power spectral densities, with special implications for membrane noise. The integral spectrum $I(\ell)$ is related to the spectral density $S(f)$ by:

$$I(\ell) = \int_0^\infty S(f)\ |L(f,\ell)|^2\, df \qquad 1$$

where:

$$L(f,\ell) = (if/\ell)/(1 + if/\ell)^2 \qquad 2$$

is a simple broadband filter centered around a peak frequency ℓ. The spectral density:

$$S(f) = a + b/f + c/[1 + (f/f_0)^2] \qquad 3$$

transforms to:

$$I(\ell) = \pi a\ell/4 + b/2 + (\pi c\ell/4)/(1 + \ell/f_0)^2 \qquad 4$$

The third term has a maximum value at $\ell = f_0$, and is symmetric about f_0 on an $I(\ell)$ - log ℓ plot. 1/f-noise is flat and does not distort the symmetry. A plot of $fS(f)$ versus log f has similar graphical properties to $I(\ell)$, but does not share its improved statistical error. For sample time T, the normalized mean square errors of the three terms in (4) are, respectively, $1/2\pi\ell T$, $2.47/2\pi\ell T$ and $\#/2\pi\ell T$, where # equals 1 for $\ell << f_0$, 3 for $\ell = f_0$ and 5 for $\ell >> f_0$. These compare favorably with spectral density estimates from the same sample time. The new method may be useful in comparing membrane noise data with theoretical expressions.

Supported in part by NIH: LM 02505 and NS 05669.

W-PM-B12 EPHAPTIC TRANSMISSION IN SQUID GIANT AXONS. F.Ramón, R.Joyner* and J.W.Moore, Department of Physiology and Pharmacology, Duke University Med. Ctr., Durham, N.C. 27710

Ephaptic effects (Arvanitaki, 1942) are those electrical effects produced by cell activity on closely apposed neighboring cells that are not coupled by specialized anatomical structures such as gap-junctions.

Two closely apposed squid giant axons were used to determine their coupling ratio for square current pulses as well as the possibility of ephaptic transmission. Experimental results include the following:

condition	ephaptic transmission	coupling ratio
ASW	no	0.03
cool (13 °C)-ASW	no	-
ASW + 4-aminopyridine	no	-
low Ca^{++} (10 mM)-ASW	yes	0.05
ephaptic region in mineral oil	yes	0.7-0.8

While in low Ca-ASW there was ephaptic transmission, there were also scattered spontaneous action potentials at different regions of both axons. All these results depend upon the ratio of the diameters of the axons, the distance between them and the length of the ephaptic region. A digital computer model (based on the core conductor representation of the axon and the HH-model) produces results similar to those obtained experimentally under comparable conditions.

These results suggest that ephaptic transmission is a possible physiological mechanism for electrical coupling between excitable cells when the external medium resistance, in the region of membrane apposition, is high.

Supported by an M.B.L. Fellowship and NIH Grant # NS03437

W-PM-B13 SODIUM EFFLUX FROM SQUID AXONS INTO LOW SODIUM SOLUTIONS. D. Landowne, Dept. of Physiology & Biophysics, Univ. of Miami, Fla. 33152.

Squid axons were loaded with ^{22}Na by microinjection and then mounted in a chamber which allowed measurement of voltage clamp currents and Na efflux from a central, guarded region of the axon. Both the resting efflux, in the presence of ouabain, and the extra efflux associated with a few thousand voltage clamp pulses were measured. The extra efflux at 22° was about 5×10^{-6} impulse^{-1} and increased linearly with the size of the depolarization, doubling in roughly 15 mV. The extra efflux was blocked by tetrodotoxin.

When sodium in the external bathing media was replaced with either Tris, dextrose, mannitol or lithium the extra efflux of sodium during the same size voltage clamp pulse was reduced 54 ± 5% (S.E., n=22) at room temperature. This is in contradiction with the 'independence principle' which has classically been used to predict the fluxes of sodium from measurements of the net current. The independence principle predicts that the efflux of sodium should be independent of the amount of sodium outside the axon. The observed decrease in sodium efflux suggests there is extensive sodium-sodium exchange during the pulse and also during the nerve impulse.

In four experiments the effect of low sodium solutions was measured at room temperature and at 8-9°C. The reduction of efflux was smaller when the axons were cold ($p<0.025$), the value measured in the cold was a 22 ± 22% reduction. Possibly this could explain the observed low temperature dependence of sodium fluxes associated with action potentials.

Supported by National Science Foundation grant BMS 73-06754 A01.

W-PM-B14 BLOCK OF SODIUM CHANNELS BY EXTERNAL CALCIUM IONS. R.E. Taylor, C.M. Armstrong, and F. Bezanilla, NINCDS, Natl Institutes of Health, Bethesda, Md. 20014, Univ. of Penn., Phila., Pa., Univ. of Chile, Santiago, Chile and Marine Biological Lab., Woods Hole, Mass.

The interaction of external calcium ions with sodium channels was examined using voltage clamped squid axons at 2°C perfused internally with approximately 200 mM K^+, 50 mM Na^+, 25 mM TEA^+, with F^- and glutamate$^-$ as the chief internal anions, and bathed externally with (usually) 10 to 120 mM $CaCl_2$, 350 mM NaCl and sucrose. The "instantaneous" I_{Na}-V curve was determined by activating the sodium channels with a depolarizing pulse, changing V to the desired level and measuring I_{Na} immediately after the change. With 10 mM Ca^{++} outside the I_{Na}-V relation, going from right (+80 mV) to left (-100mV), curves down continuously: the slope conductance is greater at -100 mV than at +60 mV by a factor of about 1.6. With 120 mM Ca^{++} outside the I_{Na}-V curve superimposes on the 10 mM Ca^{++} curve for voltages above +20 mV but inward currents are much reduced. At -80 mV, for example, I_{Na} in high Ca^{++} is approximately one-third that in 10 Ca^{++}. Mg^{++} and Zn^{++} have similar effects. The data can be fitted by a model which assumes that a calcium ion temporarily occludes the channel when it occupies a site about half way through the membrane field (Woodhull, J. Gen. Physiol. 61 687 (1973) and that calcium passes through the channel about as readily as it enters. Experiments of another type gave a P_{Na}/P_{Ca} ratio of 50 to 100 (Meves and Vogel, J. Physiol. 235:225 (1973)). Calcium is known to shift the g_{Na}-V curve; a larger depolarization is required to achieve a given level of g_{Na} in high calcium. Only a small part of this shift can be explained by the interaction described here. In normal ionic conditions the I_{Na}-V relation can be approximated by a straight line only because of interference by the calcium and magnesium with the inward currents. (CMA and FB supported by USPHS Grant NS 08951).

W-PM-B15 A SLOW GATING CURRENT COMPONENT DURING RECOVERY FROM INACTIVATION. C.M. Armstrong and F. Bezanilla. Dept. Physiology, University of Pennsylvania, Philadelphia, Pa. 19174

Opening of the sodium pores in squid axon membrane is preceded by a small outward gating current (Ig), that is the result of the molecular rearrangements that open the channels. No component of Ig yet reported has kinetics similar to inactivation of I_{Na} (sodium current). As a result of inactivation, however, a portion of gating charge (Qg) is temporarily immobilized: on return to -70mV after a long depolarization, 'off' Qg is only 1/3 of 'on' Qg at the beginning of the depolarization. Under these conditions recovery from inactivation has a half time of about 3 ms(8°C), and we postulate that the immobilized part of Qg returns to 'off' position with a similar time course, generating a current too small to detect. At -150mV recovery from inactivation has a half time of about 0.5ms. We see a slow component of 'off' Ig with similar time course after a long depolarization (-150mV→+20V, 10ms→-150mV). Under these conditions the ratio of 'off' to 'on' Qg is near one regardless of pulse duration. The slow component at -150mV is absent after pulses too short for inactivation to occur, or in axon with most of inactivation destroyed by pronase. We interpret this to mean that at -150mV the immobilized fraction of Qg (none of which moves during the 'on' transient with kinetics similar to inactivation) is freed rapidly by recovery from inactivation, and generates an easily detectable current, the slow component, as it returns to 'off' position. Our evidence indicates that charge movement associated directly with the inactivation step is small or absent.

W-PM-C1 AMMONIA DERIVATIVES AS PROBES OF THE "K CHANNEL" OF ATP-ase. Edward S. Hyman, Touro Research Institute, New Orleans, La. 70115

Hydrolysis of the high energy acyl-phosphate intermediate of Na-K ATP-ase is known to be dependent on K+ or a slightly larger monovalent cation such as Rb+, Cs+, or NH_4+. I find that Tl+ also substitutes, although it differs chemically. Hydroxylamine, used to tag the enzyme's acyl site, is known to exert a K+ effect on the intact enzyme, perhaps due to NH_4+ formed. Mono, di, and tetraalkyl amines were studied as substitutes for K+ (or NH_4+), and for their effects in the presence of 0.01M K+, using rabbit kidney microsome ATP-ase (Jorgensen, B.B.A., 365, 36, 1974) in an imidazole buffer with Na+ and Mg++. With the borderline exception of methylamine at 0.1M no stable alkylamine substituted for K+. In the presence of 0.01M K+, inhibition of Pi formation appeared to parallel lipid solubility. Methylamine does not inhibit until 1.0M, and then fully. At 0.01M monoalkylamines inhibit partially at C6 and C7, and fully at C8 or larger. Diethylamine was inert but dibutylamine inhibited slightly. Choline, $C_2(C_1)_3N$, and $(C_4)_4N$ were inert but $(C_7)_4N$ and $(C_{16})(C_2)(C_1)_2N$ inhibited fully. Hydrazine at 0.01M was inert. These observations are compatible with the belief that hydroxylamine, about equal in size to methylamine, has little access to the acyl site in the natural enzyme, but at higher concentrations has a non-specific inhibitory effect like the alkylamines. If it can be assumed that an asymmetrical mono-alkylamine would act like NH_4+ should it reach the acyl site, then access to that site must be limited to cations with bare radii no smaller than K+ but hardly any larger than Cs+. A pore in a phospholipid barrier would serve as a model for this limited access, and the assembly would serve as a model of a K+ selective membrane mechanism. NIH AM 12718

W-PM-C2 MODELLING DRUG (OUABAIN) DISSOCIATION FROM WHOLE CELLS. J.S. Cook, E. T. Brake,* and P. C. Will.*,[1] Carcinogenesis Program, Biology Division, Oak Ridge National Laboratory and University of Tennessee-Oak Ridge Graduate School of Biomedical Sciences, Oak Ridge, Tennessee 37830

^{3}H-Ouabain bound to growing HeLa cells is released slowly (days) from the cells in a non-exponential manner that implies heterogeneity of the dissociation processes. Using a program (CRICF) developed by J. P. Chandler, D. E. Hill, and H. O. Spivey (Comp. Biomed. Res. 5, 515, 1972) to estimate optimum parameters of coupled differential equations, specifically including stiff conditions, we have modelled ouabain dissociation as the sum of 3 first-order processes: 1) simple dissociation from a membrane binding site into the medium; 2) internalization of the binding site, together with bound ouabain, as a part of membrane turnover; 3) externalization of the internalized drug. Processes 1) and 2) lead to physiological recovery; processes 1) and 3) to loss of drug from the cell. Given the total-cell dissociation data, CRICF computes rate constants for these processes, compartment sizes, and statistical evaluations of the fit. Computed results based on this intact-cell analysis compare closely to data obtained from the more disruptive experimental procedures of cell fractionation and turnover inhibition. (Research jointly supported by the National Cancer Institute and the U. S. Energy Research and Development Administration under contract with the Union Carbide Corporation.)

[1]Postdoctoral Investigator supported by subcontract #3322 from the Biology Division of ORNL to the University of Tennessee.

W-PM-C3 EFFECT OF SANGUINARINE UPON SODIUM EFFLUX FROM FROG SKELETAL MUSCLE. S.Y. Chan and R.D. Moore. Biophysics Laboratory, State University of New York, Plattsburgh, 02901.

Sanguinarine (2×10^{-5}M) increased the rate of ^{22}Na efflux from Na-loaded Rana pipiens sartorius muscle into 104 Na^+ - 10 K^+ Ringer in four of five experiments ranging from 0-28% (average increase, 20%). 2×10^{-5} M Sanguinarine also increased ^{22}Na efflux into 114 Na^+-0 K^+ in each of six experiments by 30 - 103 % (average increase, 81%). The increase in ^{22}Na efflux into 114 Na^+ - 0 K^+ Ringer produced by Sanguinarine was significantly greater ($p<0.005$) than the increase in ^{22}Na efflux into 104 Na^+ - 10 K^+ Ringer. Flame photometry showed the average intracellular Na^+ content, Na^+_i, of 9 sanguinarine-treated muscles effluxed into 104 Na^+ - 10 K^+ Ringer was 27% lower than that of the paired controls ($p<0.05$) while the average Na^+_i of 11 sanguinarine-treated muscles effluxed into 114 Na^+ - 0 K^+ Ringer was 30.2% lower than the controls ($p<0.05$). This indicates that the effect of sanguinarine was to increase net Na^+ efflux. The average percent loss of Na^+_i in muscles effluxed into 104 Na^+ - 10 K^+ was not significantly different ($p>0.1$) from the average percent loss in muscles effluxed into 114 Na^+ - 0 K^+. Addition of 10^{-3}M ouabain in either 114 Na^+ - 0 K^+, or in Na^+ and K^+-free Ringer did not block the increase in ^{22}Na efflux produced by sanguinarine.

When tested upon (Na^+ + K^+)-ATPase isolated from frog sartorius. this same concentration of sanguinarine produced an inhibition of the ATPase activity which was identical in magnitude of that produced by 10^{-3}M ouabain.

The effect of sanguinarine upon Na efflux from intact muscle might be explained if the compound, which is a cation, were a potent substitute for K^+ on the outer surface of the membrane. However, its opposite action upon the isolated (Na^+ + K^+)-ATPase, as compared to its effect upon the in vivo Na pump remains an unexplained paradox.

W-PM-C4 BEHAVIOR OF THE NET HYDROGEN ION EFFLUX FROM SINGLE MUSCLE FIBRES UNDER VARIOUS STEADY STATE CONDITIONS. M.R. Menard*, J.A. Hinke, Dept. of Anatomy, University of British Columbia, Vancouver, Canada, V6T 1W5

Intact single muscle fibres from the giant barnacle were incubated for two to five hours in normal barnacle Ringer's solution, or in Ringer's solution augmented by the addition of CO_2 plus $NaHCO_3$, or the addition of $(NH_4)_2SO_4$. The intracellular pH of identically prepared single fibres was measured in parallel experiments with a pH-selective glass microelectrode and with 5,5-dimethyloxazolidine-2,4-dione (DMO). The trans-membrane difference in pH in the steady state was found to depend of the membrane potential. This dependence was not in accordance with the predictions of the Nernst-Planck equation, but agreed with a model which assumes that the hydrogen ion flux is composed of the diffusive flux and an additional non-diffusive flux equivalent to a net efflux of hydrogen ions. The magnitude of the additional flux varied from ca. 10^{-12} moles/cm^{2}sec at an intracellular pH of 6.2 to ca. 10^{-14} moles/cm^{2}sec at an intracellular pH of 7.8.

W-PM-C5 INTRACELLULAR SODIUM ACTIVITY AND SODIUM EFFLUX IN THE FROG SARTORIUS. J. F. White and J. A. M. Hinke, Dept. Physiology, Emory Univ., Atlanta, Ga. 30322, and Dept. Anatomy, Univ. British Columbia, Vancouver, B. C.

Sodium sensitive glass microelectrodes of the recessed design (R. C. Thomas, J. Physiol. 220:55, 1972) with tip diameters of 1 μm were used to measure intracellular sodium activity (a_{Na}) of isolated frog sartorii. Simultaneous measurement of cellular sodium (C_{Na}) with inulin revealed a_{Na}/C_{Na} = 0.50±0.07 (S.E.) indicating that a portion of fiber sodium is bound or compartmentalized. Myoplasmic sodium activity declined from 9.7 to 2.8 mM in 40 minutes when sodium was completely replaced with Tris or lithium. A threshold exists (2-3 mM) beyond which the activity does not decline. The decline was slowed in the presence of ouabain (10^{-4}M) and appeared to be independent of extracellular calcium and to occur in the presence of sodium concentrations which eliminate passive net diffusion. Elevation of bath potassium to 5 mM was without effect on a_{Na}. Addition of ouabain or removal of bath potassium elevated a_{Na}; reintroduction of potassium halted and in some cases reversed the increase in a_{Na}. The decline of total sodium from whole muscles determined by Na^{22} washout into Na-free media was also measured. This allowed comparisons with the ion-selective microelectrode findings. Kinetic models for sodium efflux were tested and will be discussed. (Supported by MRC 1039 and USPHS postdoctoral fellowship #F02-AM37532).

W-PM-C6 THE EFFECT OF AZIDE ON THE Na AND K PUMPS IN STRIATED MUSCLE. R.A. Sjodin and L.A. Beaugé, Department of Biophysics, University of Maryland School of Medicine, Baltimore, Md. 21201

Application of 5 mM azide to Na-enriched frog sartorius muscles resulted in a slowly increasing Na efflux with K absent from the external medium. The Na efflux reached a peak value of about 2 times the control value in from 60 to 90 min. in the presence of azide. The increased Na efflux could be abolished either by reducing $[Na]_o$ to 5 mM or by applying 10^{-4}M ouabain. When $[K]_o$ was added to the medium at or near the peak value of Na efflux in the presence of azide, a further increase in Na efflux occurred. At or near the peak value of Na efflux occurring in the presence of azide, ^{42}K influx was measured with $[K]_o$=5 mM both in the presence and absence of ouabain. Potassium influx was about 50% less in azide-treated muscles than in control muscles. The reduction in K influx was largely in the ouabain-sensitive K influx which was reduced to very low values. Reducing $[Na]_o$ to 5 mM increased by several-fold the ouabain-sensitive K influx occurring in the presence of azide. These results, and other experiments on net Na extrusion rates, suggest that azide alters the sensitivity of the Na pump to $[Na]_o$ and $[K]_o$ rendering it relatively Na sensitive. Activation by $[K]_o$ still occurs but probably at reduced capacity. Translocation of K via an inward K pump, however, is markedly reduced by azide indicating that the Na:K coupling ratio has been elevated by azide.

W-PM-C7 STROPHANTHIDIN-SENSITIVE SODIUM FLUXES IN DNFB-TREATED SKELETAL MUSCLE. B.G. Kennedy* and P. De Weer, Department of Physiology and Biophysics, Washington University School of Medicine, St. Louis, Missouri 63110.

Unidirectional fluxes of sodium-22 were measured in Rana pipiens sartorius muscles whose internal sodium levels had been elevated by storage in the cold. We studied the effect of the amino group reagent 2,4-dinitrofluorobenzene (DNFB), which Infante and Davies (J. Biol. Chem. 240: 3996, 1965) have shown to inhibit respiration and creatine phosphotransferase in this preparation. In 120 mM Na, 2.5 mM K Ringer's solution, a 30 minute exposure to 0.38 mM DNFB produced a transient increase in the rate constant for Na efflux, to approximately 1.5 x baseline level. This stimulation was blocked by 0.1 mM strophanthidin. A 2.5 fold increase in the rate constant for sodium-22 efflux was similarly observed in potassium-free Ringer's solution. In sodium free, Li substituted Ringer's solution, the DNFB effect on sodium-22 efflux was virtually abolished. Unidirectional sodium influx was also stimulated by DNFB. After a 30 minute pre-treatment, influx was approximately doubled compared to paired control muscles. This stimulation of influx by DNFB was again abolished by strophanthidin. Measurements of membrane potential and of strophanthidin-insensitive fluxes under similar conditions indicate little effect on these parameters during the period of study. Our observations are compatible with the hypothesis that metabolic effects, resulting from DNFB treatment, stimulate a strophanthidin sensitive Na-Na exchange across the cell membrane of frog skeletal muscle.

Supported by funds from the Muscular Dystrophy Association.

W-PM-C8 A TTX BINDING PROTEIN FROM FROG HEART CELL MEMBRANE. Donald D. Doyle*, Peter R. Brink*, and Lloyd Barr, Dept. of Physiology and Biophysics, University of Illinois, Urbana, IL 61801

The amount of TTX bound to a vesicular plasma membrane preparation was measured. These vesicles were purified using sucrose density gradient centrifugation (Barr et al., BBA 345, 336(1974)).

The vesicles were brought to equilibrium with a bath of known original TTX concentration. The equilibrium concentration of TTX was measured by bioassay after centrifugation of the vesicles and the amount bound was calculated from the difference in concentrations. The bioassay which allowed measurement of 2 pica moles was based on the relationship between the conduction velocity of the action potential of the median giant axon of the earthworm and the concentration of TTX in the bathing medium. The frog heart cell membrane was found to contain 16 to 60 moles of high affinity TTX binding sites/mg protein. This is equivalent to approximately 60 to 240 TTX sites/micrometer^2 of vesicular membrane. We found the dissociation constant to be approximately 8 x 10^{-9}M.

A fraction of membrane protein solubilized by 72 hour exposure to a 5 mM EDTA solution was found to include a TTX binding component by equilibrium dialysis. After electrophoresis of the EDTA solubilized fraction on 5% acrylamide gel in 5 mM Tris glycine buffer at pH 8.5 and 40 volts/cm for 1 hour, one of some twenty Coomasie blue staining bands showed appreciable binding of ^{3}H TTX. The gels were soaked in buffered ^{3}H TTX solution, sliced into 2 mm sections, dissolved in peroxide and counted in a xylene-Triton X-100 scintillation cocktail.

W-PM-C9 TRANSPORT OF CHLORIDE ION IN THE MICROCIRCULATION OF THE ISOLATED AND PERFUSED FELINE HEARTS. S.H. Song, and B.S. Kim*, Dept. of Biophysics, Faculty of Medicine, Univ. of Western Ontario, London, Ontario, Canada.

In the coronary circuit of isolated feline hearts, a 3-compartmental model for RBC and another 2-compartmental model for plasma were previously proposed from results of washout studies. Because of the marked differences in washout characteristics between RBC and plasma, we attempted to study the washout kinetics of Cl^- from the coronary vessels. Using a constant flow pump (10 ml/min) coronary vessels of isolated hearts from 26 healthy cats were perfused with Ringer-Locke solution (145 mEq/L of Cl^-) for 10 min. Then [Cl^-] in the venous outflow were measured by means of a chloride titrator (Radiometer, CMT-10) while perfusing the heart with Acetate-Ringer solution. Epicardial EKG and infusion pressures were simultaneously recorded to ensure the viability of the coronary smooth muscles and the heart. [Cl^-] decreased abruptly for the first two min. period of washout from 100 to 20%, and after five minutes (50 ml perfusion) the concentration decreased very slowly from 10 to 0%. Therefore, we concluded that the washout kinetics can be resolved into a sum of two compartments. However, the fast compartment of Cl^- can be regarded as the usual vascular pathway while the slow compartment may be due to exchange of Cl^- between the microcirculation and intracellular space.

(S.H. Song is a Senior Research Fellow of the Ontario Heart Foundation. Supported by Ontario Heart Foundation research grant 3-17).

W-PM-C10 SIMULATED RECOVERY FROM SODIUM LOADING BY AN ELECTROGENIC PUMP IN CARDIAC MUSCLE. J.B. Chapman*, C.R. Horres*, M. Lieberman, and E.A. Johnson. Dept. Physiology, Duke University Medical Center, Durham, N.C. 27710

Recovery from sodium (Na) loading and potassium (K) depletion was simulated in a model of the synthetically grown strand of cardiac muscle (J.Gen.Physiol.65:527, 1975). Active transport was idealized as a reversible chemical reaction in which a driving reaction, the splitting of one mole of adenosine triphosphate (ATP), was coupled to extrusion of three moles of Na and uptake of two (3:2 pump) or one (3:1 pump) mole of K. Passive fluxes of ions were assumed to obey constant field theory with membrane permeabilities of 50, 3.05, and 3.6 x 10^{-8}cm/s for K, Na, and chloride respectively. Active transport kinetics were assumed to obey a dissipation equation such that the ratio of the forward to reverse reaction rates was given by exp(ΔG/RT), where ΔG is the magnitude of the free energy of ATP splitting (X) not conserved in the electrochemical work of ion transport, and R and T have their usual meanings. While the control steady state contribution of a 3:2 pump to resting membrane potential was lower than that for a 3:1 pump (5.6 vs. 13.1 mV), the reverse was true for recovery from an internal Na load of 140 mM. For X = -40 kJ/mole ATP, the peak hyperpolarization developed by the 3:2 pump exceeded the passive diffusion potential by 216 mV compared with 137 mV for 3:1 pumping. These voltages contrast sharply with an upper limit of 23 mV for the hyperpolarization due to depletion of external K by an electroneutral pump. The effects of varying the values of the Na:K pump ratio and X on the magnitude and time course of the voltage changes are sufficiently dramatic to provide useful constraints for the interpretation of physiological data from cardiac muscle. Electrical equivalent circuits are altogether inappropriate as analogue models for electrogenic ion transport. Supported by NIH grants HL12157, HL11307 and Am.Heart Assn. (E.I.Award to M.L.).

W-PM-C11 OUABAIN EFFECT ON MEMBRANE AND POTASSIUM EQUILIBRIUM POTENTIALS IN SHEEP PURKINJE FIBERS. J. L. Walker, Department Physiology, College Medicine, University Utah, Salt Lake City, Utah 84132.

Potassium selective microelectrodes were used to measure the difference between the diastolic membrane potential, E_D, and the K^+ equilibrium potential, E_K, in sheep heart Purkinje fibres exposed to ouabain. Conventional KCl filled microelectrodes were used to measure E_D in the same preparations. Simultaneous measurements were not made with the electrodes but the two kinds of measurements were made within five minutes of each other. When a K^+ electrode is inserted into a cell the observed potential difference, ΔE, is $\Delta E = E_D - E_K + RT/F \log_e a_K^o/A_K^o$. a_K^o, the extracellular K^+ activity, and A_K^o, the apparent extracellular K^+ activity, are known quantities and therefore $E_D - E_K$ can be obtained from K^+ electrode measurements alone. With 1 x 10^{-8} M ouabain no change in $E_D - E_K$ or E_D was observed for up to seven hours. With 1 x 10^{-7} M ouabain the results were variable, in some cases there was no effect while in others there was a marked increase in both $E_D - E_K$ and E_D, occurring at approximately the same time. The onset of depolarization occurred after about two hours of exposure to 1 x 10^{-7} M ouabain. With higher concentrations of ouabain the increases in E_D and $E_D - E_K$ were faster in their onset. The conclusion drawn from these observations is that E_K of the Purkinje cells does not change significantly in the presence of ouabain and therefore the observed depolarization is not due to loss of intracellular K^+.

Supported by a Grant-in-aid from the AHA and NIH grant NS 07938.

W-PM-C12 EFFECTS OF THYROID FUNCTION ON SOME CARDIAC ENZYMES. Csaba Hegyvary, Departments of Medicine and Physiology, Rush Medical College, Chicago, Illinois 60612

The possible regulation by thyroid function of cardiac NaK-ATPase, adenylcyclase and actomyosin was investigated. Hyperthyroidism (2.1 mg thyroxin administered per rat in 21 days) increased the absolute and relative heart weight (heart weight/body weight) protein content, total activity of NaK-ATPase, F^- stimulated adenylcyclase and Ca^{++}-ATPase of actomyosin but did not affect the specific activity of NaK-ATPase (activity per mg protein) and the basic activity of adenylcyclase. Four weeks after thyroidectomy the absolute and relative heart weight, protein content, total and specific activities of NaK-ATPase and Ca^{++}-ATPase of actomyosin were significantly reduced. In contrast the basic and particularly the F^- stimulated activity of adenylcyclase increased so that the total activities were equal to or greater than in the controls in spite of a decrease in heart size and protein content. Thyroid hormones thus may be responsible for the maintenance of the cellular levels of NaK-ATPase and of actomyosin Ca^{++}-ATPase. On the other hand adenylcyclase level in the myocardium seems to be regulated independently of thyroid function and some mechanism "saves" this enzyme during cardiac atrophy induced by hypothyroidism.

W-PM-C13 CELL CYCLE DEPENDENT CHANGES IN POTASSIUM TRANSPORT. Barry Mills* and Joseph T. Tupper, Department of Biology, Syracuse University, Syracuse, N. Y. 13210

K transport has been investigated during progression of cultured Ehrlich ascites tumor cells through the cell cycle. Using a double thymidine block technique, Ehrlich cells carried in continuous culture have been synchronized, as verified by simultaneous monitoring of cell number, cell volume, ^{3}H-thymidine incorporation and mitotic index. Unidirectional influx, efflux and cell content of K have been monitored throughout the cell cycle. The nature of the pump mediated, ouabain-sensitive K flux and the furosemide-sensitive component of K flux, presumably representing K-K exchange, have also been evaluated. In early S period the ouabain sensitive component, representing the Na-K pump, comprises 52% of the total unidirectional K influx. During S period the pump activity increases to a maximum of 65% of the unidirectional K influx and subsequently declines during G_2 period to a minimum of 40% in mid G_2. During M and early S the activity again rises. As the ouabain sensitive component becomes maximal in late S period, the furosemide sensitive component diminishes from approximately 30% of the total influx to approximately 10%. The same pattern is observed in the G_2 period. As the pump component diminishes, the furosemide sensitive component increases. Furosemide sensitive K efflux has also been monitored and the pattern is equivalent to that observed in the influx studies. No change in net K flux is observed in the presence of furosemide. This indicates that the furosemide sensitive component represents an exchange component for K. These results are consistent with the conclusion that the alterations in exchange and pump fluxes are physiological events associated with progression of the cell cycle. Supported by grants BC-181 from the Am. Cancer Soc. and CA 17203-01 from the NIH.

W-PM-D1 COOPERATIVE VISUAL TRANSDUCTION IN LIMULUS VENTRAL PHOTORECEPTORS. Alan Fein and J. Sherwood Charlton*, Laboratory of Sensory Physiology, Marine Biological Laboratory, Woods Hole, Mass. 02543.

Limulus ventral photoreceptors were voltage clamped to resting potential and stimulated by two flashes of light. If the flashes were presented such that the responses (light induced inward membrane current) to each flash significantly overlapped in time, the overall response to the two flashes was greater than the sum of the responses to each individual flash. This indicates that there is cooperativity in the transduction process. Cells were also stimulated by two 10 μm spots of light, each focused on a different region (60 μm separation) of the voltage clamped photoreceptor. We found that the cooperativity was present when two flashes were presented at one region of the photoreceptor. However the cooperativity was nearly absent when each flash was presented to spatially separated regions of the photoreceptor. This result indicates that the cooperativity in the transduction process is localized to the region of illumination.

W-PM-D2 ADAPTATION KINETICS IN THE LIGHT RESPONSES OF PHYCOMYCES. E.D. Lipson and S.M. Block*, Division of Biology, California Institute of Technology, Pasadena, Calif. 91125

Phycomyces serves as a model system for those aspects of sensory adaptation governed within a single cell, i.e. not dependent on multicellular interactions. The light responses of the sporangiophore of Phycomyces adapt over a range of 10^9 in light intensity, similar to the range of adaptation in vertebrate vision. We have performed experiments to study the kinetics of the level of adaptation, A, as defined by Delbrück and Reichardt (see Bergman et al., Bacteriol. Rev. 33:99, 1969; Lipson, Biophys. J. 15:989, 1975). They had proposed that the dependence of A on light intensity I is described by the first-order linear differential equation $dA/dt = (I-A)/b$, where b is the time constant of adaptation. Our dark adaptation experiments on the light growth response indicate that, following a step down from $I = 10^{-6}$ W/cm^2 to $I \simeq 0$, A decays exponentially as predicted by the above equation with a time constant $b = (6.1 + 0.3)$ min. At high intensity (10^{-3} W/cm^2), A decays more rapidly at first, as predicted qualtitatively by a model associating adaptation with photochemical kinetics. To test the equation for $I \neq 0$ (light adaptation), A was measured at various times following a step up to $I = 10^{-5}$ W/cm^2. The results are incompatible with the above equation, and call for a differential equation of at least second order, with a nonlinear dependence on I. Finally dark adaptation experiments involving the phototropic response reveal that over a range from 18°C to 25°C, b is quite insensitive to temperature. (Supported by NSF grant BMS 75-11316 and NIH grant GM 21409.)

W-PM-D3 pH CHANGES INDUCED BY LIGHT IN LARGE BALANUS PHOTORECEPTORS. H. Mack Brown, R.W. Meech*, and R.C. Thomas*, Dept. of Physiology, University of Utah College of Medicine, Salt Lake City, UT, 84132, ARC Unit of Invertebrate Physiology, Cambridge University, England, Dept. of Physiology, University of Bristol, England.

Saline equilibrated with a 5% CO_2 - 95% O_2 gas mixture can substantially reduce the depolarizing receptor potential of large barnacle photoreceptors without causing appreciable changes in the resting potential or membrane conductance in the dark. Since this manipulation produces a decrease in intracellular pH in other preparations, there is the possibility that a change in intracellular pH could play an important role in light adaptation in this photoreceptor. This was investigated by penetration of the isolated photoreceptor with a H^+-sensitive glass microelectrode to measure pH and conventional KCl microelectrode to record the membrane potential. The internal pH was about 7.0 immediately after penetration of the light-adapted cell; the pH gradually increased to between 7.2 and 7.4 after about 30 min in the dark. The time course of pH recovery in the dark resembled the time course of dark adaptation. Illumination of the cell with white light for brief periods produced a decrease in the internal pH. This increase of H^+ could alter sites in the membrane decreasing gNa and resulting in the "adaptive decline" of the receptor potential. This work was supported by NIH Grant EY 00762 from the National Eye Institute.

W-PM-D4 IONIZABLE GROUPS OF THE VERTEBRATE PHOTORECEPTOR MEMBRANE. Lawrence H. Pinto and Sanford E. Ostroy. Department of Biological Sciences, Purdue University, West Lafayette, Indiana 47907.

Membrane potential and resistance were measured for vertebrate photoreceptors that were exposed to perfusion solutions having various pH's. Reduction of the pH by 0.5 to 1.0 units from pH 7.8 resulted in membrane depolarization in the dark (by 2-3mV) and an increased size of the light response (also 2-3mV). The dark depolarization was accompanied by increased membrane resistance (11-35MΩ) when the pH changes were made with 1) normal perfusate and 2) perfusate in which Cl^- was replaced by isethionate$^-$. In perfusate in which Na^+ was replaced by choline$^+$ the depolarization did not occur, but membrane resistance increased when the pH was lowered. All changes occurred as rapidly as did the change in the composition of the solution in which the retina was immersed.

From these results it is concluded that the effect of decreased extracellular pH is primarily a decrease in K^+ conductance that is mediated by external sites. The additional finding that the light-induced changes in membrane resistance disappear in Na^+-free medium confirms previous findings that the primary effect of light is to decrease Na^+ conductance.

Supported by NIH grants EY00413 and EY01221.

W-PM-D5 Ca^{++} IN THE APLYSIA GIANT CELL AND THE BALANUS EBURNEUS MUSCLE FIBER. Jeffrey D. Owen, H. Mack Brown, and James P. Pemberton*. Department of Physiology, University of Utah College of Medicine, Salt Lake City, UT, 84132.

The internal calcium ion concentrations in the Aplysia giant neuron and the Balanus eburneus muscle fiber were measured with a newly developed calcium-selective microelectrode. The microelectrode contained p-(1,1,3,3-tetramethylbutyl)phenyl in the ester linkage of the exchanger. The average value of internal calcium ion concentration from several neurons was approximately 8×10^{-7}M. This internal calcium value was higher than the value (6.7×10^{-8}M) obtained by aequorin light-emission studies (Stinnakre and Tauc, Nature New Biology, 242: 113, 1973). It was lower than the maximum value (3×10^{-6}M) suggested by Meech from prolonged action potentials induced by Ca/EGTA pressure injections (Comp. Biochem. Physiol., 48A: 387, 1974) and the range (10^{-7} - 10^{-6}M) obtained from membrane conductance changes during similar pressure injection studies (Brown, Baur, and Tuley, Science, 188: 155, 1975). The internal calcium concentration measured in the muscle fiber was approximately 10^{-6}M; this is close to the same value obtained from Ca/EGTA injections of the giant muscle fiber from Balanus nubulus. (Hagiwara and Nakajima, J. Gen. Physiol., 45: 807, 1966). (Supported by NIH Grant EY 00762 from the National Eye Institute)

W-PM-D6 ARSENAZO III. A METALLOCHROMIC DYE FOR DETECTION OF CHANGES OF INTRACELLULAR IONIZED CALCIUM IN LIMULUS VENTRAL PHOTORECEPTORS. L.H. Pinto, Purdue University, West Lafayette, IN, J.E. Brown, Vanderbilt University, Nashville, TN, and P.K. Brown,* Harvard University, Cambridge, MA.

Arsenazo III (K-salt) was pressure-injected and simultaneous measurements of membrane voltage and optical transmission at 660nm (T_{660}) were made from single Limulus ventral photoreceptors. After a small dye injection, there was a rapid transient decrease of T_{660} during a prolonged bright stimulus presented to a dark-adapted cell. The amplitude of the change in T_{660} became smaller when $(Ca)_{out}$ was decreased and was abolished after intracellular iontophoretic injection of EGTA. After a large dye injection, T_{660} decreased slowly during a prolonged bright stimulus and recovered slowly as the cell dark-adapted; absorption spectra were recorded microspectrophotometrically both before and after a prolonged bright stimulus. The light-adapted minus dark-adapted difference-spectrum had a broad minimum at about 530nm and two maxima at about 610nm and 660nm, characteristic of dye-Ca binding. This difference spectrum went to zero as the cell dark-adapted (more than 20 min). Also, the difference between spectra recorded in 0mM Ca and 50mM Ca sea waters had the same peaks. These findings indicate that in Limulus ventral photoreceptors: 1) arsenazo III can be used to detect changes of $(Ca)_{in}$, 2) changing $(Ca)_{out}$ leads to changes of $(Ca)_{in}$ in the same direction and 3) light normally induces a transient increase of $(Ca)_{in}$.

W-PM-D7 DIVALENT CATION UPTAKE AND RELEASE IN ROD OUTER SEGMENT PARTICLE SUSPENSIONS. P. A. Liebman, Department of Anatomy, University of Pennsylvania School of Medicine, Philadelphia, Pa. 19174

The metallo indicator dye, Arsenazo III, was added to absolutely dark prepared frog rod outer segment particles suspended in "intracellular" media of several compositions. Dual wavelength optical density changes upon 1% bleaching illumination were recorded. In several preparations, a small increase in optical density occurred, consistent with divalent cation release. If due to Ca^{++} (not proved), the largest of these responses would correspond to release of 200 Ca^{++}/rhodopsin bleached. Attempts to improve the responses and "recharge" the system by adding ATP, P-P, cAMP, GTP, and cGMP were unsuccessful, but cGMP produced a powerful uptake that proved on closer examination to be predominantly Mg^{++}. Uptake rate was proportional to prep, cGMP and Mg^{++} concentration, and was abolished irreversibly below pH 6.3. The Mg^{++} uptake was stoichiometrically proportional to cGMP added. EGTA is without effect and EDTA blocks uptake. After uptake, subsequent release could not be obtained via hypotonicity, syringe needle homogenization, or A23187. cAMP produced similar uptake, but 40-100X slower. I thank my colleague, A. Scarpa, for providing preliminary technical data on and clean samples of the dye.

W-PM-D8 IONIC COMPOSITION OF VERTEBRATE PHOTORECEPTORS BY ELECTRON PROBE ANALYSIS. S. Yoshikami[+] and W. A. Hagins[+] National Institutes of Health, Bethesda, Md. 20014 [+]NEI [+]NIAMDD

Live frog and rat retinas incubated in Ringer containing ferric EDTA as an extracellular marker have been quick-frozen between copper blocks at -190°C. Specimens cleaved perpendicular to the plane of the retina were mounted in vacuum on the cold stage of a scanning electron microscope at <-150°C and the cleaved surface scanned with a 10-20kV, 10 nA electron beam. Characteristic Kα x-ray emission lines of Na, Mg, K, Ca, Cl, S, P, and Fe were analyzed with a focussing crystal spectrometer. Minimum measurable concentrations of the elements in the frozen matrices were 2-5 mM. Count rates for all elements except Cl were stable. Etching rates produced by the electron beam were usually < 1 micrometer/10 mins. Elemental compositions of various retinal layers were within the range to be expected of neurons. Rod outer segments contain about 2mM Ca and 25mM K. Ouabain incubation for 5 mins. causes loss of most of the K in outer segments. Examples of analyses will be shown.

W-PM-D9 COMPARISON OF THE ELECTRON DENSITY PROFILE FOR ISOLATED, WATER-WASHED PHOTORECEPTOR DISK MEMBRANES WITH THE PROFILE FOR DISK MEMBRANES IN THE INTACT RETINA. G. Santillan* and J.K. Blasie, Dept. of Biochemistry and Biophysics, U. Pennsylvania, Philadelphia, Pa. 19174.

The electron density profile of dark-adapted, isolated, water-washed disk membranes (the "isolated case") in hydrated oriented multilayers has been determined at 8 Å resolution taking into account the effects of lattice and substitution disorders in the multilayer (Biophys. J. 15, 109a, 1975). This profile was then compared with that for the dark-adapted disk membrane (at ∿30 Å resolution) in intact retinal preparations (the "intact case") reported by Schwartz et al. (Biophys. J. 15, 275a, 1975). The comparison involved matching the coherent lamellar intensity functions corresponding to the two profiles, using equivalent inter-membrane separations within the disk, $\bar{A}$ (=88 Å), and lattice and substitution disorder parameters. The results indicate differences in these intensities which are minimized by adjusting $\bar{A}$ and the electron density of the inter-disk medium. The remaining intensity differences are attributed to variations in both the symmetric and antisymmetric components of the membrane profile and the resulting differences in the unit cell structure factor. The isolated case seems to contain a membrane with slightly greater average thickness and asymmetry. These differences, considered minor, could be due to at least the following factors: the lower temperature, the lower water content, the lower electron density level of the inter-disk medium and the removal of non-covalently bound polysaccharide matrix from the inter-disk spaces in the isolated case relative to the intact case. At present our results suggest that the lower water content in the isolated case is not an important factor giving rise to the membrane profile differences. The implications of these differences as related to the distribution of phospholipid and rhodopsin within the membrane profile will be discussed.

W-PM-D10 THE LOCALIZATION OF RHODOPSIN IN THE PHOTORECEPTOR MEMBRANES OF FROG RETINA. S. Schwartz & E.A. Dratz, U. of Cal., Div. of Nat. Sci., Santa Cruz, CA. 95064.

We have calculated a 25Å resolution electron density (ED) profile of intact ROS that is undistorted by lattice or substitution disorder (Schwartz, Cain, Dratz & Blasie, Biophys.J.,Nov. 75). An absolute ED scale for the profile was derived using the ROS composition. The average ED is .364e/A^3, while the medium is .359. The densities of the peaks are $\simeq$.39 while the trough ED is $\simeq$.32. The peak and trough ED are stable to differing assumptions of the medium ED. The area under the peaks can be mainly accounted for by phospholipid head groups implying no large concentration of protein in either head group region. Approximately 10%-15% of the Rho (about 900A^2 in cross section) could pass through each 8A thick head group region. The superposition of various fluid state phospholipid profiles demonstrates that the trough in the disk is much shallower than would be the case for pure lipid. The trough depth, modeling and the phospholipid content are all consistent with 60±10% of Rho being located in the hydrocarbon region. The above points imply that Rho is in both monolayers. Studies by several groups show that Rho has an aqueous surface on the disk exterior. The "bump" in the profile outside the bilayer region of the membrane may be due to Rho. The "bump" region could contain the remaining 0-30% of Rho (partially depending on concentration of other material here). The disk gap region is relatively flat and broad for the separation of the two membranes. Several groups have been able to get the inner surfaces of the two membranes quite close together. Hence there appears to be little Rho in the disk gap region. The slightly greater area of the inner peak may be due to the lipids in the outer monolayer being more loosely packed (allowing somewhat more Rho in the outer monolayer) and/or more Rho being in the inner monolayer. We thank Drs. Corless, Costello, Chabre & Cavaggioni for providing unpublished data. S.S. is a Fight for Sight Postdoctoral Fellow.

W-PM-D11 NEUTRON SCATTERING ANALYSIS OF THE SHAPE, MOLECULAR WEIGHT AND AMPHIPATHIC STRUCTURE OF AN INTRINSIC MEMBRANE PROTEIN: RHODOPSIN. M. Yeager*, B. Schoenborn, D. Engelman, P. Moore and L. Stryer, Department of Molecular Biophysics and Biochemistry, Yale University, New Haven, Connecticut 06520, and Department of Biology, Brookhaven National Laboratory, Upton, New York 11973.

Neutron scattering is a powerful technique for investigating the structure of detergent-protein complexes because the detergent and protein regions can be examined separately. This is achieved by the method of contrast-matching in which the scattering from one of the components is selectively eliminated by choosing the appropriate D_2O/H_2O ratio in the solvent. Our experiments indicate that the detergent Ammonyx-LO (ALO) is contrast-matched in 2.1 ± 1.7% D_2O, so that the scattering in H_2O provides information about the size ahd shape of rhodopsin alone. By comparing the zero-angle scattering from proteins of known molecular weight to that of rhodopsin, the molecular weight of rhodopsin in 0.2% ALO was found to be 38,000 ± 3,000. Since the radius of gyration of rhodopsin in 0.2% ALO (23.4 ± 0.3 Å) is much larger than that calculated for a compact spherical monomer (17.3 Å), rhodopsin must have an asymmetric shape. From the contrast-match point of the rhodopsin-detergent complex (13.8 ± 2.9% D_2O), the number of detergent molecules bound to rhodopsin was estimated to be 240. Application of the parallel axis theorem shows that the distance between the centers of mass of the detergent and protein regions is 22 ± 5 Å. Such highly asymmetric solvation by ALO indicates that rhodopsin is an amphipathic protein with a large hydrophilic surface. This hydrophilic surface would tend to restrict transmembrane rotation, making it unlikely that rhodopsin functions as a light-activated diffusional carrier. (Supported by NIH and ERDA.)

W-PM-D12 ENZYME-CATALYZED INSERTION OF A FLUORESCENT PROBE INTO THE PROTEOLYTICALLY-SENSITIVE REGION OF RHODOPSIN. J.S. Pober, V. Iwanij*, E. Reich*, and L. Stryer, Department of Molecular Biophysics and Biochemistry, Yale University, New Haven, Connecticut 06520, and the Rockefeller University, New York, New York 10021.

We have used guinea pig liver transglutaminase to insert putrescine or dansyl cadaverine into bovine rhodopsin in retinal disc membranes. This enzyme catalyzes the formation of an amide bond between an amine and the γ-carboxyl group of a glutamine residue (Clarke, et al., Arch. Biochem. Biophys. 79: 338, 1959). At saturation, the stoichiometry is about one putrescine or dansyl cadaverine per rhodopsin. We have previously shown that rhodopsin in disc membranes is cleaved by thermolysin, subtilisin, or papain into similar pairs of membrane-bound fragments, suggesting that rhodopsin contains a region that is highly susceptible to proteolysis by enzymes of different specificity (Pober and Stryer, J. Mol. Biol. 95: 477, 1975). Two observations now show that the site labeled by transglutaminase is in this proteolytically-sensitive region. First, rhodopsin labeled with dansyl cadaverine is cleaved very slowly by subtilisin or papain and not at all by thermolysin. Second, immediately after cleavage with subtilisin or papain, the dansyl label appears to be located near an end of the larger fragment; upon further proteolysis, the label is completely excised without an appreciable concomitant change in the electrophoretic mobility of this fragment. The distance between the proteolytically-sensitive region and the chromophoric site of rhodopsin was estimated by measuring the efficiency of energy transfer from dansyl cadaverine to 11-cis retinal in disc membranes. The observed efficiency of about 40% corresponds to an apparent distance of about 55 Å. (Supported by grants from the National Institutes of Health.)

W-PM-D13 TRYPSIN DIGESTION OF RHODOPSIN IN DISC MEMBRANES AND EGG PHOSPHATIDYLCHOLINE BILAYERS. B. Aton* and L. Barr (Introduced by E. Barr), Department of Physiology and Biophysics, University of Illinois, Urbana, Ill. 61801

In order to decide whether rhodopsin when recombined with phospholipid in a bilayer is oriented as it is in natural membrane, sonicated discs from outer segments of frog retinal rods and purified rhodopsin recombined with egg lecithin were digested with trypsin for various lengths of time. The protein fragments resulting from the digestion were compared by gel electrophoresis as described by Swank and Munkreys (Anal. Biochem. 39, 462). Bands corresponding to different fragments were identified after the gels were stained with Coomassie Blue and PAS reagent and by the fluorescence of the chromophore after reduction with sodium borohydride. The rhodopsin was recombined with the PC by the methods of Hong and Hubbell (PNAS 69, 2617). The pattern evolution of digestion fragments from this recombined system were indistinguishable from that of sonicated discs. Although rhodopsin was not attacked by the trypsin after exposure to light, trypsin digestion yielded large fragments after 5 minutes. The opsin to trypsin ratio by weight was 40 to 1. Digestion experiments were carried out at 37°C and pH 8. The digestion fragment migrating closest to the rhodopsin band had an apparent molecular weight of 30,000, fluoresced under ultraviolet light and did not stain for carbohydrate. The PAS positively staining fragment band with the greatest apparent molecular weight did not fluoresce.

W-PM-D14 PROTEOLYTIC STUDIES OF FROG PHOTORECEPTOR MEMBRANES. C.A. Vandenberg*, J.E. Gaw*, E.A. Dratz, and S. Schwartz, Div. of Nat. Sci., U. of Cal., Santa Cruz, California 95604.

Subtilisin (1/20 w/w rhodopsin) rapidly cleaves frog rhodopsin into two fragments, F1 and F2, running with apparent molecular weights of 25K and 18K daltons respectively, on Fairbanks, Steck and Wallach-type SDS 12% acrylamide gels. In agreement with Pober and Stryer's (J. Mol. Bio. (1975) 95:477) and Saari's (pers. comm.) results on bovine rhodopsin, the carbohydrate is associated with F1, and the N-retinyl group with F2 as shown by PAS staining of gels and reduction with borane dimethylamine (pH 1.5, dark) or sodium borohydride (pH 8.0, light). F1 is slowly degraded to fragments of apparent molecular weight of 21K and 10K daltons. The 21K fragment bears carbohydrate. F2 looses approximately 2K daltons concomitantly with the degradation of F1. Proteolysis with subtilisin releases 10-15% of the amino equivalents/rhodopsin above a 1% control. All proteolysis was conducted at room temperature on 2X water washed, dark adapted ROS membranes having a 280nm/500nm absorbance ratio of 2.2-2.4. The preparations were suspended in .115M NaCl, 10mM HEPES pH 7.5,.1mM EDTA, .15mM $CaCl_2$. Trypsin (1/20 w/w) appears not to clip rhodopsin in 1 hour as evidenced by Coomassie-blue stained and PAS stained gels and isoelectric focusing. The possibility that trypsin might be clipping rhodopsin near the C-terminus is being further investigated. Between 7.5% and 12.5% of the amino equivalents/rhodopsin are released from the membrane by trypsin, depending on the "purity" of the membrane preparation assessed by A_{280}/A_{500}. Less than 2% of the released amino equivalents/rhodopsin may be accounted for by amino sugars after treatment with trypsin or subtilisin. Regenerability remains intact after trypsin treatment, and after subtilisin treatment before F1 is degraded. We thank M. Hall for the borane dimethylamine procedure. S.S. is a Fight for Sight Postdoctoral Fellow.

W-PM-D15 DIFFERENTIAL SCANNING CALORIMETRY OF BOVINE ROD OUTER SEGMENT MEMBRANES AND TOTAL PHOSPHOLIPIDS. George Miljanich, Michael F. Brown, and Edward A. Dratz, Division of Natural Sciences, University of California, Santa Cruz, CA 95064, Susan V. Mabrey* and Julian M. Sturtevant*, Department of Chemistry, Yale University, New Haven, CT 06520.

At least two reversible, thermal phase transitions are exhibited by bovine rod outer segment (ROS) membranes and bilayers of total extracted ROS phospholipids. A relatively sharp transition is centered at ca. 7°C in sonicated or unsonicated dispersions of total ROS phospholipids and at ca. 5°C in sonicated or unsonicated 0.1 mM EGTA washed ROS membranes. A second, broader transition is apparent near physiological temperature in sonicated or unsonicated dispersions of total ROS phospholipids and ROS membranes (T_m ca. 34-36°C). Above 50°C two sharp, irreversible transitions are observed in ROS membranes which are not present in liposomes of total ROS phospholipids and most likely represent protein structural rearrangements. A sharp transition near ca. 55°C may correspond to the loss of rhodopsin linear dichroism and early receptor potential observed by Cone and Brown ((1967), Science 156, 536) upon heating rat eyes.

W-PM-D16 PROTON MAGNETIC RESONANCE STUDIES OF BOVINE ROD OUTER SEGMENT MEMBRANE MOLECULAR ORGANIZATION AND FLUIDITY. Michael F. Brown, George Miljanich, and Edward A. Dratz, Division of Natural Sciences, University of California, Santa Cruz, CA 95064.

Well resolved ^1H NMR spectra of rod outer segment (ROS) membranes and aqueous dispersions of total extracted ROS phospholipids have been obtained at 100, 220, and 360 MHz. Resonances from the vinyl (CH=CH), choline methyl (N^+Me_3), doubly allylic (CH=CH-CH_2*-CH=CH), singly allylic (CH=CH-CH_2*), methylene ($(CH_2)_n$), and terminal methyl (CH_3) phospholipid protons of ROS membranes and total phospholipid vesicles are clearly resolved above 10°C. The CH_3 resonance linewidth is frequency dependent, due in part to two components of approximately equal area which are clearly resolved at 360 MHz. The spectra of both ROS membranes and total phospholipid vesicles appear to be a superposition of at least two spectral components with different relaxation rates. The distribution between sharp and broad spectral components is sensitive to sonication and temperature over the range 5-50°C. For example, the percentage of phospholipid CH_3 protons which is observed in the relatively sharp component of sonicated ROS membranes or phospholipid vesicles increases from ca. 15% to ca. 100% over this temperature range. The ^1H NMR data provide strong evidence for a broad, thermally induced phospholipid phase transition in the ROS membrane, with a midpoint near physiological temperature and an apparent two state van't Hoff enthalpy of 22-23 kcal $mole^{-1}$. The T_1 relaxation times of ROS membranes and total phospholipid vesicles are temperature and frequency dependent and appear to be substantially longer than those of other biological membranes and phospholipid bilayers. The possibility of estimating a diffusion coefficient for lateral translation of phospholipids in ROS membranes from T_2 relaxation data is presently being explored.

W-PM-E1 STRUCTURE OF OXYGENATED HEME PROTEINS. G.H. Loew, R.F. Kirchner, Genetics Department, Stanford University School of Medicine, Stanford, CA. 94305

The electronic structure, spin state and conformation of oxy heme proteins have been investigated by molecular orbital studies of model compounds. Calculations were also made of the components of the electric field gradient at the iron nucleus, observable as quadrupole splitting in Mossbauer resonance spectra. The results indicate that the complex can be described by a normal ferrous-dioxygen ground state configuration rather than the more unusual ferric-superoxide previously proposed. The magnitude and sign of the field gradient components are very sensitive to oxygen geometry. Contributions from several low energy rotamers could account for the observed temperature dependence of the quadrupole splittings. Considerable electron delocalization between the iron and oxygen ligand and differences in the remaining iron-ligand interactions appear to be the origin of the "anomalously" large quadrupole splitting observed for all diamagnetic oxyferrous heme systems.

W-PM-E2 HYPERFINE INTERACTIONS IN HIGH SPIN FERRIC HEME COMPOUNDS AND METMYOGLOBIN. S. K. Mun,* Mahendra K. Mallick,* Jane C. Chang,* and T. P. Das, Dept. of Physics, SUNY at Albany, NY 12222

We report on our theoretical investigations on the electronic structures and magnetic hyperfine interactions in a series of high spin ferric compounds with different fifth ligands (fluoride, chloride, bromide and hydroxide) and in a model compound for metmyoglobin involving water and imidazole as fifth and sixth ligands. Self-consistent-charge-extended Huckel procedure has been used in obtaining the molecular orbitals. The hyperfine constants for Fe^{57m} and N^{14} nuclei are found to agree within 5 per cent among the four heme derivatives. For Fe^{57m} in the chloride derivative, excellent agreement is found with the Mossbauer hyperfine field in hemin. For N^{14} in the fluoride, chloride and bromide derivatives, the closeness of the predicted hyperfine constants is borne out experimentally,[1] with the theoretical values being all about 60% of experiment. For metmyoglobin, the Fe^{57m} hyperfine field agrees very well with experiment and is close to hemin. The N^{14} hyperfine constant for the porphyrin nitrogens is found to be very nearly the same as in the heme compounds, while the imidazole nitrogen bonded to iron has a hyperfine constant 60% higher, the trend being in agreement with the experiment.[2] These results indicate that electronic structures in these five molecules are quite well described by theory and that the electronic distribution on the porphyrin ring is not very sensitive to changes at fifth and sixth ligands. Arguments will be presented for expecting the imidazole nitrogen to be more sensitive to ligand changes. (Supported by a grant from National Heart and Lungs Institutes).

[1] H. L. Van Camp, C. P. Scholes and C. F. Mulks (to be published).
[2] C.P. Scholes, R.A. Isaacson and G. Feher, Biochem. Biophys. Acta 263, 448 (1972).

W-PM-E3 LIGAND BINDING STUDIES ON A CO-OPERATIVE DIMERIC MYOGLOBIN. Lawrence J. Parkhurst and Giuseppe Geraci*, Department of Chemistry, University of Nebraska, Lincoln, Nebraska 68588 and Laboratorio Embriologia Molecolare, CNR, Naples, Italy.

Oxygen equilibria and oxygen-CO partition studies have been carried out on two dimeric myoglobins isolated from the radular muscle of the mediterranean mollusc Nassa mutabilis. Both myoglobins have very similar oxygen equilibrium and kinetic properties. The Hill number, n, is ca. 1.6 and $p_{\frac{1}{2}}$ is 4.5 torr for oxygen. The Hill number for the partition studies differs significantly from 1. Measurements of CO combination and CO recombination (following flash-photolysis) were carried out in the same apparatus and the kinetic traces were identical. Furthermore, partial photolysis gave no evidence for a quickly-reacting form (Mb*) even at 4° and 0.5 mM CO. Oxygen combination measurements were made by flash-photolysis. The subsequent relaxation in the presence of CO was examined for evidence of Mb*. Kinetic manifestations of co-operativity were readily apparent in oxygen-pulse stopped-flow studies in which the rate of oxygen dissociation was found to increase as the fractional saturation decreased. A graphical method of analysis in which kinetic and equilibrium parameters are combined has been devised for testing the allosteric model on dimeric systems.

Grant Support: NIH 15284-03, Research Council (University of Nebraska) (NIH RR-07055-09), Research Corporation Grant-in-Aid, and NSF-CNR Joint US-Italy Co-operative Science Grant.

W-PM-E4 THE RELATIONSHIP BETWEEN OPTICAL ABSORBANCE AND STATE CHANGES IN CARP HEMOGLOBIN. M.J. McDonald, C.A. Sawicki* and Q.H. Gibson*, Section of Biochemistry, Molecular and Cell Biology, Cornell University, Ithaca, N.Y. 14853.

Functional studies by Tan and others have shown that Carp hemoglobin (Hb) undergoes a transition from the high affinity (R state) to the low affinity (T state) in both the unliganded and liganded forms. Since this R→T transition can be induced by increases in either hydrogen or organic phosphate ion concentrations, the pH and inositol hexaphosphate (IHP) difference spectra for both deoxy and carboxy Carp Hb in citrate, phosphate or borate buffers have been recorded. Both the pH and IHP difference spectra of deoxy Carp Hb are characterized by peaks at 430 and 443 nm and an isosbestic point at 438 nm. These spectra are similar to those correlated with an R→T transition within deoxy mammalian Hb and are seen over a pH range predicted from previous functional studies. The pH and IHP difference spectra of carboxy Carp Hb have peaks at 414 and 424 nm and an isosbestic point at 420 nm and are similar to those recently reported by Giardina and others to correspond to an R→T transition in liganded trout Hb. However, at pH 4.5 the magnitude of the pH difference spectrum is still increasing while that of the IHP difference spectrum has already declined by pH 5.5. Furthermore, spectrophotometric monitoring of the R→T relaxation of Carp Hb following laser photolysis at a wavelength (424 nm) isosbestic for ligand binding, confirms the findings from the IHP difference spectra and from previous functional studies, in revealing no R→T transitions below pH 5.5. Thus, although changes in pH generate a spectrum which is similar to that reported to correspond to an R→T transition in liganded Hb, it most probably does not reflect such a transition in this instance. Therefore, it is suggested that caution must be taken in relating spectral changes to state changes without collaborating functional evidence. (Support: PHS: GM 14276, NSF: BMS 74-08233; MJM is a NIH Postdoctoral Fellow.)

W-PM-E5 ENERGETICS OF OXYGENATION-LINKED SUBUNIT INTERACTIONS IN HUMAN HEMOGLOBIN G.K. Ackers, F.C. Mills, M.L. Johnson, and S.H.C. Ip, Dept. of Biochemistry, University of Virginia, Charlottesville, Va. 22901

The changes in intersubunit contact energy which accompany successive oxygenation of human hemoglobin have been determined by measurements on the linkage between oxygenation and dissociation of tetramers into dimeric species. In 0.1M Tris HCl, 0.1M NaCl 1mM Na_2 EDTA, pH 7.4, 21.5°C, the free energy for association of unliganded dimers into tetramers is -14.0 ± 0.3 Kcal/mole (heme) as determined by independent measurements of forward and reverse rate constants. The rate of dissociation (tetramer to dimers) was measured from haptoglobin binding experiments under deoxy conditions. The reverse rate constant was determined from stopped flow measurements on reassociation of deoxy dimers into tetramers. From this determination, and measurements of oxygenation curves as a function of protein concentration (between 4×10^{-8}M and 5×10^{-4}M heme) the following intersubunit contact energies were determined: With the first binding step $\sim$ 1.7 Kcal of "constraining" energy is released; during the second and third steps (taken together) $\sim$ 3.9 Kcal of cooperative energy is release; $\sim$ 0.75 Kcal of the energy is released at the fourth binding step. These results provide basic model-independent thermodynamic parameters which impose constraints that must be met by any models for hemoglobin function. The results provide unequivocal evidence against a concerted transition model involving only two major energetic states for the hemoglobin tetramer. They are not inconsistent with an MWC type of two-state model. They provide no information regarding the number of structural forms having substantial differences in atomic coordinates.

W-PM-E6 LASER LIGHT-SCATTERING KINETIC STUDIES OF THE ALKALINE TETRAMER→DIMER DISSOCIATION REACTION IN HUMAN HEMOGLOBIN. Duane P. Flamig and Lawrence J. Parkhurst, Department of Chemistry, University of Nebraska, Lincoln, Nebraska 68588.

Human hemoglobin dissociates into dimers at pH's above 10. We report here the first direct kinetic measurements of this process using a specially designed light-scattering stopped-flow apparatus with 200 mw Ar^+ source at 488nm. Computer simulation of planned experiments permitted optimization of the signal to noise ratio as a function of the concentration of the hemoglobins. Following a rapid jump in pH from 7 to pH values between 10 and 11.6, HbCO, HbO_2, Hb^+, and HbCN show first-order dissociation kinetics with very similar rate constants. For HbCO (7.5 μM) in 0.05 M ε-amino caproate as the final buffer, k increases from 0.2 sec^{-1} to 24 sec^{-1} for pH 10.3 to 11.6, respectively. Several models were explored to account for the pH kinetic profile using weighted Fletcher-Powell minimization. A model which predicts an increased dissociation rate solely on the basis of average net charge on the tetramer is inconsistent with the data. Models which neglect interactions among the ionizable sites do not fit the kinetic data well, whereas models which include interactions, such as Ising models, can provide excellent fits. At least two microscopic rate constants and 4 amino acids with intrinsic pK_a ~11.3 are required for a good fit to the data. The variation in the rate constant as a function of ionic strengh at pH 10.5 and pH 11.6 using KCl and KNO_3 was studied in order to investigate charge variations in the transition state. The ionic strength data can be interpreted in terms of the number of salt bridges broken in the transition state. Grant support: NIH 15284-03, Research Council (University of Nebraska) (NIH RR-07055-09), Research Corp.

W-PM-E7 ELECTROPHORETIC LIGHT SCATTERING OF HEMOGLOBIN SOLUTIONS. D.D. Haas* and B.R. Ware, Department of Chemistry, Harvard University, Cambridge, Massachusetts 02138

Electrophoretic light scattering is the determination of electrophoretic velocities by measuring the Doppler shifts of scattered laser light. We have adapted this technique for the study of dilute solutions of hemoglobin. A special electrophoretic chamber has been constructed which can be centrifuged at high speeds for final removal of particles and bubbles, and which minimizes interferences due to joule heating and electrode products. Characterization experiments which have been completed include several independent determinations of the electric field as a function of applied voltage and current, measurements of the flow profile in the scattering region, determinations of the isoelectric point of hemoglobin solutions, and quantitative studies of the linewidths of electrophoretic light scattering spectra from hemoglobin solutions. Of particular interest is the study of the dimer-tetramer equilibrium of hemoglobin by this technique. In principle both equilibrium and kinetic parameters can be measured. The experimental progress in this area will be discussed. (Supported by NSF grant MPS72-05133)

W-PM-E8 SUBUNIT DISSOCIATION, COOPERATIVITY AND THE BOHR EFFECT IN HEMOGLOBINS. D. H. Atha and A. Riggs, Zoology Department, University of Texas, Austin, Texas 78712.

The linkage between subunit dissociation and proton binding has been examined in human hemoglobin A, the variant hemoglobin Kansas, and in tadpole hemoglobin. The apparent tetramer to dimer dissociation constants for both the deoxy and oxy hemoglobins have been measured by gel chromatography and sedimentation velocity techniques at 20° in 0.05 M cacodylate, tris and glycine buffers containing 0.1 M NaCl and 1 mM EDTA in the pH range 6.5-11. Simulated oxygen binding equilibria as a function of pH were generated from these data with a pH-independent estimate of the total free energy of oxygen binding to dimer by means of the linkage relations described by G. K. Ackers and H. Halvorson (Proc. Nat. Acad. Sci. USA 71:4312,1974).Comparison of the simulated equilibria with experimental oxygen binding data has yielded a quantitative explanation of the alkaline Bohr effect and the pH dependence of the Hill coefficient of cooperativity for each of these hemoglobins.

Supported by a NIH post-doctoral fellowship (D. H. A.) and by NSF grant BMS 74-05172-A01 (A. R.).

W-PM-E9 THERMODYNAMICS OF THE TETRAMER-DIMER DISSOCIATION EQUILIBRIUM IN HUMAN HEMOGLOBIN. THE pH DEPENDENCE AND ITS POSSIBLE RELATIONSHIP TO HEMOGLOBIN FUNCTION. A.D. Barksdale*, B.E. Hallaway*, B.E. Hedlund*, E.S. Benson, and A. Rosenberg*. Department of Laboratory Medicine and Pathology, University of Minnesota, Minneapolis, MN 55455

The tetramer-dimer dissociation constant ($K_{4,2}$) of carbonmonoxyhemoglobin has been measured as a function of pH and temperature. The method of measurement -- the difference at fixed time in extent of tritium loss between the two forms, equally labeled -- provides a novel, precise, and fast evaluation of $K_{4,2}$. The results: (1) the free energy of dissociation at about 20 °C remains essentially constant from pH 6 to pH 8.6. (2) The enthalpy of dissociation increases from +2 kcal/mole at pH 6 to a maximum at pH 7.4 from which it decreases monotonically to -12 kcal/mole at pH 8.6. The subunit dissociation's pH dependence bears a striking resemblence to the Bohr effect, suggesting that the two phenomena may share a common origin. Furthermore, the results of these studies, taken together with those of others from these laboratories, indicate that the ferrohemoglobin tetramer may be poised on a conformational fulcrum at or near physiological conditions.

W-PM-E10 DIMER-TETRAMER EQUILIBRIUM OF PARTIALLY LIGANDED HEMOGLOBIN: PRELIMINARY RESULTS. Robley C. Williams, Jr., Department of Biology, Yale University, New Haven, Ct. 06520.

The dimer-tetramer association constant ($K_{2,4}$) of human hemoglobin undergoes a decrease of about six orders of magnitude between the deoxygenated state of the protein and the fully oxygenated state. Because $K_{2,4}$ is thermodynamically linked to cooperative changes in the oxygen affinity of hemoglobin, knowledge of its value for partially oxygenated species provides information about the distribution of those species at intermediate points in the oxygen-binding process. Since $K_{2,4}$ also necessarily reflects ligand-linked changes in conformation at the interface between the constituent dimers of the tetrameric molecule, it is a sensitive indicator of structural rearrangement in the partially oxygenated tetramer.

Measurements of $K_{2,4}$ as a function of saturation with oxygen are being carried out by equilibrium ultracentrifugation. Special ultracentrifuge cells have been constructed that allow stable oxygen saturation to be obtained, and conditions have been found that minimize oxidation of heme. Although resolution of the values of $K_{2,4}$ pertaining to each of the partially oxygenated intermediate species is still incomplete, preliminary results suggest that the major changes in $K_{2,4}$ occur at low degrees of saturation with ligand. These results will be discussed in the context of a number of models of cooperativity in hemoglobin.

W-PM-E11 EFFECTS OF ORGANIC PHOSPHATES, LIGANDS AND HEME SPIN STATES UPON HEMOGLOBIN CONFORMATION. M.E. Johnson, Medicinal Chemistry Department, University of Illinois Medical Center, Chicago, Ill. 60612, D. Scholler* and B.M. Hoffman*, Chemistry Department, Northwestern University, Evanston, Ill. 60201, and C. Ho, Biophysics & Microbiology Department, University of Pittsburgh, Pittsburgh, Penn. 15260

Variable temperature electron spin resonance studies of hemoglobin spin labelled at Cys β93 with 4-(2-Iodoacetamido)-2,2,6,6-tetramethyl piperidinooxyl suggest that the hemoglobin conformation, as monitored in the β93 retion, is highly sensitive to oxidation state, type of ligand, and solution conditions. At 0°C the spin label of the deoxy derivative of the ferrous state appears to experience two different environments with the relative populations changing upon addition of inositol hexaphosphate (IHP), presumably reflecting the conformational changes induced by IHP binding. The spin label on the ferric (met) derivatives appears to experience three discrete local environments under most conditions, with the relative populations being determined by pH, presence of IHP, ionic strength and, most importantly, by the type of ligand. The relation of these effects to heme-ligand stereochemistry and heme spin state will be discussed.

Supported in part by grants from Illinois Research Board, National Institutes of Health and National Science Foundation.

W-PM-E12 NMR STUDIES OF HEMOGLOBIN M MILWAUKEE AND THEIR IMPLICATIONS CONCERNING COOPERATIVE OXYGENATION. L. W.-M. Fung and C. Ho, Department of Life Sciences, University of Pittsburgh, Pittsburgh, Pa. 15260 and A. P. Minton*, National Institutes of Health, Bethesda, Md. 20014

Hemoglobin M Milwaukee (β67E11 Val→Glu) is a naturally occurring valency hybrid containing two permanently oxidized hemes on the β-chains. In this mutant, the two abnormal β-chains cannot combine with oxygen whereas the two α-chains are normal and can combine with oxygen cooperatively with a Hill coefficient of approximately 1.3. High-resolution proton nuclear magnetic resonance (NMR) spectroscopy at 250 MHz has been used to investigate the ferric hyperfine shifted resonances of Hb M Milwaukee which change as a function of oxygenation at pD 7 and 30°C. Sufficient quantities of organic phosphates can partially or completely inhibit the structural transformation which normally accompanies the binding of oxygen or carbon monoxide to Hb M Milwaukee. The hyperfine shifted resonance spectra of the ferric β-hemes of partially oxygenated Hb M Milwaukee can be described as an appropriately weighted average of the spectra of non-, singly-, and doubly-oxygenated species. The NMR spectrum of the singly oxygenated species has been calculated by a method employing least-squares analysis of the spectra of partially oxygenated Hb M Milwaukee at several values of oxygen saturation. It is different from that of fully deoxy or fully oxygenated Hb M Milwaukee and cannot be described as an average of the spectra of the fully deoxy and oxy species. These results are not consistent with a two-structure model for the oxygenation of this mutant protein. In view of the similarities between normal adult hemoglobin and Hb M Milwaukee, it is suggested that a two-state concerted allosteric model does not provide an adequate description of the structure-function relationships in normal hemoglobin. (This work was supported by research grants from NIH and NSF).

W-PM-E13 HIGH-RESOLUTION PROTON NMR STUDIES OF SICKLE CELL HEMOGLOBIN. K. J. Wiechelman*, L. W.-M. Fung, G. S. Supinski*, K.-L. C. Lin*, and C. Ho, Department of Life Sciences, University of Pittsburgh, Pittsburgh, Pa. 15260

High-resolution nuclear magnetic resonance (NMR) spectroscopy at 250 MHz has been used to investigate the aromatic proton resonances of sickle cell hemoglobin, Hb S (β6 Glu→Val). There are 38 histidyl residues per hemoglobin and more than 20 of them are located on the surface of the molecule. Thus, the histidyl residues can serve as probes to monitor the surface conformation of the hemoglobin molecule. By monitoring the C2 histidine proton resonances it is possible to detect differences in the surface conformations of Hb S and normal adult hemoglobin (Hb A) under various experimental conditions. Concentration changes bring about differences within the spectra of both Hb S and Hb A. The magnitude of the spectral differences between the two hemoglobins is also concentration dependent. The spectra of the deoxy forms of Hb S and Hb A in Bis-Tris buffer are different and change as a function of pH. The addition of organic phosphates, such as inositol hexaphosphate (IHP) or 2,3-diphosphoglyceric acid (DPG), causes changes in the spectra of the two hemoglobins. These changes are of interest since it has been reported that the minimum gelling concentration (MGC) of Hb S is lowered in the presence of these organic phosphates. Since Hb S is in the deoxy quaternary structure, these changes in the MGC may reflect some specific local environmental changes in the tertiary structure of Hb S induced by DPG and IHP. The relationship between the observed spectral features and the sickling process will be discussed. (This work was supported by research grants from NIH).

W-PM-E14 XENON, CYCLOPROPANE AND DICHLOROMETHANE PREVENT DEOXYHEMOGLOBIN S FROM SICKLING. B. P. Schoenborn , Biology Department, Brookhaven National Laboratory, Upton, N. Y. 11973

It has long been known that the substitution of glutamic acid by valine at position β6 in hemoglobin causes sickle cell anemia. This aggregation effect is thought to occur by interaction of this new hydrophobic site on the surface of the hemoglobin β chain with a complimentary site occuring probably in deoxy Hb A and S. The exposure of hemoglobin S to xenon, cyclopropane and dichloromethane does prevent sickling and even reverses sickling as shown by cell counting criteria. Xenon, cyclopropane, dichloromethane and other gases bind to myoglobin and hemoglobin at specific sites. X-ray crystallographic studies have shown that these binding sites in hemoglobin occur in the GH corner of the α chain and the AB region of the β chain. This suggests that the complimentary site involved in sickling is located in the AB corner of the β chain or the GH corner of the α chain. The concentration (gas pressure) of xenon or cyclopropane necessary to prevent sickling is in the range where these gases cause light anesthesia. Dichloromethane prevents sickling at levels that are substantially below narcotic effects and might, therefore, be useful in the prevention or reversal of sickle cell anemia.

W-PM-E15 UPTAKE AND METABOLISM OF NITROGEN OXIDES IN BLOOD. George D. Case, John C. Schooley*, and Jonathan Dixon*, Lawrence Berkeley Laboratory, Univ. of Calif., Berkeley CA 94720.

During the last forty years, numerous studies have examined the reactions of hemoglobin and whole blood with nitrogen oxides, using very high doses. This work describes the formation of nitroxyhemoglobin (Hb-NO) and its direct conversion to methemoglobin (met-Hb) *in vitro* as well as the effects of human exposure to typical combustion effluents. Whole blood from mice was exposed to an NO atmosphere, resulting in the *in vitro* formation of Hb-NO, low-spin met-Hb, and high-spin Hb (measured by EPR spectroscopy). Hematocrit analysis revealed no hemolysis. Subsequent exposure to clean air after purging results in the disappearance of Hb-NO with a 2 hr. half-time. This is accompanied by the simultaneous and stoichiometric appearance of *high-spin* met-Hb. No low-spin met-Hb is produced from the decay of Hb-NO. In addition, human and rabbit blood samples were obtained during *in vivo* exposure to 1-3 ppm NO, 0.3 ppm NO_2, and up to 50 ppm CO. These pollutant levels (especially NO and NO_2) are typical of the home environment. Blood levels of carboxyhemoglobin (Hb-CO) average 5% of the total Hb during this kind of exposure, and decay upon relocation into clean air. Blood levels of Hb-NO remain constant at 0.15 to 0.2% throughout the experiment. On the other hand, met-Hb levels in the blood rise linearly during the exposure, from 0.5% to 2% and beyond. Only high-spin met-Hb could be detected, suggesting its origin from Hb-NO. NO is therefore a toxic gas in its own right, at sub-occupational concentrations and without any need for its conversion to NO_2. If the present data are indicative, 3 ppm NO is comparable to 10-15 ppm CO in its effects on human health. NO at these levels is frequently encountered in the home during operation of combustion appliances, and is generated in such quantities regardless of the presence or absence of significant CO production. This work performed under the auspices of U.S. ERDA.

W-PM-F1 EFFECTS OF PRESSURE ON ACTIN ACTIVATION OF HEAVYMEROMYOSIN ATPASE. Ronald J. Lukasiewicz and Paul Dreizen, Department of Medicine and Program in Biophysics, State University of New York Downstate Medical Center, Brooklyn, New York 11203.

Studies are described concerning the effects of pressure on Mg-ATPase of acto-heavymeromyosin (acto-HMM), with and without troponin (Tn) and tropomyosin (TM), from rabbit skeletal muscle. HMM Mg-ATPase is activated by pressure, yielding a value for the activation volume, $\Delta V^{\ddagger}$, of ca. -20 cc/mole in 3.3mM Mg-ATP, 10mM tris, 10μM Ca, 0.1mM DTT, pH 7.6 at 25°C.. Mg-ATPase of acto-HMM is inhibited by pressure, and specific values of $\Delta V^{\ddagger}$ depend on the ratio of actin to HMM. For example, at actin to HMM ratios of 100/1, w/w, $\Delta V^{\ddagger}$ is +80 cc/mole. Smaller values of $\Delta V^{\ddagger}$ are found at lower ratios of actin to HMM, and at infinite actin, the estimated $\Delta V^{\ddagger}$ is about +100 cc/mole. Values of $\Delta V^{\ddagger}$ approach zero under conditions, including increased ionic strength and decreased temperature, that inhibit acto-HMM ATPase relative to HMM ATPase. The observed volume changes reflect an admixture of negative $\Delta V^{\ddagger}$ (-20 cc/mole), related to the steady-state rate limiting release of product from HMM, and a positive $\Delta V^{\ddagger}$ (+120 cc/mole), related to association of acto-HMM or, alternatively, to pressure enhancement of the proportion of HMM in a refractory state. Experiments were also conducted on possible effects of Tn and TM on the pressure dependence of acto-HMM Mg-ATPase at 3.3mM ATP. In 10μM Ca, values of $\Delta V^{\ddagger}$ for acto-HMM ATPase are comparable with and without Tn and TM, at ratios of actin to HMM of 4-40/1, w/w. In the absence of Ca (3.3mM EGTA), values of $\Delta V^{\ddagger}$ for acto-HMM ATPase in the presence of Tn and TM approximate those of HMM Mg-ATPase alone, presumably due to the marked inhibition of actin-activated hydrolysis. More subtle effects of regulatory proteins on $\Delta V^{\ddagger}$ for acto-HMM ATPase are not, however, excluded by the present experiments.

W-PM-F2 HEAT INDUCTION OF A POTENTIATED STATE FOR BULLFROG NATURAL ACTOMYOSIN. A. Giambalvo and P. Dreizen. Department of Medicine and Program in Biophysics, State University of New York Downstate Medical Center, Brooklyn, N.Y., 11203.

Studies of myofibrillar proteins extracted from bullfrog skeletal muscle (Rana Catesbeiana) were conducted in order to investigate possible molecular changes related to thermal acclimation. Preparations of myosin and natural actomyosin do not appear to differ in warm (25°C) and cold (5°C) acclimated frogs with respect to temperature dependence of ATPase or subunit composition, as indicated by SDS-gel electrophoresis. Unexpectedly, however, in experiments on thermal denaturation of bullfrog natural actomyosin, it was found that Mg ATPase undergoes substantial potentiation as a result of heat treatment in the absence of substrate. For example, Mg ATPase is enhanced 8 to 12 fold following incubation at 36°C. The potentiation effect is to be distinguished from conventional Arrhenius-type activation of actomyosin ATPase. The extent and time course of potentiation vary with the temperature of incubation. Although simple decrease in temperature does not restore initial levels of Mg ATPase, almost complete reversal of the potentiated state can be accomplished under appropriate solvent conditions. Heat treatment of myosin alone, or of natural actomyosin in 0.5M KCl does not result in potentiation, suggesting that interaction between myosin and thin filament proteins is essential for heat potentiation. It is speculated that the potentiation phenomenon may play some role in acclimation of frogs to different thermal environments.

W-PM-F3 THE ROLE OF THE BOUND NUCLEOTIDE OF ACTIN IN THE INTERACTION OF ACTIN WITH MYOSIN. R. Cooke, Department of Biochemistry and Biophysics, and the Cardiovascular Research Institute, University of California, San Francisco, CA 94143

F-actin contains one tightly bound nucleotide per monomer for which no definite function has been demonstrated. This study probes the possibility that the nucleotide plays some role in the actomyosin interaction which generates force. The transphosphorylation of similar tightly bound nucleotides on other proteins, e.g. tubulin, demonstrates that such nucleotides may be involved in enzymatic interactions. The actin nucleotide was replaced with an ATP analog, AMPPNP. This analog is not susceptible to hydrolysis in the present system, and its presence is expected to modify any interactions of actin in which the nucleotide plays a role. AMPPNP incorporation does not inhibit either the extent or velocity of actin polymerization, nor does it measurably inhibit the ATPase activity of actomyosin or of actoSF-1. However, analog incorporation does inhibit the velocity, but not the extent, of superprecipitation. In order to measure the effect of analog incorporation on the generation of force, actomyosin threads were formed via extrusion and their force- - velocity curves were determined. This study was made possible by the design and construction of a new type of tensiometer. Isometric tension of the threads increased with protein concentration, extrapolating to ~0.5 kg/cm^2 at protein concentrations which have been estimated for muscle fibers. This value is of the same order of magnitude as that of muscle fibers, indicating that the tensions measured in the threads are generated by a mechanism similar to that of muscle. The incorporation of the analog into actin inhibited the maximum force generated by the threads. This result demonstrates that a native nucleotide on the actin is required for the full generation of force by the actomyosin interaction. Supported by USPHS AM 17559 and NSF BMS 14793; R.C. is an Established Investigator of the AHA.

W-PM-F4 THE INTERACTION OF MYOSIN SUBFRAGMENT-1 (S-1) WITH ACTIN AND ATP: PRE-STEADY STATE KINETIC STUDIES SHOWING A SINGLE CYCLE OF ATP HYDROLYSIS. S.P. Chock*, E. Eisenberg and P.B. Chock*, Laboratories of Cell Biology and Biochemistry, NHLI, Bethesda, Md. 20014

A single cycle of interaction of acto-S-1 with ATP was studied using light scattering as a measure of binding between the actin and S-1. Fluorescence changes were also studied. The experiments were performed at very low ionic strength so that the actin-activated ATPase could be brought close to its maximal value at relatively low actin concentration and at 5° so that the measured rates would be relatively slow and thus could be more accurately measured. S-1 was used rather than heavy meromyosin because the binding of a single-headed species should be simpler than the binding of a two-headed one. Our results show that addition of stoichiometric ATP to acto-S-1 causes a cycle consisting of first, a rapid dissociation of the acto-S-1 complex; second, a somewhat slower fluorescence change in the dissociated S-1 substrate complex; and third, a much slower rate limiting recombination of the S-1-substrate complex with actin. We also find that over a ten-fold range of actin concentration, the rate of recombination of the S-1-substrate complex with actin equals the steady-state ATPase rate and most important, like it, levels off at high actin concentration. Therefore, in contrast to the Lymn-Taylor model, product release is not the rate limiting step in the cycle but rather the S-1-substrate complex undergoes two conformational changes before rebinding to actin. The first conformational change causes a fluorescence change which may be related to the initial P_i-burst. The second conformational change is about ten-fold slower than the fluorescence change, equals the maximum actin-activated ATPase rate, and thus represents the rate limiting transition from the refractory to the non-refractory state previously proposed by Eisenberg and Kielley.

W-PM-F5 MYOSIN S-1 BINDING TO ACTIN, EFFECTS OF CONCENTRATION, NUCLEOTIDES, IONIC STRENGTH AND TEMPERATURE. Stefan Highsmith, Cardiovascular Research Institute, University of Calif., San Francisco, Cal. 94143.

The technique of time-resolved fluorescence anisotropy decay measurement was applied recently to determine the association constant, K_a, for myosin subfragment-1 (S-1) binding to F-actin in solution at submicromolar concentrations. (Highsmith et.al. Proc.Nat.Acad.Sci. USA, in press). At 4°C, 0.15M KCl, 0.010M N-(tris(hydroxymethyl)methyl)-2-amino-ethane sulfonic acid (TES), pH 7.0, K_a and standard error were $(1.73\pm0.35)\times10^6 M^{-1}$ for infinitely dilute S-1 in the presence of actin. The apparent association constant, Kapp, increased when the ratio of total S-1 to total actin was increased; this was interpreted as resulting from secondary (S-1)-(S-1) interactions either in solution or when bound to actin. Magnesium pyrophosphate ($MgPPi^{2-}$) and magnesium adenylimido-diphosphate ($MgAMPPNP^{2-}$) caused complete dissociation of S-1 from actin at about 10-fold molar excess. Magnesium adenosine-5'-diphosphate ($MgADP^{-}$) reduced Kapp but failed to cause complete dissociation even at 200-fold molar excess implying formation of a ternary ADP-(S-1)-actin complex. Kapp was affected only slightly by nucleotides & analogs in the absence of magnesium. K_a increased regularly with temperature between 4 and 25°C. K_a decreased with increasing ionic strength between 0.05 and 0.5M KCl or tetramethyl ammonium chloride. Supported by USPHS Grant HL 16683, NHLI Grant HL 05251, and NSF Grant GB24992-X.

W-PM-F6 EFFECTS OF KCl UPON THE ACTIN-MYOSIN INTERACTION. R. Crooks and R. Cooke, Dept. of Biochemistry and Biophysics, University of California, San Francisco, CA 94143

In an effort to assess the relationships that exist among various *in vitro* systems used to study the actomyosin interaction, we have measured the dependence of several experimental parameters on the concentration of KCl. Previous investigators have measured the KCl concentration dependence of some of these systems under a variety of conditions. Here we report a more direct comparison between the assay systems. The association constant for acto-SF-1 in the absence of ATP (K) has been measured by Dr. Stefan Highsmith (see abstract in this volume) using a fluorescence depolarization technique. K displayed a strong dependence on [KCl], becoming weaker at high concentrations of KCl. Our results show that the following parameters display a dependence on [KCl] which is similar to that of K: i) The ATPase activity of actomyosin. ii) The 1/[actin] intercept of a double reciprocal plot of actoSF-1 ATPase activity. iii) The velocity of superprecipitation. These results are consistent with a model in which the rate limiting step determining these parameters involves the binding of myosin and actin. In contrast, ATPase activity of actoSF-1 extrapolated to infinite actin concentration (V_m) showed only a slight dependence on [KCl]. The isometric tension of glycerinated fibers and of actomyosin threads also decreased only slightly as [KCl] was increased. These results indicate that the rate limiting steps which determine V_m or the generation of tension are different from those that govern the other *in vitro* parameters. The binding of actin and myosin is probably not rate limiting in the generation of tension by muscle fibers or actomyosin threads.

Supported by USPHS AM 17559 and NSF BMS-75-14793. R. Cooke is an Established Investigator of the A.H.A.

W-PM-F7 RECIPROCAL REACTIVITIES OF SPECIFIC THIOLS WHEN ACTIN BINDS TO MYOSIN. J. Duke, R. Takashi*, K. Ue*, M.F. Morales, Cardiovascular Research Institute, University of California, San Francisco, Ca. 94143.

We report measurements of the reactivity (degree of labelling, as mole ligand/mole protein, at constant exposure time) of the reactive thiol, "SH_1", of myosin-S-1, and of Cys-10 of F-actin under various conditions, using "1,5 IAEDANS", a fluorescent/radioactive iodoacetamide analog. When either ADP or AMPPNP (simulating unhydrolyzed ATP) are bound to the enzymatic site of S-1, the reactivity of "SH_1" is slightly enhanced, but, when active ATPase is going on, reactivity is ca. (1/3)-reduced, presumably due to the species, (S-1)**ADP,P_i. The reactivity of Cys-10 alone is very low. When the complex, (S-1) F-actin, has been formed, the reactivity of SH_1 is strongly decreased, and the reactivity of Cys-10 is strongly increased. The foregoing results explain our further observation (on glycerol-treated rabbit psoas fibers) that when fibers labelled in relaxation solution are compared with fibers labelled in rigor solution, myosin is more reactive, and actin less reactive, in the former case; α-actinin and tropomyosin are also less reactive in the former case.(Proc. Nat.Acad.Sci., in press). Supported by National Heart and Lung Institute HL-16683, National Science Foundation GB-24992-X and American Heart Association CI-8.

W-PM-F8 INTERACTION OF 1,N^6-ETHENOADENOSINE 5'-DIPHOSPHATE (ε-ADP) WITH ENZYMATIC MYOSIN SUBFRAGMENTS: A FLUORESCENT PROBE STUDY. Frank Garland and Herbert C. Cheung, Department of Biomathematics, Biophysics Section, University of Alabama in Birmingham, Birmingham, AL 35294.

Equilibrium dialysis and stopped-flow kinetic experiments were done in order to elucidate the mechanism by which ε-ADP, a fluorescent probe, binds to proteolytic subfragments of myosin. All measurements were done at 4°C in 0.1 M KCl, 5 mM $MgCl_2$, 50 mM Tris, pH=8. Non-linear least squares analysis of the binding data indicates that the two active sites are identical and non-interacting. The stopped-flow experiments utilized energy transfer from the tryptophan residues to the fluorescent probe, thus allowing a direct measurement of the ligand-protein complex. Heavy meromyosin (HMM)/ε-ADP experiments showed two distinct phases: a very rapid phase which requires further elucidation, and a slow phase. The slow phase fits a single exponential yielding an apparent first order rate constant of 7 sec^{-1}, which was found to be independent of concentration, and an amplitude proportional to the amount of complex formed - the latter calculated on the basis of the equilibrium dialysis experiments. Analogous experiments with subfragment-1 (S-1) gave a concentration independent k_{obs} of 1 sec^{-1} with the amplitude again proportional to the amount of complex formed. We conclude that the observed stopped-flow traces are due to a first order transition involving the ligand-protein complex, and that apparently this transition is facilitated by the attachment of the globular heads to the rod fragment. (Support by AM17483 and GM5283 of U. S. P. H. S.)

W-PM-F9 CHEMICAL MODIFICATIONS OF SPIN-LABELED HEAVY MEROMYOSIN. D.B. Stone and P.H. Cheung*, Cardiovascular Research Institute, University of California, San Francisco, California, 94143.

It has previously been shown that a paramagnetic derivative of iodoacetamide reacts specifically with the fast-reacting thiols of heavy meromyosin (HMM). EPR spectra reveal that the spin labels are strongly immobilized by such reaction. Binding of nucleotide (ADP, AMP-PNP, or ATP in the absence of hydrolysis) partially mobilizes the spin labels, while the labels are further mobilized during steady state hydrolysis of ATP. In the present study, spin-labeled HMM (SL-HMM) has been subjected to specific chemical modifications. Reaction with four moles of trinitrobenzenesulfonate caused little change in the EPR spectrum of SL-HMM, but severely impaired the spectral changes accompanying nucleotide binding and hydrolysis. Reaction with one mole of p-nitrothiophenol in the presence of MgATP partially impaired the spectral change accompanying ATP hydrolysis without altering the effect of nucleotide binding. Reaction with one or two moles of 2-hydroxy-5-nitrobenzyl bromide at pH 6 caused partial impairment of both spectral changes. These results suggest the participation of lysyl and tryptophanyl residues in nucleotide binding and hydrolysis; glutamyl residues appear to participate only in the hydrolysis of nucleotide. Supported by USPHS Grants HL 06285 and HL 16683 and NSF Grant GB 24992-X.

W-PM-F10 AFFINITY OF CREATINEPHOSPHOKINASE FOR MYOSIN AND ITS FRAGMENTS. J. Botts and A. Wang*, Cardiovascular Research Institute, University of California, San Francisco, California 94143.

Nanosecond fluorescence depolarization studies on creatinephosphokinase (CPK) labeled with dansyl chloride indicate interaction of CPK with myosin, heavy meromyosin (HMM), subfragment-1 (S-1), and light meromyosin (LMM). Analysis of the data yields affinity constants for the binding of CPK to these moieties. Values lie between 10^5 and $10^6 M^{-1}$, the affinity for LMM being the smallest. The interaction of CPK with myosin shows a time dependence not evident with the other moieties of myosin. Experiments were carried out at 25°C and pH 8.0 - 8.3, in the presence of 0.4 to 2.0 mM MgATP, 6 to 12 mM phosphocreatine, and 0.17 to 0.25 M KCl. This work was supported by U.S. Public Health Service Grant HL 06285 and American Heart Association Grant 72-991.

W-PM-F11 BINDING OF C-PROTEIN TO F-ACTIN. C. Moos, J. H. Dubin*, C. M. Mason* and J. M. Besterman*, Biochemistry Dept., State Univ. of N.Y., Stony Brook, N.Y. 11794.

C-protein, a minor component of skeletal muscle myofibrils, is known to be located at specific positions on the shaft of the thick filaments in vivo and to bind strongly to myosin rod or light meromyosin in vitro [Offer, Cold Spring Harbor Symp. 37,87 (1972); Moos, J. Mol. Biol. 97, 1 (1975)]. We now find that C-protein can also interact with F-actin. When a mixture of C-protein and actin is centrifuged 1 hr at 100,000g the C-protein in the supernatant is depleted relative to a control centrifuged in the absence of actin, and a quantitative measure of binding may be obtained in this way. The C-protein-actin binding is reversible, and in 0.05 M KCl, 1 mM $MgCl_2$, 0.2 mM ATP, 10 mM K-phosphate, 0.5 mM DTT, pH 7, Scatchard plots give a limiting stoichiometry of 1 C-protein per 4 to 6 actin monomers and an affinity of about $10^6 M^{-1}$. The binding is not much affected by temperature between 5° and 25° or by omission of ATP. Increased salt weakens the interaction, and no binding is observed above 0.25 ionic strength. The interaction of C-protein with F-actin is accompanied by an increase in turbidity and a decrease in viscosity, possibly due to aggregation of the actin filaments. Addition of myosin subfragment-1 (S-1) in the absence of ATP inhibits the binding of C-protein to actin, and in the presence of ATP, actin activation of S-1 ATPase is inhibited by C-protein. These observations suggest a competition between C-protein and S-1 for binding to actin. Although C-protein-actin binding under physiological conditions would be weaker than C-protein-myosin binding, it might nevertheless be significant in providing weak cross-links between the thick and thin filaments at rest or in modifying the interaction of myosin cross-bridges with actin during contraction. (Supported by grants from the National Science Foundation and the SUNY Research Foundation.)

W-PM-F12 CHANGES IN CANINE CARDIAC MYOSIN ACCOMPANYING HYPERTROPHY. R. F. Siemankowski and P. Dreizen. Department of Medicine and Program in Biophysics, S.U.N.Y., Downstate Medical Center, Brooklyn, N.Y., 11203.

Studies have been conducted on canine myosins purified from left (LV) and right (RV) ventricles of normal hearts and hypertrophied hearts (approximately five weeks after aortic banding). A method of preparation involving the use of sodium sulfite and pepstatin was developed which yielded myosin that was essentially free from proteolysis, in the case of normal tissue. The following results were obtained: 1) The heavy chains (HC) from myosin of hypertrophied hearts show considerable degradation on SDS-gels; ca. 27% of LV myosin HC, and ca. 43% of the RV myosin HC appear as bands with apparent mass of 130,000-to-180,000 daltons. 2) Two weight classes of light chains (LC) are observed on SDS-gels, without significant differences in mass among myosins prepared from normal and hypertrophied LV and RV. The weight proportion of LC is somewhat greater in hypertrophied LV and RV myosin, by this method. 3) Charge electrophoresis of purified LC does not demonstrate any differences related to hypertrophy. 4) High speed sedimentation equilibrium experiments of myosin at pH 11.3 demonstrate that the mass and proportion of HC-core and LC are comparable in all cases. 5) K^+/EDTA ATPase is substantially reduced in myosins prepared from hypertrophied LV and RV, whereas Ca^{++} ATPase is relatively unchanged. The overall findings indicate that, subsequent to aortic banding, myosin HC undergo limited proteolysis; however the integrity of the HC-core is maintained via secondary interactions under benign solvent conditions. This proteolysis and concomitant decrease in myosin ATPase may, in part, account for the diminished contractility previously observed in cardiac hypertrophy.

W-PM-G1 POLAR HEAD GROUP SPECIFICITY IN LIPID-PROTEIN INTERACTIONS. P.C. Jost and O.H. Griffith, Institute of Molecular Biology, University of Oregon, Eugene, Oregon 97403.

The hydrophobic surfaces of integral membrane proteins bind (immobilize) lipids. This has been demonstrated previously by a fatty acid spin label diffused into vesicles containing lipid and integral membrane proteins (phospholipid vesicles containing cytochrome oxidase, mitochondrial ATPase, sarcoplasmic reticulum ATPase, or liver microsomal cytochrome b_5) and noting that a bound component is present as well as the expected fluid bilayer component. These data have been interpreted as evidence for a boundary layer of lipid interacting directly with the hydrophobic regions of the membrane proteins. Quantitative analyses of these data have established that the lipid immobilized by the protein remains relatively constant regardless of the extent of the competing lipid bilayer. We are now examining the ionic contribution to this lipid-protein association. Lipid spin labels differing only in the polar head group have been diffused into cytochrome oxidase membranous vesicles. Polar head groups examined include carboxyl, quaternary amine, and alcohol groups. The most striking effect is the partial exclusion of the quaternary amine from the boundary layer.

W-PM-G2 THE VIBRATIONAL FINE STRUCTURE OF PYRENE MONOMER FLUORESCENCE AS A PROBE OF LIPOPHILIC ENVIRONMENTS. V. Glushko, C. Karp*, and M. Sonenberg, Memorial Sloan-Kettering Cancer Center, New York, New York, 10021.

The fluorescence characteristics of pyrene are amenable to a wide range of biophysical investigations concerning static and dynamic properties of lipophilic environments. The monomer has vibrational fine structure that is poorly resolved with normal broadband measurement of emission. In cyclohexane, at least five distinct peaks are evident at 373, 379, 384, 389 and 394 nm with relative intensities of 1:0.96:1.58:1.11:1.17, respectively. The distribution of the peaks is characteristic of the environment with a minor temperature dependence from 8° to 50°. With increasing dielectric, the transitions undergo a limited red shift and a relative increase in the 374 nm peak until it dominates the emission. Within the experimental limits, the pattern appears independent of viscosity and quenching effects. By considering the relative intensities, an assessment independent of quantum yield can be made of the pyrene environment. This is particularly useful since the monomer excited state is sensitive to a variety of quenching mechanisms, including ground state monomers. To determine the applicability of this procedure to biological samples, high resolution spectra were obtained for pyrene incorporated into liver plasma membranes. Partial degradation by trypsin and phospholipases A and C produced different, time-dependent effects upon the fine structure, indicative of decreased dielectric. Sonication had a minimal effect on the pyrene compartment in normal or partially degraded membranes. Oxygen quenching reduced the overall emission without altering the relative peak intensities. Although the effect of more subtle measures is yet to be elucidated, it is evident that vibrational fine structure provides a useful characterization of the pyrene environment. (Supported by grants from the American Cancer Soc., BC-119, and from the NIH, CA-08748 and CA-16889).

W-PM-G3 ALTERATIONS IN MEMBRANE FLUIDITY AND GROWTH OF ENVELOPED MYCOPLASMAVIRUSES. R. M. Putzrath and J. Maniloff, Departments of Radiation Biology and Biophysics and of Microbiology, University of Rochester Medical Center, Rochester, New York 14642.

Acholeplasma laidlawii cells have only one membraneous structure, the bounding cell membrane, and the membrane order-disorder transition temperature is determined by the fatty acids available in the growth medium. A. laidlawii JA1 grown in tryptose broth containing serum fraction, JA1(t), incorporates cholesterol and a variety of fatty acids, yielding membranes with transition temperature below 0°C, as measured by differential scanning colorimetry. Cells grown in lipid extracted medium supplemented with palmitate, JA1(p), have a transition midpoint around 37°C. JA1 can be infected by MVL2, an enveloped DNA mycoplasmavirus which is bounded by a unit membrane. The infection is not lytic, as indicated by one-step growth and artificial lysis experiments and the observation that viruses produce turbid plaques on JA1 lawns. MVL2 has been grown on both JA1(t) and JA1(p) cells producing MVL2(t) and MVL2(p), respectively. Preliminary one-step growth experiments, at 37°C, show that MVL2(p) on JA1(p) cells has a longer latent period than MVL2(t) on JA1(t) cells. Reciprocal crosses, MVL2(p) on JA1(t) and MVL2(t) on JA1(p), suggest that virus growth is altered on the JA1(p) cells. Similar studies at lower temperatures are in progress. (Supported by USPHS Grant No. AI-10605).

W-PM-G4 HEXAGONAL PACKING OF PHOSPHOLIPID ACYL CHAINS AND MEMBRANE FLEXIBILITY.
D. L. Dorset[1], S. W. Hui[2], and C. M. Strozewski[1,2,*]Molecular Biophysics Department, Medical Foundation of Buffalo, Buffalo, N. Y. 14203[1], and Biophysics Department, Roswell Park Memorial Institute, Buffalo, N. Y. 14263[2]

Thin films of long chain lipids have been proposed to have enhanced stability when the polymethylene packing is hexagonal (a=4.80Å, α=120°) rather than in any of the more "crystalline" subcells (Larsson (1975) *Chem. Phys. Lipids* 14: 233). This is directly visualized in electron micrographs of microcrystals of several hexagonally-packed phospholipids. When undistorted, crystals exhibit a terraced growth around a screw dislocation with radial symmetry. Physical stresses imposed by crystallization conditions, on the other hand, are compensated by dramatic folds of the crystal surface (rather than the shear planes seen in stressed orthorhombic paraffin crystals) which demonstrate the extreme flexibility of the layers. Additionally. outgrowths are often seen on the crystal surfaces, sometimes nucleating dendritic epitaxial growths of other crystal phases. Hexagonal aliphatic packing also is correlated with membrane flexibility in electron diffraction patterns and dark field images from wet single lecithin bilayers and from several unfixed, unstained, wet cell membranes.

Research supported by NIH Grants GM 21047 and CA 15330.

W-PM-G5 NEUTRON DIFFRACTION STUDIES ON THE PURPLE MEMBRANE OF HALOBACTERIUM HALOBIUM.
G. I. King and W. Stoeckenius, Cardiovascular Research Institute and Department of Biochemistry and Biophysics, University of California, San Francisco 94143. B. P. Schoenborn, Department of Biology, Brookhaven National Laboratory, Upton, New York 11973.

The purple membrane in Halobacteria functions as a light-driven proton pump; its protein, bacteriorhodopsin, contains retinal covalently bound through a Schiff base linkage which is protonated in the dark and unprotonated in the light. Thus the Schiff base linkage may be directly involved in the proton translocation. The large difference in neutron scattering between hydrogen and deuterium allows one to perform neutron experiments analogous to isomorphic replacement with heavy metal derivatives in X-ray diffraction. Halobacteria were grown in D_2O under otherwise normal conditions. The purple membrane isolated from these bacteria contained retinal which is about 60% deuterated. Neutron diffraction data were obtained from the deuterated membranes and from deuterated membranes whose retinal was replaced with normal retinal as well as from chromophore-free "apo-membrane." Analyses of the observed differences in this data allow the position of retinal in the membrane to be determined.

W-PM-G6 THE PHYSICAL STATES OF NERVE MYELIN AS A FUNCTION OF pH USING X-RAY DIFFRACTION.
C.R. Worthington, Department of Biological Sciences and Physics, Carnegie-Mellon University, Pittsburgh, Pa. 15213.

It has been established in previous x-ray studies on peripheral nerves that after certain physical and chemical treatments, the myelin layers can be in a number of different physical states. These are the normal, the swollen, the subnormal, the separated and the condensed states. The separated and condensed states are each double depending on whether the unit cell contains one or two membranes. X-ray diffraction patterns have been recorded using immersion fluids which have a pH range of 0.5 to 13 and a total of 7 distinct states have been identified. Nerve myelin is in the normal state for a pH between 5 and 9. The nerve myelin structure goes into separated state II when the pH is made more alkaline, i.e., above 9 and finally it goes into separated state I when the pH is increased to above 12. When the immersion fluid is made more acid (from neutral pH) the nerve myelin structure goes into the swollen (or into the subnormal) state in the pH range of 2.4 to 5. In a narrow range of pH 2.0 to 2.4 anomalous swelling takes place in that swelling occurs in units of four membranes. This pH swelling of peripheral nerve myelin closely resembles that of optic nerve myelin (Lalitha and Worthington, J. Mol. Biol., 1975). In the acid pH range of 0.5 to 2.0 the nerve myelin structure is in condensed state I. There is a reversible transformation between condensed state I, the anomalous swollen state and separated state I on changing the pH of the immersion fluid.

W-PM-G7 SMALL-ANGLE X-RAY SCATTERING FROM MITOCHONDRIAL SUSPENSIONS. C.A. Mannella and D.F. Parsons, Electron Optics Lab., Roswell Park Memorial Institute, Buffalo, N.Y. 14263.

The small-angle x-ray scattering from dense, fully-hydrated, unoriented suspensions of intact rat liver mitochondria has been monitored using a Kratky camera diffraction system. The x-ray scattering characteristics of these suspensions vary with time, so that scans of the small-angle region ($1/r^* = 300$ to 30 Å) must be completed within 2 to 3 h. Suspensions of freshly isolated mitochondria at 5°C display a broad scattering maximum centered at 80 Å. Within 6 h after isolation, this scattering maximum moves to smaller angle (100 Å), accompanied by a marked decrease in the slope of the initial portion of the scattering curve. Furthermore, the integrated intensity of the x-ray diffraction maximum decreases significantly within 18 to 24 h after mitochondrial isolation. The early shift of the scattering maximum to smaller angle appears to correlate with the spontaneous swelling of isolated liver mitochondria, similar scattering changes being induced by deliberate osmotic swelling of the mitochondria. Prolonged (3 to 5 h) suspension of mitochondria in hypotonic (40 mOsm) media, followed by brief (5s) sonication, abolishes the small-angle x-ray scattering maximum, as does acetone extraction of the mitochondria. Experiments are underway to determine how the small-angle x-ray scattering of mitochondria varies with metabolic state and to identify the mitochondrial structure(s) responsible for the observed diffraction maximum. (C.A.M. is supported by Fellowship Number 5 F22 CA00785, awarded by the National Cancer Institute, DHEW).

W-PM-G8 MACROMOLECULAR CHARACTERIZATION OF AXON PLASMA MEMBRANES. G.K. Chacko*, G.M. Villegas*, F.V. Barnola*, R. Villegas and D.E. Goldman. Dept. of Physiology and Biochemistry, The Medical College of Pennsylvania, Philadelphia, Pa. and Centro de Biofisica y Bioquimica, Institute Venezolano de Investigaciones Cientificas (IVIC), Apartado 1827, Caracas, Venezuela.

The axon plasma membrane fractions isolated from garfish olfactory and lobster leg nerves were shown to contain specific tetrodotoxin receptors. In lobster nerve membrane preparation, functioning sodium channels have been detected by studying the efflux of ^{22}Na from membrane vesicles in the absence and presence of veratrine (or batrachotoxin) as well as tetrodotoxin. In the present study, the axon plasma membrane fractions from these two nerves were analysed for their polypeptide and glycopeptide components by SDS polyacrylamide gel electrophoresis. Eleven major and about ten minor polypeptides were found in garfish nerve membrane. None of the major polypeptide species present in this membrane showed any noticeable PAS staining and only trace of sialic acid could be detected in the membrane protein. Eight of the eleven major polypeptide species found in garfish nerve membrane were also found as major components in lobster nerve membrane. The molecular weights of the major polypeptides range from about 130,000 to 22,000. A very low activity of acetylcholinesterase was detected both by biochemical analysis and by histochemical technique combined with electron microscopy in the garfish axon plasma membrane whereas this enzyme was found in high concentration in the lobster nerve membrane. Assays for this enzyme in axon plasma membranes from various nerve sources showed a large variation in activity indicating that the amount of enzyme may be related to the extent of axon-glial cell membrane interactions that may exist in these nerves. Supported by NIH Grant No. NS-07595.

W-PM-G9 ALTERED INCORPORATION OF OUTER MEMBRANE PROTEINS IN MUTANTS OF ESCHERICHIA COLI DEFECTIVE IN LIPOPOLYSACCHARIDE BIOSYNTHESIS. E. J. McGroarty, Biophysics Department Michigan State University, E. Lansing, Mich. 48824.

Three mutants of E. coli D21 were studied which lack a portion of the polysaccharide component of the outer membrane's lipopolysaccharide. Cytoplasmic and outer membranes from these three mutants as well as those from the parent strain were isolated on sucrose density gradients. The outer membrane of these mutants were less dense than that of the parent strain. In addition, the mutant cells had less protein associated with the outer membrane, and when the proteins of the outer membrane were electrophoresed on sodium dodecyl sulfate (SDS) polyacrylamide gels, the mutant strains appeared to contain less of the major 36,000 to 40,000 dalton protein components than the wild type cells. The alterations in the composition of the cytoplasmic membrane of the mutant strains, as expected, were less pronounced. There was little change in the density of the inner membranes of these mutants. Separation of the cytoplasmic membrane proteins on SDS polyacrylamide gels indicated a slight increase in outer membrane proteins in the cytoplasmic membrane fractions of the mutant strains compared to that of the wild type strain. In addition, there was an increase in the amount of several cytoplasmic membrane specific proteins in the inner membrane fractions of the mutant strains.

W-PM-G10 FLUORESCAMINE AS A EXTERNAL MEMBRANE MARKER - ERYTHROCYTES AND FROG ROD OUTER SEGMENTS. L. Venkataraman, H. M. Garza* and D. S. Kirkpatrick, Dept. of Ophthalmology, Baylor College of Medicine, 1200 Moursund Ave., Houston, Tx. 77025.

Fluorescamine reacts with primary amines with $t_{1/2}$ about 0.5 sec to form fluorescent products and hydrolyses with $t_{1/2}$ about 5.0 sec to form a non-fluorescent product. The fluorescent covalent derivatives can then be identified with SDS-polyacrylamide gel electrophoresis. When intact erythrocytes were reacted with fluorescamine, plasma membrane proteins that have been shown by iodination experiments (Philips, D. R. and Morrison, M., BBRC, 40 (1970) 284) to be exposed to the external surface, were fluorescently derivatized. Fluorescent hemoglobin formation was less than 1% of control reaction. However, on reacting erythrocytes ghosts with fluorescamine, all plasma membrane components became fluorescent. Fluorescamine would become a useful tool in identifying, and isolating surface membrane components containing amino groups.

Rod outer segment proteins from "intact" plasma membrane, disrupted rod outer segments and isolated disc membranes of frog were treated with fluorescamine. The three preparations produced similar SDS-PAGE patterns. The fluorescent intensity of the rhodopsin band in the three samples was found to be different.

W-PM-G11 BARBITURATE INTERACTIONS WITH MEMBRANES. Brent Benson, Robert Hill*, and Jeffrey Sands, Molecular Biology graduate program and Physics Department, Lehigh University, Bethlehem, PA. 18015.

Because the sedative effect of barbiturate drugs is correlated with their membrane solubilities, these drugs are usually thought to act at the site of nerve membranes. We are investigating the effects of various commonly prescribed barbiturates on the physical properties of spin labelled membranes and phospholipid vesicles using ESR spectroscopy. Dipalmitoylphosphatidylcholine vesicles were labelled with a twelve carbon chain spin label 2N12 where the nitroxide group is on the second carbon. This spin label concentrates in the hydrocarbon region of lipid bilayers. The rotational correlation time τ_c of the spin label was determined as a function of temperature for vesicles exposed to a range of secobarbital concentrations. For drug concentrations in the range of 7mM to 24mM, the values of τ_c are significantly reduced from that of drug-free vesicles, indicating that the membranes have increased fluidity. For example, with 7mM drug concentration at 55°C, τ_c is reduced to 5.2×10^{-10}s from 5.8×10^{-10}s for the control. Arrhenius plots of τ_c versus 1/T show the difference of τ_c between drugged and control vesicles to be almost constant in the range of 20°C to 60°C, this difference being approximately proportional to the drug concentration. If this phenomena occurs in nerve cell membranes, it is possible that the drug induced fluidity increase interferes with normal nerve synapse processes.

W-PM-G12 ESR STUDIES TO CHARACTERIZE RADIATION DAMAGE ON THE TRANSPORT SYSTEMS OF ISOLATED E. COLI MEMBRANES. M. A. de la Rosa*, L. H. Piette, and B. McConnell, Department of Biochemistry & Biophysics, University of Hawaii, Honolulu, Hawaii 96822.

Co-60 gamma radiation decreases the active transports of α-methyl glucoside and the amino acids, glutamic acid and proline, across membrane vesicles of E. coli ML 308-225. Various spin labels have been employed to probe the lipid (4- and 15-doxyl stearic acid and androstane spin labels), and the protein (N-ethyl maleimide and iodoacetamide spin labels) portions of the membrane during irradiation. A decrease in the peak heights of the strongly (SI) and the partially (PI) immobilized components of the ESR spectrum is taken as a measure of radiation effects. Observations with the lipid probes show that radiation does not perturb the lipid bilayer to such a significant extent to account for the radiosensitivities of the transport systems. Data on the phase transition temperatures and the permeability of the irradiated membranes to ascorbate support these observations. The radiation effects on the protein probes are more pronounced. The membrane binds the N-ethyl maleimide at two sites which exhibit first-order dose-response curves and significantly different radiosensitivities the average of which parallels that of the amino acid transport system. On the other hand, the iodoacetamide-labelled membranes show second-order dose-response curves and higher radiosensitivities. The significance of these results in relation to the site and mode of radiation damage on the transport systems will be discussed.

W-PM-G13 SOLVENT PROPERTIES AND MEMBRANE MEMBRANE INTERACTIONS IN PHOSPHOLIPID MEMBRANES
Y. Katz, Room 4113, The Research Institute, The Hospital for Sick Children, 555 University Avenue, Toronto M5G 1X8, Toronto, Ontario, Canada.

Absorption of noble gases into dimirystoyllecithin lamella was used to derive the solvent properties of the hydrophobic region in phospholipid membranes and to estimate the membrane membrane interaction in this region. Free energies enthalpies and entropies of solution were derived by measuring the absorption as a function of temperature. The temperature range of measurement was between 30°C and 50°C. Typical values for absorption are the absorption coefficients for the noble gases at 30°C: helium 41.06 x 10^{-3}, neon 14.61 x 10^{-3}, argon 75.14 x 10^{-3}, krypton 112.74 x 10^{-3} and xenon 295.11 x 10^{-3}. The values for enthalpy were (in kcal): helium -4.7, argon -.032, krypton -0.94 and for entropy (in entropy units):helium 12.2, argon 24, krypton 21.2. Based on this data a rather general statistical mechanical model was used to estimate the cohesive energy density and the free volume inside the hydrophobic region of the membrane and to estimate the solvent properties of this region. The change in solubility from helium to xenon in the phospholipid was found to follow the general pattern of solubility of these gases in hydrophobic solvents, like simple hydrocarbons. This also applies to the cohesive energy densities and the free volumes. These similarities made it possible to formulate a correspondence law between solubilities in model systems, like bulk hydrocarbons, and lecithin membranes. Comparison of predicted solubilities in the hydrophobic region of the membrane with the solubilities of various compounds in lecithin membranes made it possible to estimate the solubilities of these compounds in the hydrophilic region of the membrane using some simplifying assumptions.

W-PM-H1 PROTEASE INHIBITION BY α-1-PROTEASE INHIBITOR (α-1-ANTITRYPSIN). J. W. Bloom* and M. J. Hunter, Biophysics Research Division and Department of Biological Chemistry, The University of Michigan, Ann Arbor, MI 48105.

α-1-protease inhibitor (α-1-PI) was purified from human serum by: a) adsorption on $Al(OH)_3$ gel and ammonium sulfate precipitation followed by, b) chromatography on DE-52 cellulose at pH 8.8, then c) blue dextran-Sepharose 4B affinity chromatography, and finally, d) chromatography on DE-52 cellulose at pH 6.5. The α-1-PI preparation was essentially homogeneous as determined by electrophoresis and by immunodiffusion against specific antisera. Two trace contaminants could be detected: albumin and α-1-T-glycoprotein. The specific activity of the preparation was 40-fold that of the original serum and the yield about 30%.

The molar stoichiometry of interaction of α-1-PI with both bovine trypsin and chymotrypsin was found to be 1:1 by disc gel electrophoresis and by protease inhibition assays. Trypsin and chymotrypsin were found to compete for the same binding site or for overlapping sites on α-1-PI. In the presence of both chymotrypsin and trypsin, the chymotrypsin was found to be preferentially bound by α-1-PI. α-1-PI formed a complex with chymotrypsinogen or with chymotrypsin treated with diisopropyl phospho-fluoridate in the presence of a 10-fold excess of these proteins. Under similar conditions, no binding of trypsinogen could be detected. Disc gel electrophoresis studies indicated that at a 2:1 ratio of α-1-PI to active chymotrypsin a complex was formed of mobility different from the complex formed at a 1:1 ratio. No such altered mobility occurred in the α-1-PI:trypsin interaction. These data will be discussed in terms of a mechanism of action for the inhibitor. (Supported by USPHS grants GM-1355 and HL-09739.)

W-PM-H2 PROPERTIES OF ORGANIZED ENZYMATIC PATHWAYS. E.S. Kempner, NIAMDD, NIH, Bethesda, Md. 20014

Many enzymes are associated with known cellular structures such as the endoplasmic reticulum, vacuoles and organelles. They are often part of a complex of enzymes catalyzing sequential reactions of a biochemical pathway.

Other studies involving small molecule intermediates have shown unequal mixing between exogenously and endogenously derived compounds, or non uniform labelling of a product derived from a substrate which itself has two different sources.

Restriction of enzymatic pathways to subcellular regions and the limitation on diffusion of small molecules implies unique properties of pathway reactions. Several different structures are described with varying degrees of "coupling" between enzyme and substrate. These lead to certain testable predictions including effects of exogenous competitors, the effect of genetic deletion or poisoning of a specific enzyme in the pathway, and the *in vivo* molar ratio of substrate to enzyme. Several experimental systems from the literature are shown to fit the different categories of organized enzyme systems.

W-PM-H3 STUDY OF THE STEROID BINDING SITE OF ESTRADIOL-17β DEHYDROGENASE BY DIFFERENCE SPECTROSCOPY. J.T. Lo and J.C. Warren, Department of Obstetrics and Gynecology, Washington University School of Medicine, St. Louis, Mo 63110

Homogeneous human placental estradiol-17β dehydrogenase was purified by affinity chromatography as described by C.C. Chin *et al.* (Steroids, 22:374, 1973). Difference spectroscopy was used to search for chromophore amino acid residues perturbed by the binding of steroid and therefore possibly at or close to the steroid binding site. Estradiol-17β, a substrate of the enzyme, produced a difference spectrum with a strong peak at 292 nm, a weak peak at 283 nm, and a very weak shoulder at 273 nm when it is added to the enzyme solution (in phosphate buffer, pH 7.0, containing 20% glycerol). The intensity of the difference spectrum was dependent on both enzyme and substrate concentrations. The difference spectrum is similar to the solvent perturbation difference spectrum of tryptophan produced by glycerol. The dissociation constant (Ks) of the enzyme-substrate complex was determined by measuring the difference spectrum as a function of substrate concentration. Estrone, another substrate of the enzyme, produced a similar difference spectrum, but with weaker intensities than in the case of estradiol-17β. However, estradiol-3-methyl ether and testosterone (also enzyme substrates) when incubated with the enzyme produced no difference spectrum in the 270-295 nm range. These results indicate that binding of estradiol-17β at the steroid binding site perturbs a tryptophanyl residue and suggests that this residue proximates the 3-position of the steroid.

W-PM-H4 MODULATION OF ENZYMIC ACTIVITIES THROUGH LOW ENERGY IRRADIATED SUBSTRATES. S.Comorosan, P.Murgoci*, B.Chitimia* & B.Vladescu* - Department of Biochemistry, Postgraduate Medical School, Bucharest, Romania.

We have presented evidence (Int.J.QuantumChem.1,221,1974) that irradiation of enzymic substrates in crystalline state with visible light (5461 Å Hg line) results in an enhancement of the corresponding enzyme catalyzed reaction rate. This effect appears if and only if the substrates irradiation times are sharply defined. We have termed the irradiation times of the substrates that induce enzymic rate enhancements efficient irradiation times (t_{ef}). They are obtained by the formula: $t_{ef}=t_m+n\tau$, n=0,1..... The numeric values of the t_m and τ are completely enzyme-dependent. They appear as a new type of macroscopic enzymic parameters. This effect seems to be quite general. By the same irradiation technique the growth rate of yeast auxotrophic strains (ex: tr^-, hi^-) is increased, when the corresponding growth factor (i.e. tryptophan, histidine) is irradiated. So far there is no spectroscopic evidence for the physical transition induced in substrates through this special irradiation procedure. However, the enzymic substrates activated in this manner seem to have an "excited-type" of behavior. We have observed a decay in time concerning the ability of the irradiated substrates to induce the effect. Unexpectedly this decay is particularly slow, of the order of about 1 hr. Although these long excited states have not been directly demonstrated in vivo, some symmetries with respect to the numerical values of the t_m and τ parameters, may suggest a metabolic significance.

W-PM-H5 MAGNETIC RESONANCE STUDIES OF HOG KIDNEY HISTAMINASE (DIAMINE OXIDASE). M. D. Kluetz, Department of Chemistry, University of Idaho, Moscow, ID 83843 and P. G. Schmidt, Department of Chemistry, University of Illinois, Urbana, Illinois 61801.

Our nuclear magnetic relaxation studies of the interaction of various probe molecules with the enzyme hog kidney histaminase (diamine oxidase; diamine: O_2 oxidoreductase [deaminating], EC 1.4.3.6) in an attempt to localize the Cu(II) and hence elucidate its function indicate that the only moiety which comes within a reasonable bonding distance of the Cu(II) (with the exception of at least two non-equivalently bound waters) is the imidazole ring portion of histamine analogs. These results indicate that the metal does not serve to bind and correctly orient the reacting substrate molecule, namely the amino group to be oxidized, as had been postulated. The imidazole portion of the histamine analogs only binds near the metal ion at high concentrations. This correlates with the observation of inhibition of this enzyme at high substrate concentrations with almost all of its substrates. We propose that the Cu(II) may serve as a structural factor and/or as a mediator of this process of substrate inhibition.

This work was made possible by a grant from the National Institutes of Health GM18038 (to PGS) and a Biophysical Traineeship GM00722 (to MDK).

W-PM-H6 TRANSIENT STATE KINETIC STUDIES OF ($Na^+ + K^+$) ADENOSINE TRIPHOSPHATASE. J. P. Froehlich*, R. W. Albers *, and G. Koval*, Laboratory of Molecular Aging, N.I.A., National Institutes of Health, Baltimore City Hospitals, Balt., MD. 21224, and Laboratory of Neurochemistry, N.I.N.D.C.D.S, National Institutes of Health, Bethesda, MD. 20014. Introduced by Gunther L. Eichhorn.

A rapid mixing technique was used to investigate the time course of the partial reactions of ATP hydrolysis catalyzed by a microsomal preparation of ($Na^+ + K^+$) ATPase. In the presence of 100 mM Na^+ and absence of K^+ inorganic phosphate (P_i) production lagged during the initial build up of phosphorylated enzyme and then appeared at a constant rate. This behavior is consistent with a scheme in which P is liberated as a consequence of breakdown of the acid-stable phosphoenzyme. When 2.5 mM K^+ was present in the reaction mixture with 100 mM Na^+ phosphoenzyme formation showed a transient overshoot while P_i production was resolved into two phases consisting of an initial 'burst' and slow linear phase. The burst which followed a brief lag in P_i production coincided with the transient decay in phosphoenzyme. As a possible explanation for these findings a model is proposed in which the acid-stable phosphorylated enzyme (E~P) breaks down to an acid-labile phosphoenzyme intermediate complex (E·P):

$$E + ATP \rightleftharpoons E\cdot ATP \xrightleftharpoons{Na^+} E \sim P \xrightleftharpoons{K^+} E\cdot P \longrightarrow E + P_i$$

The E·P intermediate which is dependent on K^+ for its formation decomposes in acid and is thus responsible for the initial P_i 'burst'. Examination of the substrate dependence of these reactions showed that the rate of E·P breakdown increased with ATP concentration implicating an additional role for ATP in the overall pathway.

W-PM-H7 KINETIC STUDIES ON THE MECHANISM OF BACTERIAL NAD(P)H:FMN OXIDOREDUCTASE. S.C. Tu*, J.E. Becvar, and J.W. Hastings, The Biological Laboratories, Harvard University, Cambridge, Mass. 02138.

NAD(P)H:FMN oxidoreductase (flavin reductase) catalyzes the reduction of flavin using reduced pyridine nucleotide. Such enzyme activities have been found in luminous bacteria. It is postulated that flavin reductase couples with bacterial luciferase and supplies $FMNH_2$ *in vivo* as a substrate for the bioluminescent reaction. To delineate the mechanism of flavin reductase, we have carried out kinetic studies with the enzyme partially purified from *Photobacterium fischeri*. The flavin reductase activity, at 23° in 0.1 M phosphate, pH 7, containing 0.05% or 0.2% bovine serum albumin, was first determined as a function of NADH concentration at constant levels of FMN, and then as a function of FMN concentration at constant levels of NADH. In both cases, the double reciprocal plots showed a series of parallel lines indicative of a ping-pong mechanism. The Michaelis constants for NADH (FMN saturating) and FMN (NADH saturating) were determined at 23° to be 2.2×10^{-4} M and 1.2×10^{-4} M, respectively. The suggested ping-pong mechanism was further supported by the observations that NAD^+ is a competitive inhibitor for FMN, but functions as a noncompetitive inhibitor for NADH. We also found that the reductase was not inactivated by treatment with 2.4×10^{-4} M N-ethylmaleimide (NEM) at 0° in the presence or absence of FMN, but the copresence of 10^{-4} M of NADH caused effective inactivation of this enzyme by NEM. These findings suggest that flavin reductase shuttles between an oxidized (disulfide-containing) form and a reduced (sulfhydryl-containing) form during catalysis. [Supported by an NSF grant (BMS74-23651) to J.W.H. and by NIH grants to S.C.T. (1 F32 GM00348-01) and to J.E.B. (4 F02 GM55606-03)]

W-PM-H8 LINOLEIC ACID HYDROPEROXIDE - HEME COMPOUND ACTIVATION OF THE CARCINOGEN N-HYDROXY-2-ACETYLAMINOFLUORENE. INHIBITION BY ASCORBATE. R. A. Floyd, L. Soong*, M. Stuart* and R. N. Walker*, Biomembrane Research Laboratory, Oklahoma Medical Research Foundation, Oklahoma city, OK 73104

Linoleic acid hydroperoxide (LAHP) plus either hematin or methemoglobin activates the carcinogen N-hydroxy-2-acetylaminofluorene (N-OH-AAF) into two more potent carcinogens, Nitrosofluorene and N-acetoxyacetylaminofluorene. This was shown optically as well as by thin layer chromatography. The nitroxyl free radical of N-OH-AAF was observed by ESR techniques to be an intermediate in the reaction. The kinetics of the reaction studied by optical means indicated that the rate of nitrosofluorene accumulation paralleled the rate of LAHP decrease and that N-OH-AAF decrease surveyed at 301 nm exhibited two phases, a fast phase that corresponded to the nitrosofluorene and LAHP kinetics and a much slower phase. Ascorbate inhibited N-OH-AAF activation. The carcinogen nitroxyl radical intermediate was replaced by the ascorbate free radical during ascorbate inhibition of the reaction. The carcinogen nitroxyl radical was observed with as small amount of LAHP as 1.8 μM. Supported in part by NIH grant 1 R01 CA 18591-01.

W-POS-C1 INDUCTION OF NONREJOINING DNA BREAKS IN MAMMALIAN CELLS BY HIGH-LET RADIATIONS. M.A. Ritter* and J.E. Cleaver, Laboratory of Radiobiology, University of California, San Francisco, CA 94143; G.P. Welch* and C.A. Tobias, Donner Laboratory, Lawrence Berkeley Laboratory, Berkeley, CA 94720

Chinese hamster cells (V79-S171) were irradiated with X rays and low-energy, charged particles, covering an LET range of from 9.5 keV/μm to 1950 keV/μm. The LET dependency of DNA-strand break production and the fraction of breaks that could not rejoin during postirradiation incubation were determined using alkaline sucrose gradient techniques. Results indicate that the efficiency for production of breaks decreases with increasing LET. The efficiency of nonrejoinable break production, however, increases to 4.8 times the X ray value at an LET of 150 keV/μm, and then decreases with further LET increase. This peaked LET response for nonrejoinable-break production is similar to the pattern that the RBE for cell killing exhibits as a function of LET. Work performed under the auspices of the U.S. Energy Research and Development Agency.

W-POS-C2 IN VIVO REJOINING OF DNA STRAND BREAKS IN X-IRRADIATED CEREBELLAR NEURONS AND BRAIN TUMOR CELLS. T.S. Wang*and K.T. Wheeler, Brain Tumor Research Center University of California, San Francisco, CA 94143.

The entire head of Fisher 344 rats bearing the 9L intracerebral tumor were irradiated with 4700 rads of x-rays and the tumor and cerebellum removed at various times after irradiation. Both the neurons and tumor cells were separated into single cell suspensions, and layered on 10-30% alkaline sucrose gradients in slow reorienting Ti-15 zonal rotors. The DNA sedimentation profiles were similar for unirradiated cerebellar neurons and the unirradiated intracerebral tumor cells. However, at every postirradiation time interval investigated (9 min to 30 hr) the extent of the DNA rejoining in the tumor cells was always greater than that observed in the cerebellar neurons. This differential response between neurons and brain tumor cells could be critical for the design of brain tumor radiotherapy schedules. Supported by NIH Grants CA-15203, CA-13525 and an RCDA NS70739 (KTW).

W-POS-C3 FRAGMENTATION OF CHROMATIN WITH ^{125}I RADIOACTIVE DISINTEGRATIONS. W. C. Dewey, G. Turner*, and P. Nobis*, Dept. of Radiology & Radiation Biology, Colorado State Univ., Fort Collins, CO 80523.

The DNA in Chinese hamster cells was labeled for 3 hours, first with $^{3}HTdR$ and then for 3 hours with $^{125}IUdR$. Chromatin was extracted, frozen, and stored at - 25°C until 1.0 x 10^{17} and 1.25 x 10^{17} disintegrations/gram of labeled DNA occurred for ^{125}I and ^{3}H, respectively. Velocity sedimentation of chromatin (DNA with associated chromosomal proteins) in neutral sucrose gradients indicated that the localized energy from the ^{125}I disintegrations, which gave about 1 double strand break/disintegration, selectively fragmented the ^{125}I chromatin into pieces smaller than the ^{3}H chromatin. In other words, ^{125}I disintegrations caused much more localized damage in chromatin than ^{3}H disintegrations, and fragments induced in DNA by ^{125}I disintegrations were not held together b y the associated chromosomal proteins. Use of this ^{125}I technique for studying chromosomal proteins associated with different regions in the cellular DNA is discussed. For these studies, the number of disintegrations required for fragmenting DNA molecules of different sizes is illustrated.

W-POS-C4 MODIFICATION OF THE RADIATION RESPONSE OF RAT 9L BRAIN TUMOR CELLS BY BCNU. D.F. Deen*, M.E. Williams*, S. Sheppard*, and K.T. Wheeler (Intr. By R.H. Shafer), Brain Tumor Research Center, University of California, San Francisco, CA 94143.

Rat 9L brain tumor cells were treated *in vitro* for 1 hr with either 1 μgm/ml (≈90% survival) or 3 μgm/ml (≈35% survival) of 1,3-bis(2-chloroethyl)-1-nitrosourea (BCNU) before, during or after x-irradiation. Only slight modifications of the slope and shoulder of the x-ray survival curve were observed when either concentration of BCNU was given simultaneously or 2 hrs before the x-ray dose. However, when cells were irradiated 1,5 and 15 hrs after the BCNU exposure, the shape of the survival curve depended on both the drug concentration and the time interval between the drug exposure and irradiation. The most important change was a decrease in the shoulder of the x-ray survival curve observed 5 and 15 hrs after BCNU treatment. The mechanism for this synergistic interaction between BCNU and x-rays could result in a therapeutic advantage of 1.3 to 1.7 during each radiotherapy treatment. Supported by NIH Grants CA-13525, CA-15203 and an RCDA NS70730 (KTW).

W-POS-C5 RADIATION RESPONSE OF B16 MOUSE MELANOMA CELLS. H.Z. Hill, F.Kwong,* C.F. Miller* and G.J. Hill, II,* Section of Cancer Biology, Mallinckrodt Institute of Radiology, and Department of Surgery, Washington University School of Medicine, St. Louis, Mo., 63110

Human melanomas are considered to be resistant to the lethal effects of ionizing radiation and thus radiation therapy is not often used in their control. We have initiated a study of the radiation response of transplantable mouse melanomas to determine whether they are similarly resistant. In this first report, we show that B16 mouse melanoma cells from twelve 13- to 18-day old tumors irradiated and plated in vitro have an n = 1.7 ± 0.5 and D_0 = 199 ± 16. Earlier tumors, 8 to 10 days old, tend to have larger n's and smaller D_0's. The average n for ten 8 to 10 day tumors is 4.3 ± 2.1 and the average D_0 is 159 ± 24. Computer analysis of survival curves indicates that the curves for low doses of γ-rays have a non-zero slope and that the inactivation data can be interpreted on the basis of a two-component inactivation. The first component, dominating at low doses, is a single target, high D_0 inactivation, and the second component, dominating at higher doses, is a multi-target, low D_0 inactivation. In these studies, single cell suspensions from fresh tumors are made by mincing tumors through a stainless steel mesh and suspending the resulting single cell suspension in medium (MEM- alpha + 10% fetal calf serum), plating and irradiating. In most experiments, plates are incubated at constant cell number by adjusting the final cell number per 60 mm dish before incubation to 10^5 cells with heavily irradiated (5000 rads) tumor cells from the same suspension. The plating efficiency at zero dose is between 20 and 40% of the viable cells plated. (Supported by NCI Grant # CA13053).

W-POS-C6 ASYMMETRICAL CHARACTERISTIC OF UV-MUTAGENESIS IN E. COLI. R. Bockrath and J. Palmer*, Microbiology, Indiana University School of Medicine, Indpls., Ind. 46202

The production of nonsense suppressors and the conversion of nonsense suppressors are both alterations in tRNA genes, and may be used to indicate GC to AT transitions resulting from ultraviolet irradiation. The premutational lesion for both phenomena is thought to be a pyrimidine dimer. We have studied mutation frequency decline (MFD) for these two mutation processes. MFD is a decline in the mutation frequency which occurs during post-UV incubation with protein synthesis restricted. Using E. coli WU 36-10-11 (contains a class 2 UAG suppressor) and selecting tyrosine revertants, we followed three types of reversion by the phage test method: true backmutation, de novo class 2 UAA suppression, and conversion (class 2 UAG suppressor to class 2 UAA suppressor). MFD for de novo suppression was rapid as expected (2-3 min half-life). However, MFD for conversion was slow (20-25 min half-life). This large difference in kinetics suggests: (a) MFD is not simply the result of a high rate of dimer excision at tRNA genes in general and (b) the mutation processes for these two examples are affected differently by cellular DNA metabolism. The second point is particularly interesting because the genetic alterations in these two examples are only slightly different. The target base-pair for transitions (GC) is at one or the other end of the anticodon, and has its C in the transcribed strand of DNA in one instance and its G in the transcribed strand in the other. The possibility of an asymmetrical interaction between repair and mutation processes is indicated. (Supported by NIH Grant GM 21788.)

W-POS-C7 KINETICS OF THYMINE DIMER EXCISION FROM PHAGE T4 DNA IN VIVO. G. Pawl*, R. Taylor*, and E.C.Friedberg, Laboratory of Experimental Oncology, Dept.of Pathology, Stanford University, Stanford, CA 94305. (Sponsored by C.A. Smith)

We have studied the kinetics of excision of thymine-containing pyrimidine dimers from prelabeled phage T4 during infection of E. coli. With wild-type hosts excision of dimers was observed immediately after infection, reaching a maximal level of 40-60% 4-6 minutes later. No further loss of thymine dimers from acid-precipitable DNA was observed up to 17 minutes after infection.

Excision was not observed when infection was carried out in the presence of chloramphenicol. When a pol A-1 mutant was used as host, there was a significant reduction in both the rate and extent of excision. In a res-1 mutant (defective in DNA polymerase I activity) no significant loss of dimers was observed within the first 4 minutes after infection. Between 4-7 minutes a slight but reproducible loss of dimers (10-15%) occurred. This time course corresponded with the kinetics of synthesis of phage-coded 5' → 3' exonuclease activity measured in cell-free extracts.

The kinetics of dimer excision was normal in rec B hosts. Normal excision was also observed under conditions restrictive for phage T4 DNA synthesis. In the latter situation excision again terminated at about 6 minutes after infection, suggesting that the cessation of dimer excision at this time is not obviously related to phage DNA replication.

These studies suggest that E.coli DNA polymerase I plays a primary role in the excision of thymine dimers from phage T4 DNA in vivo. (Studies supported by grant #CA 12428 from the U.S.P.H.S. and contract #AT-(04-3)-326 with the U.S.E.R.D.A.)

W-POS-C8 THYMINE DIMER EXCISION BY CELL-FREE PREPARATIONS OF NORMAL & XERODERMA PIGMENTOSUM CELLS: K. Mortelmans[1], E.C.Friedberg[2], H.Slor[3], G.H.Thomas[2] &J.E.Cleaver[2], Lab.of Exp.Oncology Dept.of Pathology,Stanford University,CA[1]Dept.of Human Genetics,University of Tel Aviv,Israel[2] & Laboratory of Radiobiology, University of California, San Francisco, CA.[3]

We have determined experimental conditions for the selective excision of thymine containing pyrimidine dimers by crude extracts of human cells. Extracts of diploid human fibroblasts (WI-38) and of human peripheral blood lymphocytes effect the loss of 50-90% of thymine dimers from the acid-precipitable fraction of UV-irradiated E.coli DNA, with the release of only 1-2% of the total DNA into the acid-soluble fraction. Similar results are obtained with crude extracts of skin fibroblast strains from xeroderma pigmentosum (XP) patients belonging to complementation group A. Extensive testing has failed to demonstrate mycoplasma or other contamination in the xeroderma cultures. Loss of thymine dimers from E.coli DNA during incubation with either normal or XP cell extracts is not light-dependent, but freezing of either whole cells or cell extracts destroys dimer excising capacity.

Extracts of normal fibroblasts prelabeled in their DNA with [^{3}H] thymidine, effect excision of thymine dimers from chromatin present in the crude extracts. However extracts of XP cells (complementation group A) fail to release dimers from their chromatin into the acid-soluble phase. These extracts still effect dimer excision from [^{14}C] labeled E.coli DNA however. The addition of crude extract from unlabeled WI-38 cells results in excision of dimers from the labeled chromatin in extracts of XP cells. These studies suggest that XP cells contain nucleases capable of excising thymine dimers from DNA, but cannot excise dimers from chromatin. (Studies supported by grants from the U.S.P.H.S., A.C.S., Binational U.S.-Israel Science Foundation, and contracts with the U.S.E.R.D.A.)

W-POS-C9 EVIDENCE FOR A 2-PHOTON REACTION IN THE PHOTOENZYMATIC REPAIR OF UV-IRRADIATED DNA. W. Harm, Biology Program, University of Texas at Dallas, Richardson, Texas, 75080.

Photoenzymatic repair of lesions in UV(254 nm)-irradiated transforming DNA of Haemophilus influenzae by yeast photoreactivating enzyme (PRE) in vitro has been studied, using polychromatic light flashes (1 msec) and monochromatic continuous light (320 to 450 nm) [1]. This permits investigation of the photolytic reaction (i.e., the repair in the strict sense) independently of the formation of PRE-substrate complexes. The photolytic reaction rate constant k_p, which characterizes for a given wavelength the product of the molar absorption coefficient of the complexes (ε) and the quantum yield of the reaction (φ), was found to be 3-4-fold increased if complexes were formed by PRE that had been illuminated prior to its binding to substrate [2]. The action spectrum for this preillumination effect resembles that for photolysis in the near UV and short visible wavelengths range, but extends to greater wavelengths with a secondary maximum around 575 nm. Enzyme-substrate complexes formed by non-preilluminated PRE, in contrast to those formed by preilluminated PRE, show enhanced photolysis if the photoreactivating light is applied at very high fluence rate. Evidence will be presented that this is due to absorption of $\geq$ 2 photons within a period of 10^{-2} to 10^{-3} sec.

-- Support by NIH Grant GM 12813.

[1] W. Harm, C. S. Rupert, and H. Harm (1971). In: Photophysiology (A.C. Giese, ed.) Academic Press, N.Y. pp.279-324.

[2] H. Harm (1976). Mutation Research, in press.

W-POS-C10 CONFORMATIONAL PROPERTIES OF ACIDIC GLYCOSAMINOGLYCANS FOR DIFFERENT IONIZATION AND SOLVATION STATES. R. Potenzone Jr. and A.J. Hopfinger. Department of Macromolecular Science, Case Western Reserve University, Cleveland, Ohio 44106

We have extended our conformational analyses of acidic glycosaminoglycans to include behavior of the neutral form in vacuo and water. We have studied the charged form in vacuo and water, and also the charged-counterion form in water. The calculations are probably most meaningful relative to dilute solution behavior since only intramolecular chain energetics are considered. The results are presented in terms of preferred conformations and general hydrodynamic properties including $\langle r^2 \rangle$ for the different molecular species and environments. A discussion focuses upon the relative dominance of the various types of molecular interactions responsible for the predicted conformational properties. Our results are also compared to available crystal structure data on the acidic glycosaminoglycans. Hyaluronic acid has been the main focus of our work.

W-POS-C11 SEMI-EMPIRICAL APPROACH TO THE MOLECULAR DIELECTRIC CONSTANT BY ENERGY MINIMIZATION OF AMINO ACID CRYSTALS. David A. Greenberg*, C.David Barry*, F.Scott Mathews and Garland R. Marshall. Dept. of Physiology and Biophysics, Washington University School of Medicine, St. Louis, Missouri 63110.

The dielectric properties at the molecular level of amino acid crystals were investigated by energy minimization. The energy was considered as sum of non-bonded and electrostatic interactions. The non-bonded and hydrogen bond functions of Hagler et al., (J. Amer. Chem. Soc. 96: 5319, 1974) and the partial charges calculated by Del Re (BBA, 75: 153, 1963) were used since the amino acids crystallize in the Zwitterionic form. Variables included the unit cell lengths and angles, the six positional variables of a molecule, and all rotatable bonds. Using a dielectric constant (ε) equal to 1, agreement between the calculated minimum energy structure and that observed was poor. When an ε of 2 was applied to interactions involving atoms more than 5Å apart, agreement improved considerably. Other formulas describing ε as a function of distance were tried. Thus far, best agreement was obtained when ε was set to 1 at distances less than 2Å, and to 2 at distances greater than 5Å, then made a parabolic function of distance in between. The above approach has been applied to alanine, proline, serine, threonine, and glycine crystals. Agreement has been good in each case. These findings indicate that the macroscopic property defined as the dielectric constant must be modified when one is considering events at the molecular level. The improvement between the calculated and observed crystal structures in all cases examined suggests strongly that the empirical parameterization proposed is a valid approach. Extension to crystals containing water of hydration and solution studies is under current investigation.

W-POS-C12 DYNAMIC LIGHT SCATTERING FROM SOLUTIONS OF DNA. S.-C. Lin, J.M. Schurr, and W.I. Lee, Department of Chemistry, University of Washington, Seattle, WA 98195, and K.S. Schmitz, Department of Chemistry, University of Missouri, Kansas City, MO 64110

Polarized light scattered quasi-elastically from solutions of DNA (of molecular weight $\gtrsim 5 \times 10^6$) has been found to manifest two unusual characteristics: (i) at sufficiently high concentration and molecular weight, or at sufficiently low ionic strength ($\gtrsim .02$), the autocorrelation function exhibits a long-tail with a time constant too large by an order of magnitude to be attributable to translational diffusion of the center of mass; (ii) at low DNA, and high salt, concentrations, where the long-tail is absent, the correlation functions are simply exponential, and plots of reciprocal relaxation time vs. K^2 resemble closely the theoretical curve predicted by the independent-segment, mean-force model of Lee and Schurr.

An explanation for the long-tail has been constructed, based on the couplingbetween rotation of the instantaneously non-spherical DNA coils and a severe, congestion-induced anisotropy of translational diffusion. Semi-quantitative agreement with literature data for the K^2 dependence of both fast and slow relaxation times is obtained. Satisfactory agreement is found also with well-known behavior in the long-wavelength limit, where the congestion has little effect.

Using the Lee-Schurr theory as a curve-fitting tool it has been possible to obtain translational diffusion coefficients for calf-thymus DNA as a function of pH, through its pH-denaturation region, under high-salt conditions. Significant differences between pH and thermally induced transitions have been found, principally a markedly enhanced diffusion coefficient in the pH-transition region. Using also sedimentation data the decline in molecular weight has been observed.

W-POS-C13 ANOMALOUS TEMPERATURE-DEPENDENT SOLUBILITY OF A MONOCLONAL CRYOGLOBULIN. C.R. Middaugh*, M.E. Aberlin* and G.W. Litman, Sloan-Kettering Institute for Cancer Research, New York, N.Y. 10021.

Monoclonal cryomacroglobulins are proteins of the IgM class which display a sharp temperature and concentration dependent precipitation at reduced temperatures. Systematic series of low molecular weight solutes have been utilized to perturb this phenomenon with McE, an IgM, k cryoglobulin and it has been found that: 1) neutral salts are inhibitory relative to their positions in the lyotropic series, 2) inhibitory effects of ureas and amides are relieved by increasing degrees of alkyl substitutions, 3) enhancement of cryoprecipitation by alcohols parallels their increasing hydrophobicity, 4) tetraalkylammonium salts enhance cryoprecipitation with increasing chain length, 5) sugars display nonsystematic inhibition of cryoprecipitation and 6) D_2O enhances cryoprecipitation. At the minimum concentrations at which a complete effect is obtained, the agents do not produce detectable changes in secondary and tertiary structure as monitored by CD in the near and far UV, UV difference spectroscopy and intrinsic fluorescence at 37°C. However, analyses of the temperature dependence of intrinsic fluorescence and kinetics of precipitation as monitored by light scattering suggest the possible involvement of a low temperature induced conformational change as a component of the cryoprecipitation process. The results of these studies, along with the observation that D_2O induces cryoglobulin-like behavior in many normal IgM proteins suggest that cryoprecipitation may reflect a nonspecific solubility phenomenon possibly involving dispersion forces as opposed to interactions of a more defined nature (e.g. hydrophobic and ionic). Supported in part by NCI CA-17404 and NCI CA-08748.

W-POS-C14 THE TRANSITION FROM RIGID ROD TO STIFF COIL BEHAVIOR. CONFORMATION OF SMALL DOUBLE STRANDED DNA MOLECULES IN SOLUTION. R. T. Kovacic and K. E. Van Holde, Department of Biochemistry and Biophysics, Oregon State University, Corvallis, Oregon 97331

Large DNA molecules of discrete size can be readily obtained from bacteriophage. But, to investigate the size range which covers the transition from rigid rod to stiff coil behavior, smaller DNA fragments than can be obtained from intact viral DNA are necessary. Sonicated or enzymatically degraded DNA can be fractionated by column chromatography but the resulting material may be nicked or partially single stranded and the homogeneity of the preparation is limited by the resolving power of the fractionation technique.

We have isolated 15 Endonuclease R Hae III fragments of PM2 DNA by preparative gel electrophoresis to obtain a discrete set of DNA molecules which spans the transition region. The isolated restriction fragments were homogeneous on analytical gel electrophoresis while formamide gel electrophoresis indicate that the preparations were unnicked. Hydrodynamic behavior in solution was studied by sedimentation velocity experiments. No concentration effects are found for moving boundary sedimentation velocity measurements made over the range of 5-40 μg/ml. Preliminary molecular weight calibrations by analytical gel electrophoresis combined with the results of sedimentation velocity measurements are generally consistent with the Yamakawa-Fujii theory for wormlike cylinders. (Supported by NSF Grant BMS 73-06819 A02).

W-POS-C15 EQUILIBRIUM AND KINETIC MELTIUG STUDIES ON RODLIKE DNA FRAGMENTS. Charles P. Woodbury, Jr. and M. Thomas Record, Jr., Institute of Molecular Biology, University of Oregon, Eugene, Oregon 97403 and Department of Chemistry, University of Wisconsin, Madison, Wisconsin 53706.

Equilibrium and kinetic aspects of the melting of low molecular weight DNA have been studied in a solvent that equalizes the stability of the A·T and G·C base pairs (2.4 M Et_4NBr). Following preliminary experiments with fragments of calf thymus DNA, we have investigated two low molecular weight samples of T7 DNA, prepared by sonication and agarose gel fractionation. Melting experiments on the latter samples followed to equilibrium the change in UV absorbance after a temperature perturbation. The observed equilibrium behavior is consistent with that predicted for all-or-none melting of intact double helices. Using small temperature perturbations in the transition region, we observed two resolvable kinetic relaxation processes in downward temperature perturbations; two corresponding processes were observed in upward perturbations, as well as faster kinetic events of substantial amplitude. The faster of the two relaxation processes may represent the all-or-none melting of intact double helices. The kinetic experiments showed unusually slow melting behavior, with some experiments taking longer than 10^4 seconds to reach a constant absorbance. The slow kinetics may be due to conformational rearrangements in the reacting species.

W-POS-C16 INTRODUCTION OF SINGLE-STRAND SCISSIONS IN DNA BY IRRADIATION OF ETHIDIUM BROMIDE-DNA COMPLEXES. Phillip A. Martens* and David A. Clayton, Program in Biophysics and Department of Pathology, Stanford University, Stanford, CA 94305

It is possible to induce scissions in the deoxyribose-phosphate backbone of DNA molecules by irradiating DNA-ethidium bromide (EB) solutions with incandescent light. This effect was studied by monitoring the conversion of various closed circular (form I) DNA molecules to open circular (form II) molecules. The EB-DNA solutions used contained 100 μg/ml EB, 1M NaCl, 50 mM Tris (pH 8.5), 10 mM EDTA, and <1 μg/ml DNA. The light source used was a Kodak Carousel Model 850 slide projector adjusted to maximize the light intensity on the sample. The sample was stirred in a quartz cuvette 8 cm from the projector lens. The conversion of form I DNA to form II DNA follows zero order kinetics until a substantial amount (>80%) of the molecules are nicked. Alkaline sedimentation velocity analyses of the nicked molecules indicate that breaks occur in both strands. These results do not preclude the possibility that further nicking occurs preferentially in one strand or at sites near a prior nicking site. The frequency of nicks in single-strands cannot be represented by a Poisson distribution. It appears that the second and subsequent nicks are introduced at a faster rate than the first. This may be due to the extra EB bound by form II molecules. The nicked strands are not rejoined by E. coli polynucleotide ligase.

This research was supported by grant CA-12312 from the National Cancer Institute and a NSF Predoctoral Fellowship to P.A.M.

W-POS-D1 A NEW METHOD FOR CALCULATION OF LV EJECTION FRACTION IN COMPARISON WITH EIGHT CLASSICAL TECHNIQUES. I. Beranek*, R. Moore, S. Kim*, and K. Amplatz*. Department of Radiology, University of Minnesota Hospitals, Minneapolis, Minnesota 55455.

Systolic ejection fraction (EF) is commonly used for estimating the left ventricular performance, especially for patients with ischemic heart disease. Many radiographic methods are described for calculating EF.

The main goal of this study was to compare values of the EF calculated by nine different methods using single plane cine left ventriculography in the RAO projection. Models described by Davila, Chapman, Dodge, Arvidsson, Green, Snow, and Beranek, and our new method were tested. The new method under study was based on area and diameter ratios. A method described by Davila, using a modification of Simpson's rule (each slice represented a truncated cone) was chosen as a reference. 25 patients with a normal contraction pattern of the left ventricle (Group 1) and 25 patients with akinesia or dyskinesia (Group 2) were used. Statistical analysis was performed separately for each group of patients.

The new technique to be described was highly correlated in both groups (correlation coefficient = 0.972 and 0.988) with a small standard deviation of the differences ($\pm$ 1.58 and $\pm$ 2.85). This method is simple and gives rapid results without a computer.

If one accepts the assumption that a model based on modification of Simpson's rule can serve as a reference method, then only mathematical models such as those proposed by Davila, Chapman, Dodge, Beranek, and our new method can give comparable results (with acceptable errors) in estimating systolic EF regardless of the shape of the left ventricle.

This work was supported in part by Public Health Service Grant No. HL-16484 from the National Heart and Lung Institute.

W-POS-D2 DOPPLER-SHIFTED ULTRASOUND MONITORING OF GAS BUBBLES FOLLOWING DECOMPRESSION M. R. Powell, and M. P. Spencer *, Hyperbaric Laboratory, Institute of Applied Physiology and Medicine, Seattle, Washington 98122.

Decompression sickness, which can manifest itself in many forms, appears to have gas phase formation as a common etiologic agent with the differing pathologies being the result of the gas phase in different anatomical regions. Prevention of a phase transition to completely eliminate bubble formation does not appear to be feasible within realistic economic constraints. Thus much work has been directed towards the pathophysiological consequences of in vivo bubble growth and rational medical treatment for serious cases. In addition, considerable work has been focused on detection of bubbles in the body attempting to be temporally and anatomically as close to the initial phase transition as possible. The application of such a technique would be of great value to both researchers involved in calculation and testing of decompression tables and to deep sea divers, especially those involved in deep-ocean oil recovery. We present data obtained from experiments which monitored human divers as they returned from simulated 1000 feet sea water dives. Times at which bubbles were detected in the central venous system were correlated with the observed dives of decompression sickness. Final stages of decompression from deep dives are of the "saturation" type where tissues well perfused with blood are not thought to influence the decompression profile. We have tested the hypothesis that "fast" tissues do not produce a gas phase in controlled decompressions. Ultrasound monitoring of blood in the renal vein in sheep gave clear evidence of bubbles in this highly perfused organ. This can also occur in cases where U.S. Navy Diving Tables were followed. Supported by the Office of Naval Research with funds made available by the Bureau of Medicine and Surgery.

W-POS-D3 TRANSMEMBRANE IONIC FLUX MEASUREMENTS VIA 250 AND 25 MSEC RESOLUTION MICROPERFUSION TECHNIQUES. D.F. Juncker* (Intr. by C. Terzuolo), Departments of Physiology and Health Computer Science, University of Minnesota, Minneapolis, MN 55455.

In an attempt to directly measure cardiac transmembrane ionic fluxes during the contraction cycle, relatively insensitive tracer efflux and influx techniques were re-designed. The methods developed have been used to obtain both efflux and influx profiles for ^{42}K (Circ. Res. 30:350, 1972 and Circ. Res. 37: Nov., 1975). Additional efflux profiles have been obtained for Na^+ and Ca^{++}. It is the purpose of this presentation to describe the rapid microperfusion techniques developed in terms of theory, resolution, and definitive results. Both influx and efflux methods are based on specific attention to simple test chamber geometry and minimal fluid boundary layer thickness within the test chamber. The homogeneous tissue isolated for examination (amphibian atrial fiber) and the test environment are confined to cylindrical geometry. The region of perfusate flow thus formed is annular, and its description and manipulation are well understood. A two-phase (flurocarbon and Ringer's) system is employed to obtain the higher resolution and to ensure tracer uptake only during specific 25-50 msec intervals during the cardiac cycle. Boundary layer stability is maintained by damping or blocking the cardiac contraction with high flow velocity, or perfusion with 5 mM $NiCl_2$-Ringer's, or "zero"-Ca^{++} Ringer's. In addition, Ni^{++} and "zero"-Ca^{++} perfusates prolong the plateau of the action potential to different (but reproducible) degrees, thus providing two additional test states for comparison of the action potentials with corresponding flux profiles. Some of the working details of the method, its versatility, and limitations will be presented and discussed.

W-POS-D4 DETECTION OF REDUCING METABOLITES USING A STABLE FREE RADICAL
P. W. Benda, A. E. Sherry*, and M. S. Blois, Department of Dermatology, University of California Medical Center, San Francisco, California 94143.

Diphenylpicrylhydrazyl (DPPH) is a stable free radical that has long been known in the chemical and physical literature. DPPH exhibits a free spin, and in solution has a violet color with a broad absorption maximum centered at 520 nm. DPPH is also a mild oxidizing agent that will react with suitable electron donors, bleaching the absorption. DPPH has been used in the past largely as a spin marker, and as an indicator of radical reactions in organic solvents. We have found that DPPH also reacts with a wide range of compounds of biological significance, including reducing agents such as ascorbic acid and cysteine, substituted aromatics such as dihydroxyphenylalanine (DOPA) and the catecholamines, and restricted drugs such as morphine and tetrahydrocannabinol. We have developed an ion-exchange chromatographic system similar in outline to an amino acid analyzer, but which uses DPPH as the colorimetric reagent. Our primary interest in DPPH is for the detection of pigment-related catecholic and indolic metabolites in the urine of patients with malignant melanoma. We find that urines from patients with disseminated disease contain several major chromatographic peaks that are absent from normals. Most of the peaks remain to be identified, but the metabolite most characteristic of the disseminated urines is 3-methoxytyrosine (MOPA), not DOPA. The chromatogram of 30 to 50 DPPH-reactive compounds is unique for each patient, and detects common urinary constituents, such as uric acid and creatinine, as well as many drug metabolites. Since DPPH reacts in high molar ratios with hydroxy-/methoxy-substituted aromatics, comparison runs for hydrolyzed and non-hydrolyzed urine are a sensitive indicator of conjugation and liver function. We believe that the DPPH analytical system has many other clinical and research applications.

W-POS-D5 CIRCULAR DICHROISM OF MONOSACCHARIDES IN THE VACUUM ULTRAVIOLET.
R. G. Nelson* and W. C. Johnson, Jr., Department of Biochemistry and Biophysics, Oregon State University, Corvallis, OR 97331.

Circular dichroism spectra in the vacuum ultraviolet to 165nm have been measured for the individual anomeric forms of five aldopyranoses, three ketopyranoses, and twelve methyl aldopyranosides. These spectra have Cotton effects in the region of intrinsic absorption for cyclic sugars which are sensitive in sign and magnitude to small changes in the configuration and conformation of the monosaccharide. Difference spectra are used to study changes in group interactions between the two molecules compared. These reveal that the aldopyranoses and methyl aldopyranosides have the same conformation where comparisons are possible. The difference spectra also indicate that α- and β-D-galactose have different rotameric populations of the hydroxymethyl group which we tentatively attribute to differences in water structure at about the two sugars. The data allow tentative assignment of the transitions for the monosaccharides.

W-POS-D6 A MULTIPLE-WAVELENGTH SPECTROMETER.
K. Ogan, K.W. Beach,* S.R. Caplan, and A. Essig, Department of Physiology, Boston University School of Medicine, Biophysical Laboratory, Harvard Medical School, Boston, MA., and Laboratory of Membranes and Bioregulation, Weizmann Institute of Science, Rehovot, Israel.

We have developed a multiple-wavelength scanning (MWS) spectrometer which can be used as a dual-wavelength spectrometer, but which is easily adapted to monitor several pairs of wavelengths. Scanning is accomplished by focusing the image from a monochromator grating onto a mirror mounted on a galvanometer rotor. The mirror orientation rapidly and accurately follows the waveform applied to the galvanometer driver amplifier, allowing a 79 nm band to be scanned at a rate up to 60 Hz. In the step mode, a square wave input to the driver amplifier alternates the monochromator output between two wavelengths; a multiple-step waveform results in several wavelengths. In the sweep mode, a voltage ramp input causes a linear variation of wavelength with time. Electronic timing circuits cause sample-and-hold amplifiers to sample the photomultiplier output at appropriate times. Operation in the step mode permits observation at a few wavelengths with reduced photon noise. Alternatively, operation in the sweep mode allows the study of a shifting absorption peak or, in conjunction with a signal averager, the study of small absorbance changes (0.0001 A). We are now using the MWS spectrometer in studies of active sodium transport in epithelial tissues.

W-POS-D7 VOLTAGE TO FREQUENCY CONVERSION AS AN INTEGRATION PROCEDURE FOR IMPROVED FLUORESCENCE DETECTION. V. Glushko, R. Caley*, and C. Karp*, Memorial Sloan-Kettering Cancer Center, New York, New York, 10021.

The ability of certain fluorophores to reflect environment and mobility is a useful property for many biophysical studies. However, it is often necessary to use low probe concentrations in order to avoid serious perturbation effects. Many commercial fluorometers are unable to provide sufficient accuracy for the measurement of weak fluorescence. At present, single photon counting represents the optimum approach for the detection of weak optical signals. Budget constraints, or inherent limitations in instrument design, may limit the conversion of available equipment to photon counting detection. In such cases, a significant improvement in precision is possible by integration over longer periods of time. The recent development of low-cost, high resolution voltage to frequency converters (VFC) provides for direct integration with the simple addition of a TTL compatible event counter. The VFC procedure bypasses the common drawbacks of analog integrators, such as limited storage capacity, low resolution, and dissipation of stored signal. The precision and accuracy of the VFC at mid-scale were better than 1 part in 10,000, which represents the limit of stability for our voltage source. The linear correlation coefficient exceeded 0.999 for a 4000 fold range in input voltage. The VFC procedure introduces negligible noise providing the typical relationship of an increase in the signal to noise ratio as the square-root of the increase in the integration period. This improvement in signal measurement ability was used to provide an 81 fold enhancement in the detection of quinine, in comparing a 1 s to an 8000 s integration interval. By directing the output of the VFC to a multi-channel scaler, a similar improvement is obtained for spectral analysis. (Supported by grants from the American Cancer Soc., BC-119, and from the NIH, CA-08748, and -16889).

W-POS-D8 ELECTROPHORETIC LIGHT SCATTERING: ELECTROPHORETIC AND HYDRODYNAMIC PROPERTIES OF CELLS AND VIRUSES. J. Josefowicz* and B.R. Ware, Department of Chemistry, Harvard University, Cambridge, Massachusetts 02138. Intr. by F.R. Hallett

Electrophoretic light scattering is an objective instrumental technique for the rapid determination of the electrophoretic mobility distribution of a suspension of particles by spectrum analysis of the Doppler-shifted scattered laser light. This technique is ideal for fast, accurate determinations of the respective electrophoretic mobilities of different populations of particles in the same sample. We have used this technique to quantify the extent of hydrodynamic interaction during electrophoresis of a solution containing both rat thymus lymphocytes and rat red blood cells. Such information will be of particular significance for the design of preparative cell electrophoresis experiments, for which hydrodynamic interaction must be minimized. A significant advantage of electrophoretic light scattering over classical methods is that it allows the investigation of both microscopic and submicroscopic particles. We have utilized this technique for the electrophoretic analysis of solutions of viruses. Results of electrophoretic mobility measurements and isoelectric point determinations are presented. (Supported by NSF grant MPS72-05133 and the Killam Program of the Canada Council)

W-POS-D9 BIOLOGICAL CELL CLASSIFICATION BY A MULTI-ANGLE LIGHT-SCATTERING FLOW SYSTEM. B. J. Price, G. C. Salzman, J. M. Crowell*, M. Ingram*, K. M. Hansen*, and P. F. Mullaney, Biophysics and Instrumentation Group, Los Alamos Scientific Laboratory, University of California, Los Alamos, New Mexico 87545, USA.

Classification of biological cells by their light-scatter patterns has been accomplished by a multi-angle flow-system instrument, which is described. Unfixed, unstained cells are passed through a focused helium-neon laser beam (6328 Å) at speeds up to 1000 cells/sec. The scattered intensity from each cell is measured simultaneously at 32 angles between 0° and 25° with respect to the laser beam axis. The scatter patterns are stored in a computer where the various classes of cells can be distinguished by a mathematical clustering algorithm. The boundaries between the classes are found by a linear-separation algorithm. The light-scatter criteria thus developed for each cell type can then be used to sort the different cell populations for subsequent visual inspection and possible further analysis. Preliminary results on both horse and human peripheral blood as well as exfoliated gynecological specimens will be presented. (This work was performed under a joint ERDA/NCI agreement #Y01-CB-10055.)

W-POS-D10 A POSITION SENSITIVE LIGHT DIFFRACTOMETER UTILIZING LINEAR IMAGE SENSOR CHARGE COUPLED DEVICES. P.J. Paolini, Dept. of Biology, San Diego State University, San Diego, CA 92182, K.P. Roos*and R.J. Baskin, Dept. of Zoology, and J.W. Cline*, Crocker Nuclear Laboratory, University of California, Davis CA 95616.

A position sensitive dual channel light diffractometer has been developed to allow the real time monitoring of light diffraction patterns produced by the myofibrillar sarcomeres of single skeletal muscle fibers and small bundles of fibers during contraction. The diffractometer utilizes two linear image devices to permit the analysis of two or more diffraction lines. These units are highly sensitive (1.5×10^{-5} fcs), lag-free, self-scanning 256 element charge coupled devices driven by Shottky and standard TTL logic circuitry at a selectable data transfer rate/element from 20 to 400 KHz. Video output from the diffractometer can be displayed directly on an oscilloscope screen, or can be connected to an analog-to-digital converter and minicomputer system so that diffraction spectra can be corrected for dark signal and element non-uniformities and displayed on-line by the computer CRT. The computer evaluated spacing between diffraction lines provides an accurate measure of mean sarcomere length within the muscle, while line shape and width are indicative of the length distribution among sarcomeres. Sarcomere length resolution attainable with the instrument ranges from about 10 to 100 A at a nominal length of 2.5 u, depending upon muscle-to-sensor spacing and whether one or two channels of the diffractometer are used.

W-POS-D11 TRANSIENT VELOCITY SEDIMENTATION OF MAMMALIAN CELLS. N. Catsimpoolas, R. Rossi*, S. Agathos*, and A.L. Griffith, Biophysics Laboratory, Dept. of Nutrition and Food Science, Massachusetts Institute of Technology, Cambridge, MA 02139

A new method has been developed for the determination of the mean sedimentation velocity ($\bar{s}$) of cells at unit gravity in a shallow density gradient. Fewer than 5×10^5 cells can be used for analysis. The distribution of sedimenting cells is followed as a function of time by repetitive optical scanning of the transport path. The data are digitized on-line and processed by a computer program which produces the statistical moments of the distribution as well as the skewness and excess. The slope of the plot of the mean position (first moment) of the distribution vs. time gives a direct measure of $\bar{s}$ in cm/sec. In addition, measurement of the distribution variance (σ^2, second central moment) as a function of time produces an estimate of the dispersion coefficient (degree of spreading). The latter parameter is important in predicting the expected resolution in the preparative separation of cells (varying in size) by velocity sedimentation. The method has been applied successfully to the study of erythrocytes in normal and diseased states and to lymphocyte subpopulations. (Supported by National Cancer Institute Contract No. NO1-CB-43928 and National Science Foundation Grant No. MPS 74-19830)

W-POS-D12 BIOLOGICAL ION EXCHANGER RESIN THEORY AND THE DEVELOPMENT OF THE NUCLEAR RESONANCE METHOD FOR DETECTING CANCER. R. Damadian, Department of Medicine and Program in Biophysics, State University of New York at Brooklyn, Brooklyn, New York 11203.

The Biological Ion Exchanger Resin Theory (BIER theory) is a "fixed charge" model for ion transport. Data will be presented to show that the fixed anion composition of the cell, as determined by protein amino acid analysis, organic phosphate analysis, nucleic acid analysis and metal analysis, adequately accounts for the alkali cation accumulation of E. coli without the necessity of invoking membrane pumps (R. Damadian, Ann. N.Y. Acad. Sci. 204:211, 1973; R. Damadian, Critical Reviews in Microbiology, CRC Press, p. 377-422, 1973). The energetics of ion accumulation in E. coli was investigated and results questioning the adequacy of cell ATP stores for supplying the energetic needs of membrane pumps will be presented. Requirements for a mechanism in the BIER theory to regulate cell hydration and thereby control ion selectivity led to the discovery of an actin-like protein in E. coli which formed the basis of a cytotonus hypothesis for control and regulation of cellular physiology. The action of contractile proteins in the control and regulation of ion transport and cell respiration through the mechanism of cytotonus will be discussed. The BIER theory and the use of nuclear resonance in its investigation led to the discovery of the Nuclear Resonance Effect in Cancer (R. Damadian, Science, 171:1151, 1971; Zaner, K., and Damadian, R., Science, 189:729, 1975; R. Damadian, et al., Ann. N.Y. Acad. Sci., 222:1048, 1974). Nuclear resonance data of human and malignant tumors using four nuclei, K^{39}, Na^{23}, P^{31}, and H^1 will be presented.

W-POS-D13 INTERACTION OF WATER WITH N-ACETYL L-ALANINE N-METHYL AMIDE. F.Jordan*, V.Renugopalakrishnan, Dept. of Chemistry, Rutgers, The State University, Newark, New Jersey 07102

This study reports the interaction of water with a simple dipeptide, N-acetyl L-alanine N-methyl amide in fully extended (C_5), C_7 equatorial and C_7 axial conformations using ab initio quantum mechanical method. Due to the size of the molecular systems involved, the calculations were performed using minimal basis set (STO-3G) approximation. Water molecule was allowed to approach the peptide carbonyl and NH protons linearly with a hydrogen bond angle of 180°. No attempt was made to optimise the geometries of the interacting species. A potential well with a minimum typical for hydrogen bond formation was oberved except in the case of C_7 axial conformer. Hydrogen bond energies of 2.91 and 5.97 kcals/mole respectively were obtained for C_5 and C_7 equatorial conformers. An attempt towards a calculation for the simultaneous interaction of the H atom of water with C'=O and oxygen of water with the peptide NH, (i.e.) forming a bridged structure (experimentally observed), is discussed. Some details of the potential energy surface around the peptide using electrostatic approximation based on ab initio wave functions, is presented. The potential energy surface clearly reveals the vulnerable regions of attack by the approaching water molecule. A decomposition of the hydrogen bond energy into components, is discussed.

W-POS-D14 HYDROXYL RADICAL GENERATION DURING NADPH OXIDATION BY LIVER MICROSOMES. P.B. McCay*, R.A. Floyd, E.K. Lai*, J.L. Poyer*, and K-L Fong*, (intr. by J.J. Killion) Biomembrane Res. Lab., Okla. Medical Res. Found., Okla. City, OK 73104

Earlier work has provided indirect evidence that NADPH oxidase activity in rat liver microsomes, which is known to form H_2O_2, also produces a sufficient flux of $O_2^{\cdot}$ to promote HO· generation via the reaction $O_2^{\cdot} + H_2O_2 \rightarrow HO\cdot + HO^- + O_2$ and that hydroxyl radical formation is augmented by the presence of very low concentrations of Fe^{3+} to the point that the radicals initiate lipid peroxidation in the microsomal membrane (Fong, et al., J. Biol. Chem. 248: 7792, 1973). We have now obtained an electron spin resonance spectrum with this reaction system characteristic of an adduct of the hydroxyl radical with phenyl-t-butyl nitrone described by Harbour, Chow and Bolton (Can. J. Chem. 52: 3549, 1974). The signal obtained with the spin trap is dependent on the activity of the enzyme system. No signal was observed, 1) if the substrate for the reaction (NADPH) was omitted from the system; 2) if an enzyme inhibitor was added, such as p-chloro-mercuribenzoate; 3) if the microsomes were heated to 70° to denature the enzyme before addition to the reaction system; or 4) if inorganic iron was removed from the system. The results are entirely consistent with our hypothesis that enzyme-catalyzed generation of reactive free radicals may be inherent property of certain oxidoreductase systems which produce superoxide. Superoxide itself, however, was shown to be completely unreactive with lipids except in the presence of inorganic iron. The results are consistent with the illustrated sequence of reactions which are dependent on the activity of the NADPH oxidase system. Reaction [3] and [4] described the role of Fe^{3+} in augmenting the reaction. Reduction of the iron by $O_2^{\cdot}$ formed in this system has been demonstrated.

$$\text{NADPH} + O_2 \xrightarrow{H_2O_2} O_2^{\cdot} \quad [1]$$

$$O_2^{\cdot} + H_2O_2 \rightarrow HO\cdot + HO^- + O_2 \quad [2]$$

$$O_2^{\cdot} + Fe^{3+} \rightarrow O_2 + Fe^{2+} \quad [3]$$

$$Fe^{2+} + H_2O_2 \rightarrow Fe^{3+} + HO\cdot + HO^- \quad [4]$$

W-POS-D15 THE ION EXCHANGE RESIN AND SOLID STATE APPROACH TO CHARGE TRANSPORT AND SALT AND WATER METABOLISM. F.W. Cope, Biochemistry Laboratory, Naval Air Development Center, Warminster, Pa. 18974

Cation pumps across cell walls are thermodynamically impossible (Amer. J. Phys. Med., 34, 89, 1955; Int. Rev. Cytol., 26, 1, 1969; Biophys. J. 13, 167, 1973). In dead muscle, cations diffuse as if free in solution (Science, 166, 1297, 1969). In living muscle, cations diffuse as if associated with macromolecules in structured water (Science, 181, 78, 1973). NMR observations are as expected for structured cell water (Biophys. J., 10, 843, 1970; Nature New Biology, 237, 215, 1972) and for Na^+ and K^+ associated with fixed charge sites like on an ion exchange resin (Biophys. J., 10, 843, 1970; Physiol.Chem. & Physics, 6, 17, 1974). The classical hypothesis of free cations in liquid cell water persists only because scientists and granting agencies cannot admit to students and to Congress that they have been wasting their time and money, resulting in control of grants and of journal publication (e.g. of the Biophysical Journal) to prevent investigation and publication of the new concepts. One must now regard the cell as an ion exchange granule with Na^+ and K^+ associated with fixed charge, surrounded by structured cell water (Int. Rev. Cytol., 26, 1, 1969; Biophys. J., 13, 167, 1973). Therefore, all kinetic analyses and nerve conduction theories based on free cations and liquid water are wrong. A solid state physical approach to ion leakage kinetics is valid in concept and agrees with experiment (Bull. Math. Biophys. 29, 691, 1967). Solid state electron transport (semiconduction in cytochrome oxidase; P-N junction conduction in photobiology; superconduction in growth) is favored by much evidence (Adv. Biol. Med. Phys., 13, 1, 1970; Ann. N.Y. Acad. Sci., 204, 1973; J. Biol. Physics, 3, 1, 1975).

W-POS-D16 SODIUM-23 MAGNETIC RESONANCE OF BIOLOGICAL AND NON-BIOLOGICAL ION EXCHANGER SYSTEMS. M. Goldsmith and R. Damadian, Department of Medicine and Program in Biophysics, State University of New York at Brooklyn, Brooklyn, New York 11203.

The sodium-23 spin-lattice relaxation time (T_1) was determined at 10 MHz on Dowex 50W-X2 as a function of the dielectric constant of the solvent. The relaxation time varied from 24.8 milliseconds in distilled water (D = 78.5) to values too short to determine in media of dielectric constant below 35. Sodium-23 T_1 of normal and cancerous tissues of rats and mice consistently fell within this range, with the shortest T_1 being demonstrated by rat liver (6.5 msec) and the longest T_1 being shown by rat hepatoma (23.7 msec). Control studies indicated that the dielectric constant of the intra-resin media appeared to be 63. The possible values of the tissue dielectric constants are discussed based upon a comparison of the NMR and electrochemical properties of the two systems.

W-POS-D17 DNA MOLECULAR WEIGHT MEASUREMENT BY FLUCTUATION SPECTROSCOPY.† M. B. Weissman, H. Schindler,* and G. Feher, Department of Physics, University of California, San Diego, at La Jolla, CA 92093.

A rapid method for determining the weight-average molecular weight of large DNA molecules in solution has been developed. The number/volume concentration (n) of DNA molecules was obtained by measuring the magnitude of concentration fluctuations $(\Delta n/n)^2$ between different subvolumes of a sample cell. The molecular weight is then given by $MW = 6 \cdot 10^{23} \cdot c \cdot n^{-1}$, where c is the ordinary weight/volume concentration. We used the fluorescence of a dye, Ethidium Bromide, as a convenient probe of the DNA concentration in the fluctuation measurement. A cell rotating at 0.25 revolutions/sec, illuminated with an exciting beam from an argon laser and microscope-like fluorescence collecting optics, allowed for continuous sampling of successive independent volumes of $\sim 10^{-5}$ cc without requiring any shear forces. An autocorrelator was used to obtain the autocorrelation function $A(\tau) = \langle \Delta V(t)\ \Delta V(t+\tau) \rangle$ of the output V(t) of the fluorescence detecting phototube. By observing $A(\tau)$ at $\tau = 4$ sec, the periodicity of the concentration fluctuations with the turning time of the cell was used to separate undesired noise sources. About one minute of data accumulation time is required to measure the concentration fluctuations. For phenol extracted T-2 viral DNA, we obtained $MW = 1.15 \pm .15 \times 10^8$ daltons and for DNA from log phase E. coli B chromosomes, $MW = 3.75 \pm .5 \times 10^9$ daltons. The method is applicable to much larger molecules; we are currently planning experiments on DNA from eukaryotes. We wish to thank Brian Bowen, Randy Adam, Ruth Kavenoff, and Bruno Zimm, who supplied both the DNA and helpful advice on its handling and properties.

†Work supported by an NIH Grant, GM-13191.

W-POS-D18 A LASER FLYING SPOT FLUORESCENCE MICROSCOPE FOR THE QUANTITATIVE STUDY OF FLUOROPHORE DISTRIBUTIONS IN SINGLE CELLS. L. Rimai, I. Salmeen (Research Staff, Ford Motor Co., Dearborn, Mich. 48121) J. W. Levinson*, J. J. McCormick, (Mich. Cancer Found., Detroit, Mich. 48201) Supported by NCI Contract NO1CP33226

We describe a scanning fluorescence microscope system with object illumination by a diffraction limited spot obtained by a focused laser beam. The spot is scanned over the object by deflecting the beam, prior to focusing, off a pair of orthogonally rotating mirrors mounted on flexural piezoelectric transducers. The transmitted beam is monitored by a photovoltaic detector. The fluorescence emission is collected over a wide angle and focused through a monochromator onto a photomultiplier tube. Thus absorption and fluorescence images can be obtained simultaneously. The detector output is stored in a 1024 word memory whose address is advanced by the clock controlling the timing of the voltages driving the piezoelectric transducers. The 1024 spots of a 100 x 100 μ field can be scanned in one second. Multiple scans can be integrated in the memory. Thus for weak signals long exposure can be realized with full linearity, but without continuous illumination of any given spot. The system was tested on acriflavin-Feulgen stained preparations of cultured human fibroblasts and on SV-40 infected 3T3 mouse cells treated with fluorescent antibody against the viral T-antigen. The absorption data allow the quantitative determination of the chromophore density (typically 1.5×10^8 acriflavin molecules per diploid fibroblast nucleus). From the chromophore density, the absolute sensitivity of the system for a given chromophore can be determined: with 441.6 nm laser excitation at 2 mW, receiver monochromator tuned to 530 nm, slit width of 500 μ, 1500 acriflavin molecules in one fibroblast nucleus yield a signal-to-noise ratio of about 3 after 2 hours of data accumulation.

W-POS-D19 LASER DOPPLER SPECTROSCOPY OF THE PROTOPLASMIC STREAMING IN NITELLA AND PHYSARUM. R.V. Mustacich, F. Lanni,* and B.R. Ware, Department of Chemistry, Harvard University, Cambridge, Massachusetts 02138

Laser light scattered from particles in the streaming protoplasm of the cells of Nitella flexilis is shifted in frequency by the Doppler effect. The spectrum of the scattered light can be measured and interpreted to infer details of the velocity distribution of the cytoplasm. A comparison to model laminar flow systems indicates a narrower distribution of velocities than parabolic laminar flow. Photo-inhibition of the protoplasmic streaming in Nitella by laser light has been spatially mapped using a double beam technique. The photo-inhibition extends only a few beam diameters from the inhibiting beam and has a greater effect downstream than upstream. Long exposure times exfoliate the chloroplasts to produce a "window" region in which photo-inhibition of streaming after recovery requires three orders of magnitude more intensity. Frequency spectra obtained from the streaming protoplasm of the slime mold Physarum depict velocity distributions which include velocities greater than 1 mm/sec. Interpretations of the data in terms of the spatial distribution of velocities within the organism have been illustrated by comparison with data from model flow systems. The streaming is oscillatory, and a technique for measuring the fluctuating spectral width is used to monitor the flow oscillations in real time. (Supported by NIH grant 21910-01)

W-POS-D20 ELECTROPHORETIC LIGHT SCATTERING OF HUMAN PERIPHERAL BLOOD LYMPHOCYTES. B.A. Smith, B.R. Ware, and Roy S. Weiner,* Department of Chemistry, Harvard University, Cambridge, Massachusetts 02138 and Harvard Medical School, Boston, Massachusetts 02115.

Electrophoretic light scattering is a technique for determining electrophoretic mobility distributions of a suspension of particles by measuring the Doppler-shifted frequency spectrum of laser light which is scattered from the particles. We have obtained electrophoretic mobility profiles for samples of human peripheral blood lymphocytes which were purified by isopycnic centrifugation over Ficoll-Hypaque. Extensive studies have been performed to verify that cells which have been cryopreserved by a DMSO method under optimized conditions have electrophoretic mobility distributions which are experimentally indistinguishable from the mobility distributions of fresh cells from the same source. Cryopreserved samples from patients have been analyzed, and the differences in the electrophoretic mobility profiles of normal and abnormal lymphocyte populations have been characterized. (Supported by NSF grant MPS72-05133 A02 and National Cancer Institute contract NO1-CB43885)

W-POS-D21 HOW DO LIVING CELLS RETAIN WATER? G.N. Ling & C. Walton; Department of Molecular Biology, Pennsylvania Hospital, 8th and Spruce Streets, Philadelphia, Pennsylvania 19107.

Three types of evidence were presented showing that the retention of cell water does not necessarily rely upon the possession of an intact cell membrane. The data agree with the concept that water retention in cells is due to multilayer adsorption on proteins and that the maintenance of the normal state of water relies on the presence of ATP as a cardinal adsorbent, controlling the protein conformations.

W-POS-D22 DIFFERENTIAL ^{51}Cr UPTAKE BY ELECTROPHORETICALLY SEPARATED HUMAN PERIPHERAL LYMPHOCYTES. A.L. Griffith[1], E.M. Skrabut*[2], C.D. Platsoucas*[1], C.R. Valeri*[3] and N. Catsimpoolas[1], [1]Biophysics Laboratory, Department of Nutrition and Food Science, Massachusetts Institute of Technology, Cambridge, MA 02139, [2]Department of Hematology, Boston University Medical Center, Boston, MA 02118, and [3]Naval Blood Research Laboratory, Chelsea, MA 02150.

Human peripheral lymphocytes, incubated with ^{51}Cr for 30 min. prior to and after electrophoresis, respectively, have been separated by preparative density gradient electrophoresis (A.L. Griffith, N. Catsimpoolas and H.H. Wortis, Life Sciences 16:1693-1702, 1975). In both cases a bimodal distribution was obtained consisting of high mobility cells (HMC) and low mobility cells (LMC). The LMC incorporated several-fold less ^{51}Cr/cell than did the HMC. This differential chromium uptake was obtained both with labelling before and after electrophoresis. Furthermore, it was shown that the rate of chromium uptake reached a plateau at about 2 hrs for the LMC but continued to increase for 4 hrs for the HMC. This phenomenon may contribute to variability of results in cytotoxic assays when ^{51}Cr-labelled lymphocytes of undetermined charge are used as target cells. In addition, preparative electrophoresis of peripheral lymphocytes after incubation in Dulbecco's phosphate buffered saline containing 40% plasma for 2 hrs with and without ^{51}Cr gave an approximate unimodal distribution, suggesting an alteration in cellular surface charge upon prolonged incubation. (Supported by NCI contract No. NOl-CB-43928).

W-POS-D23 AFFINITY FACTORS OTHER THAN MEMBRANE SURFACE CHARGE INVOLVED IN THE PARTITION OF CELLS IN TWO-POLYMER AQUEOUS PHASES. H. Walter, and D. E. Brooks, Laboratory of Chemical Biology, VA Hospital, Long Beach, CA 90801 and Department of Pathology, University of British Columbia, Vancouver, B.C.

When aqueous solutions of dextran (D) and of polyethylene glycol (PEG) are mixed above critical concentrations immiscible, liquid two-phase systems are obtained with a PEG-rich top and a D-rich bottom. Made isotonic, such phases are highly useful in separating cells by partition. Some salts (e.g., phosphate) partition unequally when the polymer concentrations are at some distance from the critical point (e.g., 5% D:4% PEG). An electrostatic potential between the phases results and accounts for the finding that membrane surface-charge-associated properties are a major determinant in cell partition. We now report two instances, one of general applicability and one a more specific illustration, in which membrane charge either does not determine or is not the main determinant of cell partition. (1) Cell partition coefficients in phase systems approaching the critical point (e.g., 5% D:3.5% PEG) increase (probably due to the decrease in interfacial tension) even in phase systems in which the bulk phase potential is zero. Furthermore, in systems close to the critical point, the partition coefficient of some cells is not affected by complete removal of cell surface charge components (e.g., sialic acid from human erythrocytes). (2) Rat and mouse erythrocytes have sizeable partition coefficients in a phase system away from the critical point with no potential between the phases (i.e., 5% D:4% PEG containing NaCl, a salt which itself partitions equally between the phases). Cell surface interaction with the polymers, particularly with PEG, is probably responsible for cell partition in these phases.